Inaugural dissertation

submitted to the

Combined Faculties for the Natural Sciences and for Mathematics

of the Ruperto-Carola University of Heidelberg, Germany

for the degree of

Doctor of Natural Sciences

Presented by

Dipl.-Biol. Markus Krieger

Born in Ludwigsburg

Date of oral examination: 27.10.2011

Declaration

I hereby declare that this thesis is my own work and effort.

Where other sources of information have been used, they have been acknowledged

Date

Signature

THE HEMATOPOIETIC CYTOKINE GRANULOCYTE-MACROPHAGE COLONY STIMULATING FACTOR IS INVOLVED IN COGNITIVE PROCESSING

Referees: Prof. Dr. Stephan Frings

Prof. Dr. Armin Schneider

ABSTRACT

The hematopoietic cytokine Granulocyte/Macrophage Colony Stimulating Factor is involved in cognitive processing

Granulocyte/macrophage colony stimulating factor (GM-CSF) is a growth factor originally discovered in the hematopoietic system. Recently presence of GM-CSF and its receptor (GM-CSFR) was reported on CNS neurons. Here we investigated whether this system is involved in cognition by evaluating learning and memory formation in GM-CSF deficient (GMko) mice. In a complementary approach, GM-CSF signalling was bidirectionally manipulated specifically in the adult hippocampus by adeno-associated virus (AAV) mediated GM-CSF receptor α (GM-CSFRα) overexpression or knock-down. In GMko mice, broad cognitive deficits were observed in all behavioural paradigms tested. Animals showed impairments in fear memory to conditioned cue, in spatial learning in an active place avoidance paradigm, and in spatial memory and re-learning flexibility in the Morris Water Maze. Additionally, knock-outs also showed diminished exploratory drive. The inferior cognitive performance was not due to secondary factors such as motor function, inherent anxiety, or pain threshold levels. Corroborating these data, spatial memory of AAV-injected mice in the MWM was enhanced or impaired dependent on GM-CSFR alpha overexpression or knock-down, respectively. GMko mice showed diminished overall dendritic length and branching complexity in the dentate gyrus (DG) and reductions in both dendritic spine density and the percentage of mature spines in the hippocampus. Despite these morphological alterations and the strong memory deficits, induction of long-term potentiation (LTP) was not impaired in the hippocampus of knock-out mice, providing an example for the complicated relationship of LTP and memory performance. Collectively, these results suggest that GM-CSF signalling plays a major and hitherto unrecognized role in neuronal structural plasticity relevant to learning and memory. This finding is of particular therapeutic relevance, as GM-CSF readily passes the intact blood-brain barrier.

ZUSAMMENFASSUNG

Das hämatopoetische Zytokin Granulozyten/Makrophagen-Kolonie stimulierender Faktor ist beteiligt an kognitiver Verarbeitung

Granulozyten/Makrophagen-Kolonie stimulierender Faktor (GM-CSF) ist ein ursprünglich aus der Hämatopoese bekannter Wachstumsfaktor, der kürzlich samt seinem Rezeptor (GM-CSFR) auch auf Neuronen im Gehirn nachgewiesen wurde. Gegenstand der vorliegenden Studie war eine mögliche Beteiligung dieses Systems an kognitiven Prozessen. Hierzu wurde die Lern- und Gedächtnisfähigkeit GM-CSF-defizienter (GMko) Mäuse untersucht. In komplementären *in vivo* Experimenten wurde mit Hilfe Adeno-assoziierter Virusvektoren (AAV) ausschließlich im Hippocampus adulter Mäuse die neuronale Molekülzahl der alpha-Untereinheit des GM-CSF Rezeptors (GM-CSFRα) erhöht oder verringert, und so entsprechende Signalwege jeweils aktiviert oder gehemmt. GMko-Mäuse zeigten kognitive Defizite in sämtlichen angewendeten Verhaltenstests inklusive verringertem Angstgedächtnis für einen konditionierten auditorischen Reiz, geringerem räumlichen Lernen in einem Active Place Avoidance Test, sowie verringertem räumlichen Gedächtnis und eine geringere Umlernfähigkeit in einem Morris Water Maze (MWM). Zudem zeigten diese Tiere reduziertes Explorationsverhalten. Diese Befunde waren unabhängig von möglichen sekundären Einflüssen betreffend die Motorik, Ängstlichkeit oder Höhe der Schmerzschwelle. Unterstützt werden diese Daten durch Ergebnisse mit AAV-behandelten Tieren, die abhängig vom Expressionsniveau des GM-CSFRα im MWM je verbesserte oder verringerte räumliche Gedächtnisleistung zeigten. Die zelluläre Gesamtlänge der Dendriten im Gyrus dentatus, sowie deren Verzweigungsgrad, waren in GMko-Mäusen geringer, ebenso die hippocampale Besatzdichte mit dendritischen Dornfortsätzen sowie die relative Anzahl reifer Dornfortsätze. Trotz dieser morphologischen Veränderungen und des Gedächtnisdefizits war die Ausbildung von Langzeitpotenzierung (LTP) im Hippocampus nicht beeinträchtigt, was ein Beispiel darstellt für die komplizierte Beziehung zwischen LTP und Gedächtnisbildung. Insgesamt legen diese Ergebnisse den Schluss nahe, dass GM-CSF eine zuvor unbekannte Rolle in neuronalen Plastizitätsvorgängen spielt, die für Lernen und Gedächtnisbildung notwendig sind. Dieser Befund hat möglicherweise eine besondere therapeutische Relevanz da GM-CSF die intakte Blut-Hirn-Schranke überquert.

CONTENTS

1 INTRODUCTION

1.1 GM-CSF Biology

1.1.1 GM-CSF and the hematopoietic system

THE mammalian granulocyte/macrophage colony stimulating factor (GM-CSF) is a secretory glycoprotein of 15-35 kDa which was named after its ability to generate both granulocyte and macrophage colonies from bone marrow-derived hematopoietic progenitor cells *in vitro* (Metcalf, 1989). Its existence was first postulated in the 1960s when it was found that formation of these neutrophilic colonies did not occur unless progenitor cells were co-cultured with either cells or medium conditioned by cells from other tissues including spleen, kidney, lung, uterus, testis, and ovary (Bradley and Metcalf, 1966; Ichikawa et al., 1966; Robertson and Seamark, 1992). Hence, a variety of tissues appeared capable to generate and secrete this factor (Fig. 1).

Partly due to the presence of only minute amounts of GM-CSF protein in all of these tissues (Hill et al., 1995), however, its biochemical isolation was only achieved more than a decade later from the murine lung (Burgess et al., 1977), and human GM-CSF was not purified until the mid 1980s (Gasson et al., 1984). The subsequent observation that addition of purified GM-CSF to hematopoietic progenitor cells was sufficient even in serum-free media to induce formation of granulocyte and macrophage colonies revealed that GM-CSF had a direct effect on these progenitor cells that did not require intermediate serum factors (Metcalf et al., 1980; Hill et al., 1995).

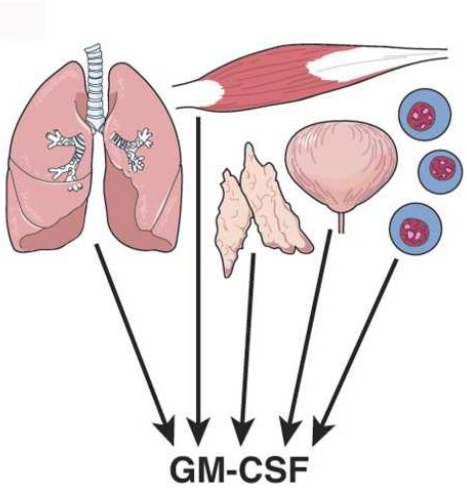

Figure 1. GM-CSF is expressed and secreted by a variety of different tissues and cell types including but not restricted to lung, muscle, and hematopoietic cells. From (Metcalf, 2008).

However, purification of GM-CSF from tissue did not yield sufficient amounts of protein to conduct *in vivo* studies. This only became possible when both the murine and human GM-CSF genes were molecularly cloned (Gough et al., 1984; Wong et al., 1985), thus facilitating recombinant GM-CSF (rGM-CSF) expression in large quantities. Subsequent studies confirmed a dose-dependent increase in granulocyte and monocyte-macrophage counts following repetitive injections of rGM-CSF in both mice (Metcalf et al., 1987) and human AIDS patients (Groopman et al., 1987).

Further clinical investigations established GM-CSF as a therapeutic option to ameliorate both chemo- and radiotherapy-induced neutropenia and for the myeloid recovery after bone-marrow transplantation (Brandt et al., 1988; Nemunaitis et al., 1988; Visani et al., 1990; reviewed in Lieschke and Burgess, 1992). Moreover, GM-CSF was shown to expand the circulating compartment of hematopoietic progenitor cells by mobilization of bone marrow stem cells (Socinski et al., 1988). This greatly facilitated the harvesting of peripheral blood stem cells which could be used as a substitute for bone marrow cells in transplantation procedures (Gianni et al., 1989; reviewed in Metcalf, 2008). To date, GM-CSF has proven a valuable agent in these indications, and has demonstrated an excellent safety and tolerability profile in its 20 years of clinical use.

Apart from its activity as a regulator of hematopoietic progenitor cell proliferation and differentiation, however, GM-CSF is also a key determinant in the functional activation of terminal effector cells in the hematopoietic system. For example, a large body of evidence indicates GM-CSF to exert tight control over the efficiency of antigen presentation by dendritic cells (Sallusto and Lanzavecchia, 1994), leukocyte chemotaxis and cell-cell adhesion (Arnaout et al., 1986), oxidative metabolism and phagocytic activity of neutrophils (Fleischmann et al., 1986; Weisbart et al., 1987), fungicidal activity of monocytes (Smith et al., 1990), and the transition from resting to activated T-lymphocytes (Shi et al., 2006). These pleiotropic functions implicate an additional pro-inflammatory role for GM-CSF (reviewed in Hamilton, 2008; Hercus et al., 2009). Moreover, by controlling both dendritic cell and lymphocyte activity, GM-CSF provides a link between the innate and the adaptive immune system. A summary of the various effects GM-CSF exerts on different target cell types is shown in Figure 2.

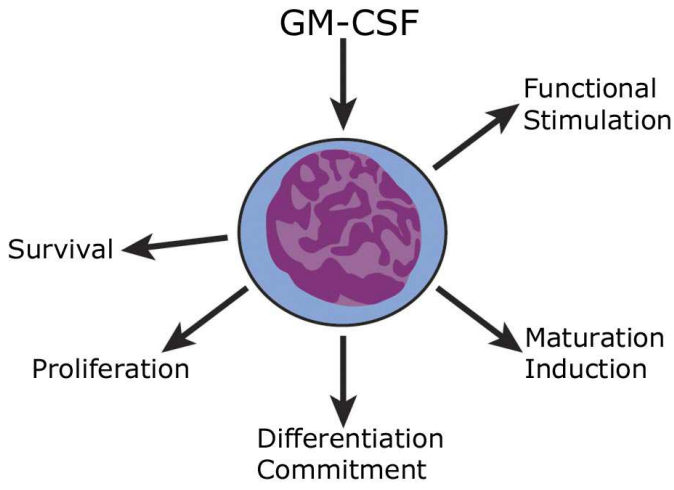

Figure 2. GM-CSF is a pleiotropic hematopoietic cytokine. A variety of different cellular functions are mediated by GM-CSF in the hematopoietic system including regulation of proliferation, lineage commitment, and functional activation of effector cells. After (Metcalf, 2008).

On the background of combined GM-CSF-regulated leukocyte generation and regulation of activity, clinical relevance has been established for GM-CSF in the

etiology of both hematopoietic and inflammatory disorders. For example, dysregulated GM-CSF signalling plays a central role in the development of juvenile myelomonocytic leukemia (JMML), a rare but devastating disease that leads to juvenile death in the majority of cases (Chan et al., 2005; Iversen et al., 1996; Birnbaum et al., 2000). This myeloproliferative disorder is characterised by a combination of excessive GM-CSF secretion by transformed hematopoietic progenitor cells and a concomitant autocrine hypersensitivity of these cells to this cytokine (Yoshida et al., 2009). Rheumatoid arthritis (RA), on the other hand, is an autoimmune disease characterized by chronic inflammation of synovial joints, synovial hyperplasia, and massive infiltration of lymphocytes, macrophages, dendritic cells, and neutrophils into both synovial tissue and fluid. Enhanced levels of GM-CSF have been observed in the synovium of RA patients (Jang et al., 2006) and blockade of GM-CSF signalling was shown to alleviate RA symptoms (Cook et al., 2001; reviewed in Cornish et al., 2009). A third condition associated with malfunctions in the GM-CSF system is pulmonary alveolar proteinosis (PAP), a lung pathology related to dysfunctional alveolar macrophages that is characterized by dysregulated surfactant homeostasis and a subsequent accumulation of lipoproteinaceous material in alveoli that renders patients at risk of secondary infection and respiratory failure (Seymour and Presneill, 2002). The genetic loss of essential GM-CSF signalling components has been linked to congenital PAP, while autoimmunity against GM-CSF protein has been shown to underlie an idiopathic form of this disorder (Trapnell et al., 2003). In fact, it was the phenotypic characterization of a GM-CSF knock-out (GMko) mouse line that revealed the central role this cytokine plays in PAP (Dranoff et al., 1994).

Surprisingly, however, in these GMko mice no effect was observed on the counts of bone marrow hematopoietic progenitor cells, peripheral leukocytes, and hematopoietic cells in tissues (Dranoff et al., 1994), and these findings were confirmed by a different group that generated an independent GMko mouse line (Stanley et al., 1994). Indeed, lethally irradiated GMko mice could be rescued by bone marrow transplants from untreated GMko donors (Dranoff et al., 1994). While these *in vivo* findings demonstrated GM-CSF to play an essential role in basal lung physiology, unexpectedly, no such impact was detected on basal hematopoiesis which appears governed, at least to some extent, by functional cytokine redundancy. Hence, the notion that GM-CSF was an essential regulator

of basal myelopoiesis *in vivo* had to be rejected. Rather, a large and growing body of evidence now suggests that GM-CSF plays an essential, non-redundant role in emergency myelopoiesis after infection where it leads to accelerated neutrophil production by hematopoietic progenitors in the bone marrow and to survival and activation of this progeny at the site of infection (Zhan et al., 1998; Metcalf, 2008; Hercus et al., 2009; Shibasaki et al., 2007; Guthridge et al., 1998). In the course of such immune responses, activated T-cells seem to be a main source of GM-CSF secretion.

1.1.2 GM-CSF receptors, ligand binding, and signal transduction pathways

GM-CSF exerts its biological activities by binding to GM-CSF receptors (GM-CSFR) located in the plasma membrane of target cells. These receptors are heteromeric complexes consisting of two different subunits: the GM-CSF receptor alpha (GM-CSFRα) which confers ligand-specific binding, and a common beta (β_c) subunit that acts as the signal transduction chain and is shared with the closely related receptors for interleukin (IL)-3 and IL-5 (Metcalf, 1989). While β_c alone does not show any detectable ligand binding activity, GM-CSFRα alone binds GM-CSF with low affinity (K_D = 0.2-100 nM), but it is only after the ligand-induced aggregation of GM-CSF:GM-CSFRα complexes with β_c that ligand binding is converted to a high-affinity state (K_D = 100 pM), thus generating a stable ternary complex with functional signalling activity (Hoang et al., 1993; Hansen et al., 2008). However, one report also indicated that preformed GM-CSFRα:β_c complexes may exist in the plasma membrane of a human leukemic cell line (Woodcock et al., 1997). Notably, abundance of GM-CSFRs in the plasma membrane is very low with only 100-1000 molecules per subunit (Hansen et al., 2008). Expression of GM-CSFRs has been confirmed in myeloid cells, lymphocytes, and a variety of non-hematopoietic cells including endothelial cells, small-cell lung carcinoma cells, neurons, and neural stem cells.

Both GM-CSFRα and β_c are typical single-pass type I transmembrane proteins with an extracellular domain, a small transmembrane region, and a cytoplasmic tail. They belong to the superfamily of cytokine receptors which is characterized by conserved structural features in the extracellular domain such as two conserved pairs of cysteine residues that form stable disulfide bridges and thus contribute to structural integrity of the polypeptide chain (Guthridge et al., 1998). Moreover, they contain a characteristic Trp-Ser-X-Trp-Ser (WSXWS) motif in the membrane-proximal region that mediates protein folding and protein-protein interaction between membrane-bound cytokine receptors (Rosas et al., 2007). Both the cysteines and the WSXWS motif are incorporated into two fibronectin III (FNIII) folds containing seven antiparallel β strands each (Bazan, 1990; Rajotte et al., 1997) designated A-G and A'-G' for the N- and C-terminal folds, respectively. Together, these two FNIII folds form a characteristic cytokine receptor module (CRM). While the extracellular region of GM-CSFRα comprises one CRM, and hence two fibronectin III domains (αD1, αD2), β_c consists of two CRMs, and hence four fibronectin III domains (βD1-βD4).

In GM-CSFRα, the bulk of the 388 amino acids that constitute the whole polypeptide are contained within the extracellular domain, while the cytoplasmic tail is rather short with a length of only 40 amino acids. This tail contains a proline-rich Pro-Pro-X-Pro domain (PPXP) that contributes to signal transduction via the β_c subunit in functional ligand-receptor complexes (Doyle and Gasson, 1998), and deletion of the cytoplasmic tail abrogates GM-CSF signalling but has no effect on ligand binding (Polotskaya et al., 1993). This structural principle also applies for the closely related ligand-specific alpha receptor chains for IL-3 (IL3Rα) and IL-5 (IL5Rα) whose cytoplasmic tails provide equivalent, yet distinct contributions to intracellular signal transduction via the β_c subunit, thus explaining the overlapping functional effects these cytokines exert on target cells co-expressing β_c with combinations of GM-CSFRα, IL3Rα, and IL5Rα (Hercus et al., 2009; Muto et al., 1995). Apart from that, alternatively spliced soluble GM-CSFRα isoforms have been described both *in vitro* and *in vivo*, and have been shown to modulate GM-CSF bioactivity by scavenging circulating cytokine molecules (Brown et al., 1995; Sayani et al., 2000).

The cytoplasmic domain of the signal transducing β_c subunit is much larger and very similar in size to the extracellular domain. Nevertheless, it does not contain intrinsic tyrosine kinase or any other enzymatic activity to initiate signal transduction. Instead, via two conserved motifs in the juxtamembrane region termed Box 1 and Box 2, constitutive binding of Janus kinase 2 (JAK2) is achieved, and transphosphorylation of JAK2 molecules upon receptor activation initiates intracellular signal transduction via activation of signal transducer and activator of transcription (STAT) molecules (Quelle et al., 1994). It has been shown recently that the structure of the GM-CSFR complex comprises a 2:2:2 hexameric assembly of two intertwined β_c chains, two GM-CSFRα chains, and two GM-CSF molecules (Hansen et al., 2008). However, JAK2 transactivation within these hexamers is prevented by a gap of 120 Å between the cytoplasmic domains of the two β_c chains, a distance too wide to allow enzymatic interaction of associated JAK2 molecules. As illustrated in Figure 3, it is only via the formation of an unusual dodecamer complex that close association (~ 10 Å) and subsequent transactivation of JAK2 molecules is facilitated (Hansen et al., 2008). In this configuration, transphosphorylation takes place between JAK2 molecules associated with different hexamers.

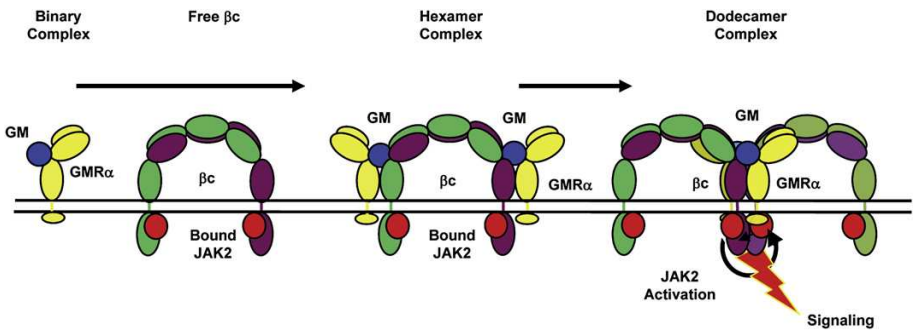

Figure 3. Model for functional activation of GM-CSF receptors. Low-affinity binary complexes of GM-CSF-bound GM-CSFRα associate with free β_c dimers to form stable high-affinity hexameric complexes. Subsequent assembly of hexamers into dodecameric complexes is required to facilitate close proximity and transactivation of β_c-bound JAK2 molecules (red circles) of different hexamers, thus inducing intracellular signalling. From (Hansen et al., 2008).

Extensive structure-function analyses of GM-CSF, GM-CSFRα, β_c, and ligand-bound receptor complexes led to a detailed understanding of the molecular events during ligand binding and receptor complex formation. The structure of the 127 amino acids GM-CSF ligand has been determined by x-ray crystallography which revealed a non-spherical configuration dominated by four α helices (Diederichs et al., 1991), a tertiary structure known from other cytokines including IL-2, IL-5, and growth hormone (Hercus et al., 1994). In conjunction with results from earlier studies (Clark-Lewis et al., 1988; Kaushansky et al., 1989; Shanafelt et al., 1991) receptor binding could thus be assigned to the first and fourth helices of GM-CSF and residues Lys14, His15, Glu21, and Asp112 were shown to be indispensible for bioactivity of the murine cytokine (Meropol et al., 1992; Hercus et al., 1994). Residue Arg280 in the F'-G' loop of GM-CSFRα also plays an essential role in GM-CSFR activation by providing electrostatic interaction with Asp112 of GM-CSF (Fig. 4a), and charge reversal mutations of Asp112 led to a 1000-fold decrease in receptor binding affinity of the cytokine (Rajotte et al., 1997). On the other hand, charge reversal mutations by arginine substitution of GM-CSF residue Glu21 (E21R) led to near-complete retention of low-affinity binding to GM-CSFRα but abolished formation of high-affinity receptors, and hence abrogated stimulation of cellular proliferation and mature cell function (Lopez et al., 1992). In fact, E21R was found to act as a dominant negative inducer of apoptosis in primary human hematopoietic cells (Iversen et al., 1996). From these findings it was deduced that Glu21 plays a crucial role in the association of GM-CSF:GM-CSFRα complexes with β_c to form stable ternary signalling complexes, a notion corroborated by the three-dimensional location of Glu21 within the receptor complex (Fig. 4b).

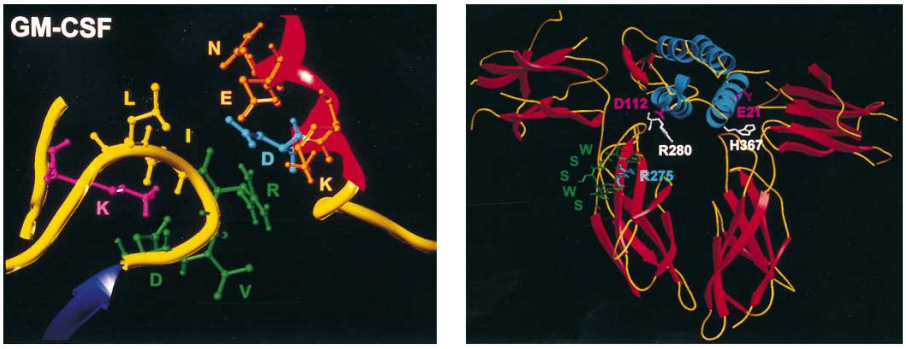

Figure 4. Three-dimensional model of GM-CSF binding to its receptor. (***Left panel***) Low-affinity binding is mediated by interaction between the F'-G' loop of GM-CSFRα (*left, yellow*) and helix D of the GM-CSF ligand (*red*) through electrostatic interaction between residues R280 of the receptor (*green*) and D112 of the ligand (*blue*). Other side chains of minor importance are shown as well. (***Right panel***) Three-dimensional model of extracellular portions of a liganded GM-CSF receptor complex containing GM-CSF (*top*), GM-CSFRα with its WSXWS motif (*left, green*), and β_c (*right*). Basic receptor side chains involved in ligand binding are shown in white (R280 of GM-CSFRα and H367 of β_c) while interacting acidic ligand side chains are shown in magenta. Note the interaction of GM-CSF residue E21 with the β_c subunit which is required for high-affinity binding. From (Rajotte et al., 1997)

This was recently confirmed by high-resolution analysis of isolated β_c at 3.0 Å (Carr et al., 2001) and 2.7 Å (Carr et al., 2006), and by the crystal structure of GM-CSF receptor complexes at 3.3 Å (Hansen et al., 2008) where Glu21 of the cytokine was shown to critically interact with Tyr365 and His367 in the B-C loop, and with Tyr421 in the F-G loop of βD4 (Fig. 5). Any alanine substitution of these three β_c residues completely abolished high-affinity GM-CSF binding (Lock et al., 1994; Woodcock et al., 1994).

Elucidation of the crystal structure of the GM-CSF receptor complex led to detailed models of both hexameric and dodecameric assemblies of GM-CSF receptor complexes (Fig. 6).

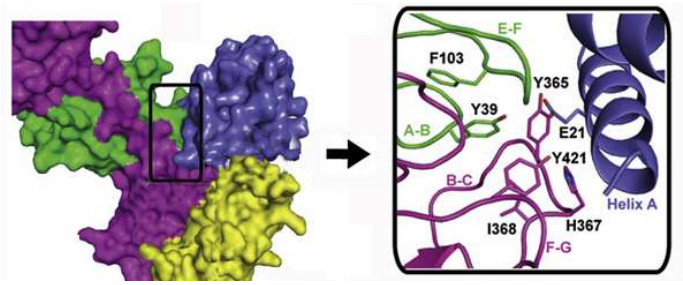

Figure 5. High-resolution model of GM-CSF binding to β_c. (***Left panel***) GM-CSF (blue) bound to GM-CSFRα (yellow) interacts with a composite surface provided by two different β_c subunits, i.e. by domain 1 of one β_c chain (green) and domain 4 of the second β_c chain (purple). (***Right panel***) Magnification of boxed area in left panel illustrating the critical position of GM-CSF residue Glu21 relative to β_c residues Tyr365 and His367 in the B-C loop, and Tyr421 in the F-G loop of β_c, respectively. After (Hansen et al., 2008).

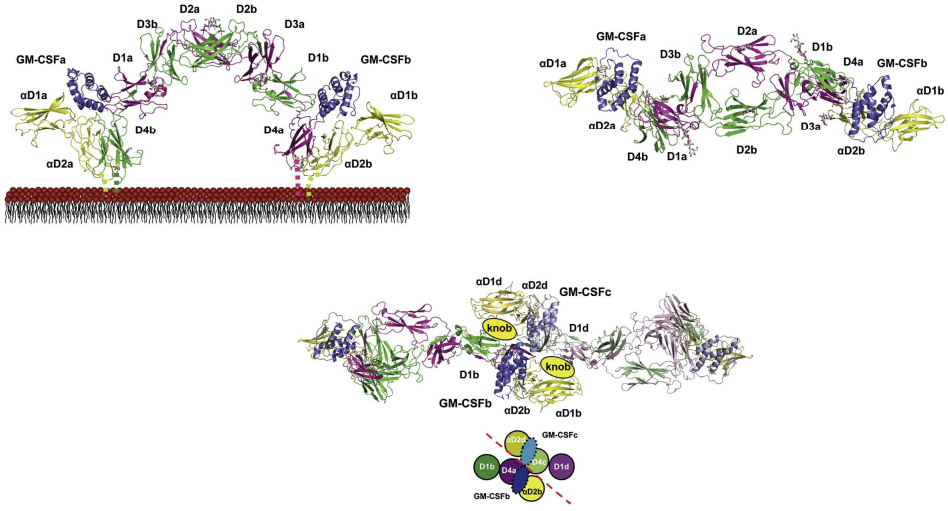

Figure 6. Structure of the hexameric and dodecameric GM-CSF receptor complexes. (***Top left***) Side view of a GM-CSF receptor hexameric assembly consisting of two molecules of GM-CSF (blue), GM-CSFRα (yellow) and β_c (green and purple), respectively. Domain names are denoted for all molecules. Dashed lines indicate C-terminal anchoring of the receptor chains to the membrane. (***Top right***) Top view on same hexameric assembly. The membrane would lie underneath the hexamer but is not shown for enhanced clarity. (***Bottom***) Top view on dodecameric assembly with different hexamers depicted in different shades. N-terminal portions of GM-CSFRα are shown as a knob domain for which high quality structural data is missing. A simplified illustration of the dodecameric assembly is shown in the lower panel which highlights the relative positions of the individual modules. Chains of β_c are labelled a-d, chains of GM-CSFRα are labelled likewise but start with an α. "D" indicates a domain. After (Hansen et al., 2008)

Apart from the aforementioned JAK/STAT pathway, GM-CSF is known to induce at least two other signalling cascades: the mitogen-activated protein kinase (MAPK) and the phosphoinositide 3-kinase (PI3K) pathway. These multiple pathways are not mutually exclusive but, instead, may overlap to a considerable degree and thus contribute to a network signalling response that may help to explain the pronounced pleiotropic effects of GM-CSF.

In JAK/STAT signalling following GM-CSFR activation, JAK2 molecules pre-associated with β_c subunits of different hexamers transactivate each other and subsequently also phosphorylate tyrosine residues in the cytoplasmic tail of β_c such as Tyr577, Tyr612, Tyr695, Tyr750, Tyr806, and Tyr866 which are conserved between mouse and human (Guthridge et al., 1998). These phosphotyrosines then provide docking sites for proteins containing Src homology 2 (SH2) domains such as members of the STAT family. While STAT5 appears to be the predominant member of the STAT family involved in GM-CSF signal transduction, isoforms STAT1, STAT3, and STAT6 play differentially important roles in a variety of target cell types as well (de Groot et al., 1998). Following JAK2-mediated phosphorylation, STATs dimerize to form functional transcription factors and subsequently translocate to the nucleus to regulate expression of target genes including *oncostatin M*, and *pim-1* (Yoshimura et al., 1996; de Groot et al., 1998).

In parallel, GM-CSF-induced phosphorylation of β_c tyrosine residues also triggers docking of adaptor proteins Shc and Grb2 to Tyr577 and Tyr612/Tyr695, respectively, which leads to activation of these adaptors followed by the formation of Shc/Grb2 heterodimers. These dimers, in turn, can activate Ras-GTPase, thus triggering the MAPK signalling pathway which leads to activation of different members of the MAPK family including ERK1, ERK2, p38, and JNK/SAPK (reviewed in de Groot et al., 1998). Indeed, GM-CSF has been shown to rapidly induce activation of both Ras and its downstream target c-Raf (Kanakura et al., 1991; Satoh et al., 1991), as well as phosphorylation of ERK1 and ERK2 (Schallenberg et al., 2009). The MAPK pathway is likely involved in mediating GM-CSF induced proliferation, although cross-talk between signalling cascades makes it difficult to fully dissect contributions of individual signalling pathways to distinct functional outcomes.

Activation of the PI3K pathway is the third major signalling cascade initiated by GM-CSF. The heterodimeric, cytosolic PI3K is composed of the regulatory and catalytic subunits p85 and p110, respectively, and although the molecular details initiating this pathway are less well understood, tyrosine phosphorylation of p85 seems to play an important role in p110 activation (al-Shami et al., 1997) and phosphorylation of β_c Tyr577 and Tyr612 may be important in this process, a finding that indicates an upstream role for JAK2 (Dijkers et al., 1999). The lipid kinase PI3K phosphorylates its plasma membrane-bound substrate phosphatidylinositol 4,5-bisphosphate (PIP_2) to generate phosphatidylinositol (3,4,5)-trisphosphate (PIP_3) to which the PI3K downstream effector phosphoinositide dependent kinase 1 (PDK1) can subsequently bind via its pleckstrin homology (PH) domain. PDK1 acts as a master regulator of several downstream kinases including p70 ribosomal S6 kinase (S6K), p90 ribosomal S6 kinase (RSK), serum and glucocorticoid-induced protein kinase (SGK), several isoforms of protein kinase C (PKC), and Akt (for review see Bayascas, 2008), with the latter appearing as the most significant for GM-CSF function (Perugini et al., 2010; Guthridge et al., 1998). Signalling via Akt, also known as protein kinase B, has potent anti-apoptotic effects that contribute to cytokine-induced survival of target cells. These protective effects of the serine/threonine kinase Akt are partially mediated via phosphorylation-induced inactivation of the pro-apoptotic protein BAD, an inhibitor of anti-apoptotic Bcl-2 family members, and further Akt-related survival signals are transmitted by direct activation of IκB kinase (IKK) leading to disinhibition of transcription factor NFκB, and hence to expression of a variety of pro-survival genes. Moreover, there is additional evidence that activated GM-CSFRs can bind IKK directly via GM-CSFRα, and hence activate NFκB signalling in a more direct way (Ebner et al., 2003).

1.1.3 GM-CSF in the central nervous system

Apart from its functions in the hematopoietic system, GM-CSF has also been shown to exert effects on cells in the central nervous system (CNS). For example, an early study on primary glial cells revealed the presence of functional

GM-CSFRs in plasma membranes of oligodendrocytes (Baldwin et al., 1993). Later reports demonstrated neuromodulatory effects of peripherally applied GM-CSF such as indirect inhibition of scopolamine-induced anterograde amnesia (Bianchi et al., 1996), regulatory actions on hypothalamic levels of glutamate and GABA neurotransmitters (Bianchi et al., 1997), and modulatory effects on the electrical activities of both the medullary gigantocellular reticular formation in the CNS and the efferent splenic nerve in the peripheral nervous system (Lukashenko et al., 2004). Moreover, centrally administered GM-CSF was shown to induce somnogenic effects with impacts on both rapid eye movement (REM) sleep and non-REM sleep in rats (Kimura et al., 2000) and also to decrease food intake and body weight in both rats and mice (Reed et al., 2005).

A study by McLay and co-workers revealed that GM-CSF is able to cross the intact blood-brain and blood-spinal cord barriers by means of a selective and saturable transport system, thus providing initial explanation for the observed central effects (McLay et al., 1997) after peripheral application of GM-CSF. In extension to this, both GM-CSF and GM-CSF receptor expression was found in neurons and neural tissues in the developing human fetus at 8 and 16 weeks postconception (Dame et al., 1999).

Respective expression data for the adult mammalian CNS, however, was only recently obtained in a study by Schäbitz and colleagues which demonstrated constitutive co-expression of both GM-CSF and GM-CSF receptor in the CNS by the neuronal subpopulation (Schabitz et al., 2008). This endogenous expression of GM-CSF indicates that the CNS is independent, to some extent, from influx of peripherally produced GM-CSF via the blood-brain barrier, and further suggests an autocrine mode of action in the healthy brain. This study also revealed selective upregulation of both GM-CSF and GM-CSFRα under conditions of experimental ischemic stroke and demonstrated infarct volumes to be reduced after GM-CSF application. Induction of Akt signalling was shown to contribute to this neuroprotective mechanism (Schabitz et al., 2008). These functional outcomes were confirmed by an independent study also using a middle cerebral artery occlusion rat model (Kong et al., 2009). Neuroprotective effects were also observed in a 1-methyl-4-phenyl-1,2,3,6-tetrahydropyridine (MPTP)-induced murine model of Parkinson’s disease where subcutaneous application of GM-CSF

promoted survival of dopaminergic neurons in the substantia nigra and partially rescued the MPTP-induced locomotor deficit (Kim et al., 2009).

Beneficial central effects of GM-CSF were additionally demonstrated in rodent models of spinal cord injury (SCI) where GM-CSF provided anti-apoptotic neuroprotection in a spinal cord contusion model (Ha et al., 2005), inhibited glial scar formation (Huang et al., 2009), and activated neural stem/progenitor cells in the injured spinal cord (Hayashi et al., 2009).

Additional *in vitro* studies further suggest that GM-CSF also induces proliferation of neural stem cells (Kim et al., 2004) and subsequently drives their differentiation into neurons (Kruger et al., 2007), thus indicating positive effects on neuronal plasticity for this cytokine. Apart from its neuroprotective functions, GM-CSF consequently appears to mediate some degree of neuronal replenishment and induction of brain plasticity in the CNS under disease conditions, and hence to exert beneficial effects in a dual mode.

Nevertheless, only scarce information exists regarding the role of GM-CSF in the healthy brain. In particular, virtually no information is available on the impact of neuronal GM-CSF signalling on learning and memory, despite the constitutive neuronal co-expression of GM-CSF and GM-CSFR in a wide variety of brain regions including cortex and hippocampus (Schabitz et al., 2008). While a recent report has shown reversal of cognitive deficits in a mouse model of Alzheimer's disease (AD) after GM-CSF application, the authors related this effect to a GM-CSF-induced reduction in amyloidosis. The ability of GM-CSF to regulate Aβ levels both *in vitro* and in the brains of a transgenic AD mouse model has also been shown previously (Volmar et al., 2008; Manczak et al., 2009). Hence, it remains unknown whether GM-CSF signalling in the brain exerts genuine neuronal actions that affect learning, memory, and an animal's ability to process complex information.

1.1.4 Other hematopoietic factors in the brain

Hematopoietic GM-CSF is functionally related to the cytokines granulocyte-colony stimulating factor (G-CSF) and erythropoietin (EPO) although these proteins do not share any considerable sequence homology. Like GM-CSF, both other cytokines are heavily glycosylated *in vivo* and bind to cytokine type I receptors (G-CSFR and EPOR, respectively) located in the plasma membranes of target cells. They act as growth factors on myeloid lineage stem cells in the hematopoietic system and induce proliferation and subsequent differentiation into the various effector cell types after which they were named, respectively.

In recent years, however, additional important functions in the CNS have been assigned to these well-known hematopoietic factors, and receptors for all three cytokines have recently been demonstrated in the brain (Digicaylioglu et al., 1995; Schneider et al., 2005; Schabitz et al., 2008). It has been suggested that these cytokines exert important neurotrophic functions by employing basal cellular mechanisms similar to those in the blood (for review see Maurer et al., 2008; Tonges et al., 2007). Indeed, enhanced adult neurogenesis has been described for EPO (Shingo et al., 2001; Wang et al., 2004), G-CSF (Schneider et al., 2005), and GM-CSF (Kruger et al., 2007), and it is interesting to note that a comparison of gene expression profiles between neural and hematopoietic stem cells has revealed a high degree of similarity (Terskikh et al., 2001).

Similar to GM-CSF, neuroprotective actions with beneficial effects in a variety of neurodegenerative diseases have been established for both EPO and G-CSF in rodent models for stroke (Schabitz et al., 2003; Wang et al., 2004), amyotrophic lateral sclerosis (Grunfeld et al., 2007; Henriques et al., 2011; Pitzer et al., 2008) and Parkinson’s disease (Ganser et al., 2010; Kim et al., 2009; Meuer et al., 2006). Hence, all three factors present potential clinical options in neurological conditions, particularly in light of their ability to cross the blood-brain barrier, thus facilitating peripheral application (McLay et al., 1997; Brines et al., 2000; Schneider et al., 2005).

1.2 Cognition and the Hippocampal Formation

1.2.1 Facets of cognition and memory

Cognition is a broad term describing a variety of mental activities associated with the neural processing of information. These activities include aspects of perception, learning, memory, association, judgment, thinking, reasoning, knowing, problem-solving, planning, imagination, and language, and hence some of the frequently cited but ill-defined higher functions of the brain. As some of these mental processes are inextricably linked to conscious experience for which non-linguistic behavioural indexes are missing, their existence remains elusive in non-human animals, and hence not all of these aspects are amenable to experimental testing in rodents (Griffiths et al., 1999; Eichenbaum, 1997). Of those who are, learning and memory are by far the most prominent subjects of investigation in cognitive neuroscience.

In general, different types of memory systems exist in parallel. Some of them may be specific to humans, and are governed by different brain regions. The first level of discrimination between memory systems is merely based on the time span of information storage, and hence the categories are short-term or working memory on the one hand and long-term memory on the other. The latter is further subdivided by the capacity to access its content consciously into non-declarative (not consciously accessible) and declarative (consciously accessible) memory and further subdivisions exist within each group (Fig. 7). Despite its frequent and widespread use, however, this classification system has also been challenged recently (Henke, 2010).

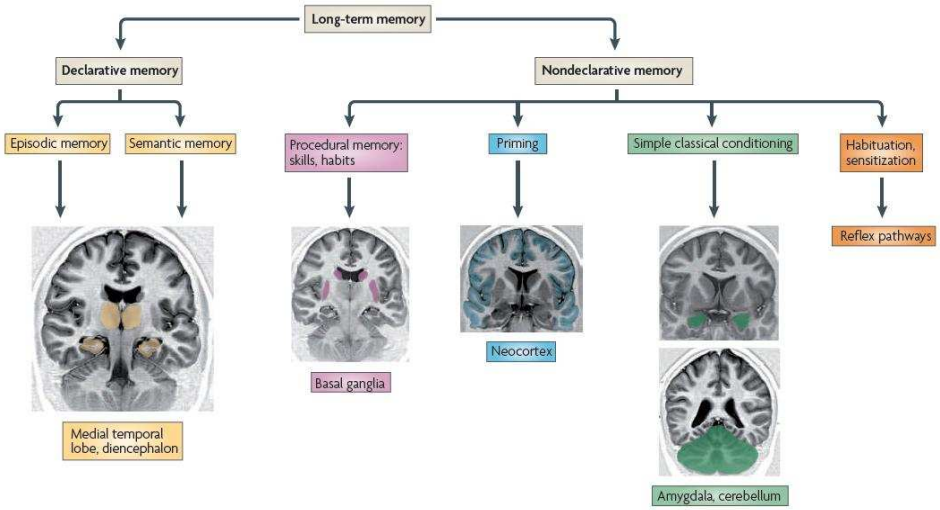

Figure 7. A classification system for subtypes of long-term memories. The first level of discrimination classifies long-term memories into declarative or non-declarative memory depending on whether its content is consciously accessible (declarative memory) or not (non-declarative memory). Declarative memory consists of episodic and semantic memory systems which store personal, autobiographical experiences and impersonal, factual knowledge about the world, respectively, and is highly dependent on medial temporal lobe structures. Non-declarative memory comprises procedural learning, priming, classic conditioning, and sensitization which are explained in the main text. All subtypes of non-declarative memory appear predominantly governed by brain regions other than the medial temporal lobe. From (Henke, 2010)

Non-declarative or implicit memory comprises several types of memory including procedural memory, priming, classic conditioning, and sensitization, and its existence is uncontroversial in non-human mammals including rodents. The term procedural memory, describes the ability to execute a practiced set of procedures, mostly movements, without a need and mostly without a possibility for conscious control. Examples include playing an instrument, walking, reading, or swimming. This type of long-term memory is often a result of motor learning (Kelley et al., 2003). Priming is another form of non-conscious memory which describes the enhanced ability of a subject to either recognize an item or discriminate between different items following a previous encounter with identical or similar items. This effect is based on activation of context information in the brain by the priming stimulus (Tulving and Schacter, 1990; for review see Schacter et al., 2004). Classic conditioning refers to a kind of associative memory that mentally

links two stimuli based on their repetitive co-appearance in the past in such a way that one of these stimuli alone elicits behavioural responses that are typical for the other. This type of memory was discovered by the Russian physiologist Ivan Pavlov (Pavlov, 1927). Finally, sensitization describes a non-associative form of memory eliciting increasing response intensities to repetitive administration of a stimulus. This is exemplarily illustrated by the hyperlocomotor behaviour observed in subjects after frequent abuse of amphetamines which modulate mesolimbic dopamine transmission (Ujike and Sato, 2004).

The term declarative or explicit memory, on the other hand, refers to those types of memories which can be consciously recalled, and which may thus be human-specific to some extent. Declarative memory contains two subcategories, namely episodic and semantic memory. Episodic memory is defined as a repository for autobiographical experiences that stores memories of personally experienced events including their multi-faceted spatio-temporal and emotional contexts (Tulving and Markowitsch, 1998), and this type of memory appears to exist in rodents (Henke, 2010). Semantic memory, on the other hand, comprises factual knowledge about the world that is not directly related to personal experience, and is widely believed to be a human-specific trait. While, for example, remembering having chicken for dinner last Wednesday is episodic memory, knowing that chickens are birds which are a group of animals that lay eggs and derived from reptiles during evolution is semantic memory.

One of the best-studied types of memory in rodents is spatial memory which describes the ability of an animal to know about its location in a familiar environment and, particularly, to navigate it in a goal-directed manner by using both self-centered (idiothetic) and external (allothetic) cues for orientation. Spatial memory does not fully fit in any of the aforementioned groups as it appears to comprise components of both implicit and episodic memory, and two competing hypotheses are actively debated to explain the mode of action underlying spatial memory, namely the cognitive map hypothesis and the relational memory hypothesis (Eichenbaum et al., 1999; Redish, 2001; Kumaran and Maguire, 2005).

The cognitive map hypothesis originally proposed by Edward Tolman assumes the existence or construction of an internal coordinate system into which external cues may be integrated and used for orientation (Tolman, 1948; O'Keefe and

Nadel, 1978). This hypothesis has received important corroboration through a seminal study by O'Keefe and Dostrovsky whose *in vivo* electrophysiological recordings in behaving rats demonstrated that distinct neurons display action potential firing patterns that highly correlate with an animal's position and orientation in a test arena (Fig. 8). Individual neurons of this type, whose existence was more recently confirmed in the human brain as well (Ekstrom et al., 2003), displayed high firing rates at certain locations, and reduced or no firing activity after the animal changed its position or orientation relative to the external cues. These cells were hence termed "place cells" as they appeared to encode the occupancy of a specific location in space which was correspondingly termed a "place field" (O'Keefe and Dostrovsky, 1971). Interestingly, once these firing patterns are established in a given environment, place cells maintain these patterns even in the subsequent absence of landmarks (O'Keefe and Speakman, 1987) and in the dark (Quirk et al., 1990). It appears very tempting to correlate this independence of acute presence of external cues with spatial memory formation.

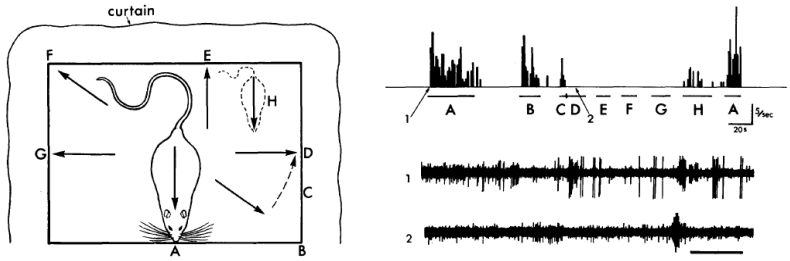

Figure 8. Place cells as location detectors. (***Left panel***) Schematic representation of a rat in a recording stand where hippocampal electrical activity was recorded *in vivo*. Letters A-H denote animals' positions and orientations in which electrical activity was recorded. (***Right panel, top***) Continuous firing frequency histogram illustrating firing activity of a particular recording unit at A-H. Note that this unit was fully active only when rats faced position A or B, and was active to a lesser extent when animals were moved from B to D, a process represented by letter C. This unit was also weakly active in position H indicating the importance of both position and direction. (***Right panel, bottom***) Raw data recorded at time points 1 and 2 in the upper panel illustrating high (1) and low (2) firing activity, respectively, in the particular recording unit. Reference bar, 400 ms. After (O'Keefe and Dostrovsky, 1971)

These findings received further important refinement through experiments showing that place fields are preferentially formed near locations that provide a high degree of spatial information, rather than being formed comprehensively all over the Cartesian plane. Furthermore, information about the relative distances between these saliently cued spots appears neurally encoded in connections between place cells, which may thus serve as anchors to which the cognitive map is aligned (Hetherington and Shapiro, 1997).

However, such findings highlighting the non-continuous, non-homogeneous character of spatial representation paved the way for a competing relational memory hypothesis which essentially assumes spatial memory as a consequence of associative memories that were formed during previous encounters with a given coordinate in the environment (Eichenbaum, 2000). Spatial memory is hence understood as a by-product of overlapping representations of cue-configurations associated with neighbouring coordinates (Fig. 9). According to this view, location-specific firing of place cells would represent the recognition of a certain configuration that is associated with multimodal experiences in the past, instead of being merely a gauge for geometric properties of space (Eichenbaum et al., 1999).

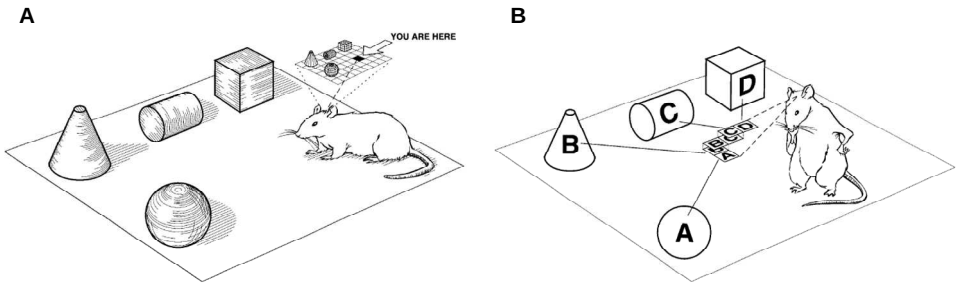

Figure 9. Cognitive map hypothesis versus relational memory coding. (***A***) According to the cognitive map hypothesis, sensory information is integrated into a mental coordinate system which provides an animal with an internal spatial map. (***B***) The relational memory hypothesis assumes spatial memory to emerge as a by-product of associative memory through overlapping representations of distinct cues with different but overlapping sets of relational information content. After (Eichenbaum et al., 1999)

While such fundamental aspects of spatial memory currently remain a matter of active investigation, it is uncontroversial that the hippocampus is a key brain region in this process, with one argument being that place cells appear to be exclusively found among the population of hippocampal pyramidal neurons.

1.2.2 Structure and function of the hippocampal formation

The bilateral hippocampal formation is part of the limbic system, a set of evolutionarily primordial mammalian brain structures, and is physically located in the medial temporal lobes nestled between the brainstem and the neocortex (Fig. 10).

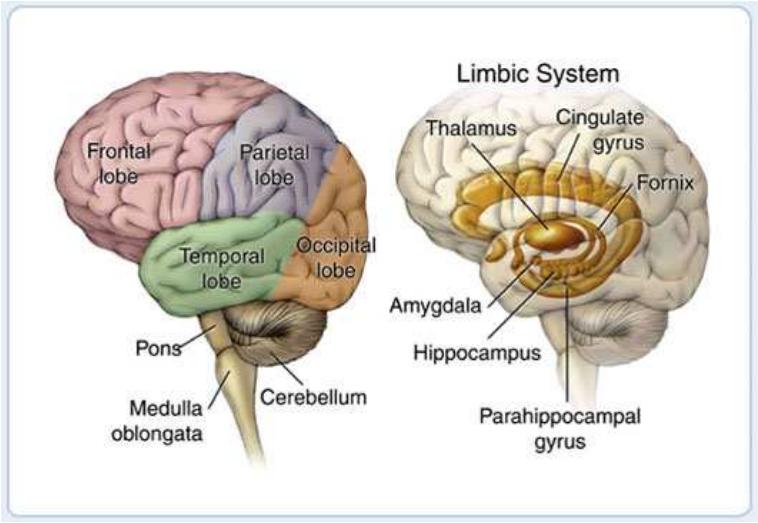

Figure 10. Anatomy of the brain. (***Left panel***) The cerebral cortex consists of four major lobes. Cerebellum and brain stem structures are shown as well. (***Right panel***) The limbic system comprises several brain structures including the hippocampus and is located between the brain stem and the cerebral cortex. (The medical illustrations are provided courtesy of Alzheimer's Disease Research, a program of the American Health Assistance Foundation. © 2011 http://www.ahaf.org/alzheimers)

Its functional roles include the integration of sensory information to generate a singular and coherent perception of the environment and the temporal sequence of events (Sweatt, 2004), thus acting as a real-time integrator of information. Closely linked to this function, the hippocampus also plays a key role in the retrieval of previously formed memories, in the updating of these memories by integration of novel information, and in the subsequent re-consolidation or initial consolidation of adjusted and novel memory traces, respectively. Hence, the hippocampus determines and initiates the formation of stable long-term memories from instable memory traces, and can thus be regarded as the mammalian brain structure most prominently and directly involved in the storage and maintenance of complex memory (Kandel, 2001).

At the structural level, the hippocampal formation presents as a highly organized array of neuronal cells which constitute two main substructures, i.e. the cornu ammonis (CA) or hippocampus proper consisting of densely packed pyramidal cell bodies and the dentate gyrus (DG) consisting of densely packed small granule cell bodies. Moreover, the hippocampal formation comprises the entorhinal cortex (EC) and the subicular complex which connects the CA1 subfield of the hippocampus proper with the EC. The extraordinary degree of organization within the hippocampal formation is not restricted, however, to the localization of cell bodies, but extends to the network level where specific axonal projections exist between individual subregions. Particularly, the hippocampal formation contains a characteristic information relay and processing circuit encompassing a tri-synaptic pathway that grossly defines the overall signal flow path through the hippocampus. As shown in Figure 11, the bulk of incoming signal is transmitted from layers II and III of the EC to the DG via axonal projections of the perforant path (PP), although minor branches of the PP also feed into all four CA subfields (CA1-CA4), and a distinct projection, the temporoammonic pathway, leads directly from the EC to CA1 (Deng et al., 2010). Information transmitted from the EC has been pre-processed in cortical areas and includes both sensory information of various modalities and information about ongoing cognitive processes. In the DG, information is relayed to CA3 neurons via non-myelinated axons termed mossy fibers that traverse the hilar region. The CA3 target neurons then form the third synapse in this tri-synaptic pathway on CA1 pyramidal neurons to which they project the efferent Schaffer collateral bundle of axons. The flow of

information is subsequently closed to form a circuit via projections from CA1 pyramidal neurons back to the EC, partially via the subicular complex which, in addition, also receives direct input from the EC that has not passed through the tri-synaptic pathway. Additional CA1 projections also feed fully processed information into the lateral septum, amygdala, and cortical regions, thus providing integrated output signals to other brain areas (Sweatt, 2004).

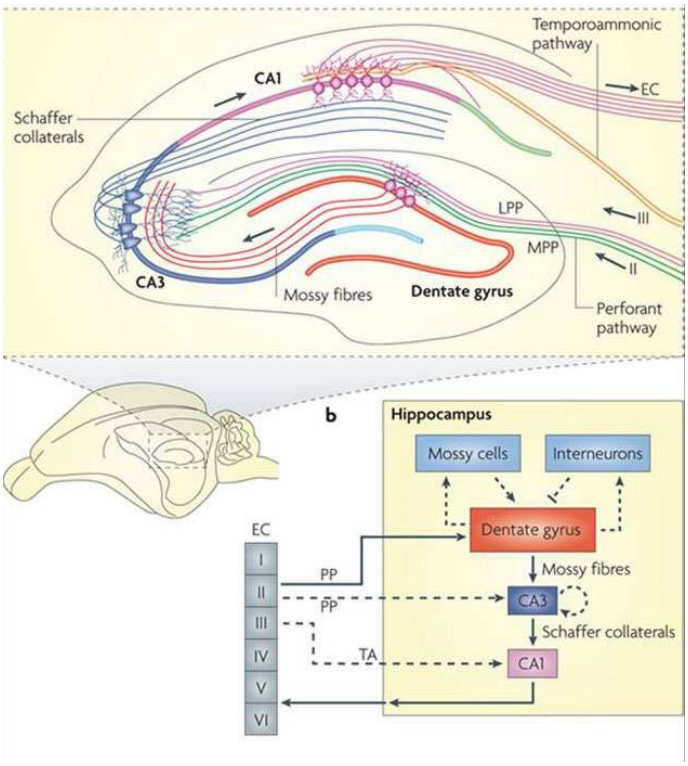

Figure 11. Hippocampal circuitry. (***Upper panel***) Gray arrows denote the classical tri-synaptic hippocampal pathway through the DG-CA3-CA1 subfields. The bulk of signal enters the hippocampus via axonal projections of the perforant pathway connecting EC layer II with the DG which relays processed signal via mossy fibres to CA3 pyramidal cells. These, in turn, project to CA1 neurons via the Schaffer collateral bundle of axons. Processed signal is subsequently returned to the EC, albeit to deeper layers. In parallel to this circuit, the PP, which splits into lateral (LPP) and medial (MPP) portions, also feeds directly into the CA3 subfield, and CA1 receives direct input from EC layer III via the temporoammonic pathway. (***Lower panel***) Simplified model illustrating flow of information within the hippocampal formation. From (Deng et al., 2010)

Early evidence for a specific and important role of the hippocampus in memory formation came from a seminal study by Scoville and Milner who observed severe memory deficits in patients after bilateral mesio-temporal lobectomy that included the anterior two thirds of the hippocampus to alleviate severe and recurrent epileptic seizures resistant to anticonvulsant therapy (Scoville and Milner, 1957). The most famous of these, patient HM, exhibited severe and permanent global anterograde amnesia following surgery that virtually abolished HM's ability to acquire novel episodic memories in the 55 years between surgery and his death in 2008 (Milner et al., 1968; Corkin, 1984; for review see Corkin, 2002). Retrograde amnesia extending to a limited period of time prior to surgery was also apparent in HM. These observations indicated that the ablated aspects of the medial temporal lobes (MTLs) including the hippocampus were highly relevant for the formation of novel memories, and that ablation probably prevented proper consolidation of novel memory traces. However, the partial MTL ablation did not appear to interfere with memories that were already firmly consolidated at the time of surgery since childhood memories were spared. In line with a specific memory consolidation problem, short-term memory was unimpaired in HM (Sullivan and Sagar, 1991; Corkin, 2002).

The paramount role the hippocampus plays in memory formation has later been confirmed in non-human primates and rodents where hippocampal lesions of varying extent were shown to impair spatial learning and memory, particularly when dorsal aspects of the hippocampus were lesioned (Zola-Morgan and Squire, 1990; Moser et al., 1993; Moser et al., 1995). Since this body of evidence strongly indicates the hippocampus to be primarily, maybe uniquely, involved in several aspects of memory, experimental manipulations of the hippocampus in animal models render mnemonic functions amenable to analysis by behavioural assessment in hippocampus-dependent tasks under laboratory conditions.

1.2.3 Molecular determinants of hippocampus-dependent spatial memory

Today, through application of pharmacological and genetic engineering techniques, the investigation of hippocampus-dependent learning and memory has reached the molecular level. These efforts spawned a long and growing list of gene products that act as mediators of long-term memory formation both in mice and men, and a compilation of these genes is publicly accessible via a curated database hosted by the *Genes to Cognition* programme (G2C) centered at the Wellcome Trust Sanger Institute, Cambridge, UK (Croning et al., 2009). Of note, however, the G2C compilation focuses on synaptically expressed proteins and may thus be intrinsically non-comprehensive, although synaptical processes are undoubtedly essential for the structural and functional plasticity events underlying memory formation. While cognitive deficits are frequently observed as a consequence of dysfunctional learning and memory-related gene products, the opposite, cognitive enhancement following increased gene product activity, is found less commonly. This particularly interesting subgroup of genes has been surveyed in a recent review which listed the few dozens for which transgenic mouse models with enhanced cognitive abilities have been reported (Lee and Silva, 2009).

In general, the bulk of learning and memory-related gene products appear to be mediators of synaptic plasticity, an activity-dependent process that affects both the strength and efficiency of cell-cell communication by inducing structural remodelling of the synaptic connection between neurons. However, transcription factors regulating the abundance of such effector proteins are clearly important players in the context of memory formation as well. To exemplify this, three prominent members of fundamentally different protein families shall be briefly discussed here for illustration, i.e. the *N*-methyl-*D*-aspartate (NMDA) type glutamate receptor as a membrane receptor / ion channel, the cAMP response element binding protein (CREB) as a transcriptional regulator of long-term memory-related gene expression, and the brain-derived neurotrophic factor (BDNF) as a member of the nerve growth factor family of proteins.

The NMDA subtype of ionotropic glutamate receptors in the postsynaptic membrane plays a central role in the neurobiological mechanisms mediating certain types of long-term memory formation (reviewed in Riedel et al., 2003). These ion channels, which facilitate charge transfer by Na^+, K^+, and Ca^{2+} conductance, are unique in their combined ligand and voltage-dependent gating mechanism that requires binding of glutamate neurotransmitter and concomitant membrane depolarization to remove a Mg^{2+} block from the channel pore, thus rendering the receptor a coincidence detector for pre- and postsynaptic activity (Seeburg et al., 1995). As such, the NMDA receptor appears as a formidable molecular correlate for Hebb's postulate that learning relies on the enhancement of synaptic efficacy between simultaneously activated neurons. This heterotetrameric receptor is composed of two obligatory NMDA receptor 1 (NR1) subunits and two of six known regulatory subunits comprising four NR2-type (NR2A-NR2D), and two NR3-type (NR3A, NR3B) isoforms (Seeburg, 1993; Ciabarra et al., 1995; Yashiro and Philpot, 2008). Every specific subunit combination endows the holoreceptor with unique overall functional properties by influencing its channel kinetics and ion conductance characteristics, and hence the receptor's ability to mediate synaptic plasticity.

Particular attention has been paid to the two predominant regulatory NMDAR subunits NR2A and NR2B which are widely expressed throughout the mammalian brain. Here, an interesting differential developmental regulation pattern has been found which involves a general shift from low to high ratios of synaptic NR2A versus NR2B expression as the animal progresses from perinatal to juvenile and adult stages of ontogeny (Monyer et al., 1994; Gambrill and Barria, 2011). Hence, while NR2B dominates the early phases of postnatal development NR2A becomes more important during later stages. The study by Monyer and co-workers also established longer excitatory postsynaptic potentials (EPSPs) in recombinant NR1/NR2B compared to NR1/NR2A di-heteromers (Monyer et al., 1994). In agreement with this, overexpression of NR2B in the murine forebrain of the transgenic *Doogie* mouse line was found to prolong NMDA receptor channel opening, and hence the time window for charge transfer and coincidence detection (Tang et al., 1999). Strikingly, these mice displayed superior cognitive abilities when compared to age-matched adult wildtypes, thus implying the developmental shift from NR2B to NR2A expression as a possible

explanation for the decline of memory performance observed in adult mammals. A more recent study further indicated that the developmental shift in favour of NR2A likely led to increased formation of NR1/NR2A/NR2B tri-heteromers rather than to a higher preponderance of NR2A- over NR2B-containing di-heteromers (Rauner and Kohr, 2011).

While the body of evidence implicating NMDA receptor signalling as a key determinant of memory formation is much larger, it shall suffice to mention that the genetic knock-out of the murine NR2A subunit led to severe impairments of both spatial learning abilities and induction of long-term potentiation (Sakimura et al., 1995), and that both effects were confirmed by specific pharmacological blockade of NMDA receptors (Bannerman et al., 1995). Moreover, spatial memory consolidation was elegantly demonstrated to critically depend on the presence of the NR1 subunit in the hippocampal CA1 subfield. By genetic engineering, Shimizu and colleagues were able to reversibly switch NR1 expression on and off in the CA1 field during the memory consolidation phase (Shimizu et al., 2000). However, while deficiency for NR2B in the forebrain was associated with electrophysiological abnormalities and specific memory deficits in adult conditional knock-outs, hippocampus-specific NR2B ablations did not significantly affect long-term spatial memory formation (von Engelhardt et al., 2008). This latter finding might indicate that the hypothesis of hippocampal NMDA receptor-mediated facilitation of long-term memory formation may need some careful adjustment to fully accommodate all relevant experimental results.

At the molecular level, NMDA receptors are closely associated at their intracellular side with a multiprotein complex called the postsynaptic density which provides a scaffold for downstream signalling molecules on the one hand, but also regulates NMDA receptor stability, function, subunit shuttling and composition on the other (van Zundert et al., 2004). While the NMDA receptor-mediated inward and outward currents of Na^+ and K^+, respectively, predominantly affect the neuronal membrane potential, Ca^{2+} influx provides additional important functions by triggering intracellular signal transduction cascades which ultimately facilitate synaptic remodelling and nuclear adaptations in gene expression. One important transducer of NMDA receptor signalling is the Ca^{2+}/calmodulin (CaM)-dependent protein kinase II (CaMKII) which has been

shown to bind the C-terminal domain of the NR2B subunit (Bayer et al., 2001; Bayer et al., 2006). Interestingly, this domain has previously been shown to be important in all NR2 subunits, but only truncation of NR2B led to perinatal lethality (Sprengel et al., 1998).

The CaMKII pathway also links NMDA receptor signalling to activation of transcription factor CREB by CaMKII-mediated phosphorylation of CREB residue Ser133 (Sheng et al., 1991). CREB has received particular attention in memory research since it was found to act as a master regulatory switch for long-term memory formation across phyla including molluscs (Dash et al., 1990), insects (Yin et al., 1994; Perazzona et al., 2004), and mammals (Barco et al., 2002). Upon Ser133 phosphorylation-dependent activation in neurons, CREB induces expression of target genes required for long-term facilitation, a protein synthesis-dependent process involving stable enhancement of synaptic transmission (Casadio et al., 1999), by regulating expression of target genes through binding to regulatory DNA elements termed cAMP response elements (CREs). In line with this, CREB-hypomorphic mice were profoundly impaired in both contextual and cued fear conditioning, as well as in spatial long-term memory, but not short-term memory formation (Bourtchuladze et al., 1994). The fear memory deficits could be completely rescued in these animals, however, when CREB was provided in *trans* to neurons of the lateral amygdala (Han et al., 2007), thus highlighting the acute need for CREB in this context. Moreover, Han and colleagues further showed that participation of individual neurons in the process of consolidation of a fear memory trace depended on their respective CREB expression levels at the time of fear acquisition (Han et al., 2007). Fear memory consolidation impairments were also noted in a transgenic mouse line expressing a dominant-negative CREB mutant (S133A) in an inducible, tamoxifen-dependent manner (Kida et al., 2002). Furthermore, enhanced excitability of CA1 pyramidal neurons has been demonstrated in transgenic mice that ectopically express a constitutively active form of CREB (VP16-CREB) specifically in these cells (Lopez de Armentia et al., 2007).

As a transcription factor, CREB mediates its effects indirectly by regulating expression levels of target genes including other transcription factors like *c-fos* and *zif268* which mediate expression of genes involved in synaptic plasticity

(Sheng et al., 1990; Sakamoto et al., 1991), the alpha subunit of CREB-activating Ca^{2+}/calmodulin-dependent kinase II (Olson et al., 1995), and neurotrophins like BDNF which modulate synaptic activity (Tao et al., 1998).

Among the neurotrophic factors which also include nerve growth factor (NGF) and glial cell line-derived neurotrophic factor (GDNF), BDNF plays a particularly important role in learning and memory formation as evidenced by the substantial impacts on these systems associated with manipulations of BDNF function. For example, BDNF-deficient mice were shown to be severely impaired in synaptic transmission and induction of long-term potentiation (Korte et al., 1995), and both effects could be rescued when BDNF was subsequently provided in *trans* (Korte et al., 1996). Moreover, BDNF was shown to enhance synaptic responses to high-frequency stimulation in both the early postnatal and adult rat hippocampus, and to be indispensible for the induction of LTP (Figurov et al., 1996). At the behavioural level, severe spatial memory deficits were found in a conditional knock-out mouse line in which the BDNF gene was ablated specifically in the hippocampus of adult animals (Heldt et al., 2007), and it was shown that BDNF signalling is required within 12 hours after acquisition of a learning task to facilitate long-term memory formation (Bekinschtein et al., 2007). Moreover, hippocampus-dependent contextual learning was shown to cause a rapid increase in BDNF transcript levels in the rat hippocampus (Hall et al., 2000), and antibody-mediated scavenging of BDNF molecules in the adult rat brain led to impaired spatial learning and memory (Mu et al., 1999).

This neurotrophin exerts its functions by binding to the transmembrane tyrosine receptor kinase B (TrkB), to which at least three important intracellular signalling cascades are coupled, i.e. the Ras-MAPK pathway, the PI3K-Akt pathway, and the phospholipase $C\gamma$-Ca^{2+} pathway, all of which may contribute to memory formation to some extent (reviewed in Minichiello, 2009). Remarkably, binding of BDNF to TrkB leads to rapid depolarization of target cells by Na^{+}-influx on a timescale comparable to glutamate receptor activation (Kafitz et al., 1999), thus BDNF function clearly encompasses more than mere synapse-to-nucleus signal transduction.

1.3 Adeno-associated Virus

1.3.1 Basic virology of adeno-associated virus

Adeno-associated virus (AAV) was originally discovered more than 40 years ago as a contamination in adenovirus preparations from cultured rhesus monkey kidney cells (Atchison et al., 1965) and was also isolated from human tissue shortly after (Blacklow et al., 1967). It was noted very early that these parvoviruses were inherently replication-deficient and required superinfection with either adenovirus or herpes simplex virus to provide essential helper functions for propagation (Hoggan et al., 1966; Conway et al., 1997). Due to this characteristic and previously unknown feature, AAV was classified as a unique genus termed dependovirus within the Parvoviridae family. In the absence of superinfection with a helper virus, wildtype AAV is able to establish latency which, in the human genome, occurs specifically by integration at a site termed AAVS1 physically located on chromosome 19 at 19q13.4 (Kotin et al., 1990). A murine AAVS1 homologue was more recently discovered on chromosome 7 in a region syntenic with human chromosome 19 (Dutheil et al., 2004). However, no apparent pathogenicity is associated with AAV infection since AAV was never related to any disease symptoms despite high infection rates as indicated by a prevalence of antibodies against AAV in approximately 80 % of the human population (Erles et al., 1999). The immune response to AAV infection appears to involve only negligible amounts of cytotoxicity and seems more limited to the production of neutralizing antibodies (Hernandez et al., 1999).

With no more than 25 nm in diameter, AAV is a very small, non-enveloped virus that packages a linear single-stranded DNA (ssDNA) genome of approximately 4.7 kb. Individual virions are packed with a ssDNA of either (+) or (-) polarity such that double-stranded DNA (dsDNA) can form after host cell infection by annealing of complementary DNA strands from different virions (Crawford et al., 1969; Rose et al., 1969). However, the majority of dsDNA after infection is generated by replication which, given the existence of (+) and (-) oriented ssDNA, requires initiation at both ends of the genome. The underlying mechanism for this was found to include inverted terminal repeats (ITRs) of 145 nucleotides which

facilitate hairpin loop formation via palindromic sequences, and hence self-priming at either end of the duplex (Koczot et al., 1973; Hauswirth and Berns, 1977).

The AAV genome contains two open reading frames (ORFs) designated rep and cap which code for non-structural and structural proteins, respectively. Gene product diversity is achieved at both ORFs via alternative splicing of messenger RNAs (mRNAs) and the use of alternative promoters (Fig. 12). Hence, the rep ORF generates four different Rep proteins (designated Rep78, Rep68, Rep52, and Rep40) implicated in replication, genome packaging, and establishing latency, while the cap ORF facilitates expression of capsid proteins VP1, VP2, and VP3 which autonomously assemble into icosahedral virions (Daya and Berns, 2008). In the absence of a polymerase coding sequence, AAV is entirely dependent on host cell mechanisms for replication.

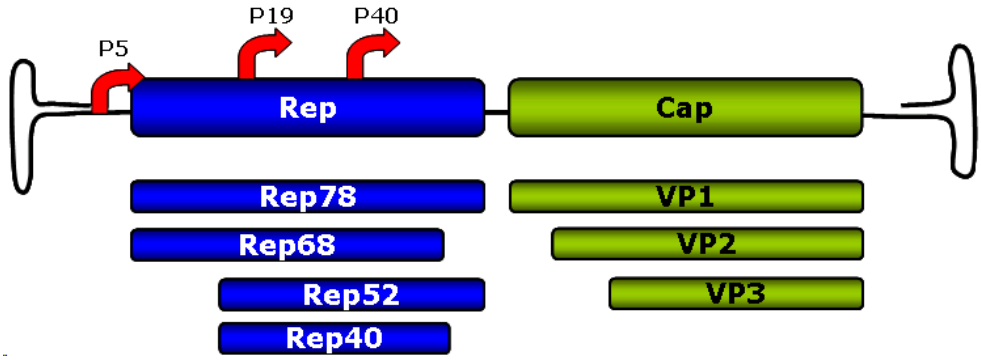

Figure 12. AAV genome structure. The wildtype AAV genome contains two ORFs, rep and cap, which generate non-structural and structural proteins, respectively. This is facilitated by the use of both alternative promoters (P5, P19, P40) and alternative splicing.

As of 2008, twelve different AAV serotypes (AAV1 - AAV12) were described and demonstrated to infect human cells and tissues (Daya and Berns, 2008), and efforts to characterize each of them in terms of tissue tropism and transduction efficiency *in vivo* are ongoing. The present literature indicates differential general susceptibilities to AAV infection between organs, and maximal transduction efficiency for each type of tissue seems to depend on the viral serotype. For

example, hepatic tissue seems to be readily transduced by a variety of AAV serotypes, most efficiently by AAV8 and AAV9, while renal tissue appears relatively inert to AAV infection although AAV was originally discovered in kidney cells (reviewed in Schultz and Chamberlain, 2008).

Of these serotypes, AAV2 is by far the best-studied. Extracellular docking of AAV2 to host cells is primarily facilitated by binding to heparan sulphate proteoglycans (Summerford and Samulski, 1998), while $\alpha_v\beta_5$ integrin and receptors for fibroblast growth factor, among others, act as co-receptors that help facilitate clathrin-dependent endocytosis of AAV2 virions (Summerford et al., 1999; Qing et al., 1999; Duan et al., 1999). The use of ubiquitous heparan sulphate proteoglycans as primary receptors explains the broad tropism of AAV2 which can infect a wide variety of cell types including quiescent, non-dividing cells. A schematic representation illustrating the initial steps of AAV transduction is depicted in Figure 13 which highlights that the route to the nucleus includes endosomal escape of intact viral particles. However, details of nuclear translocation thereafter remain to be determined (Daya and Berns, 2008).

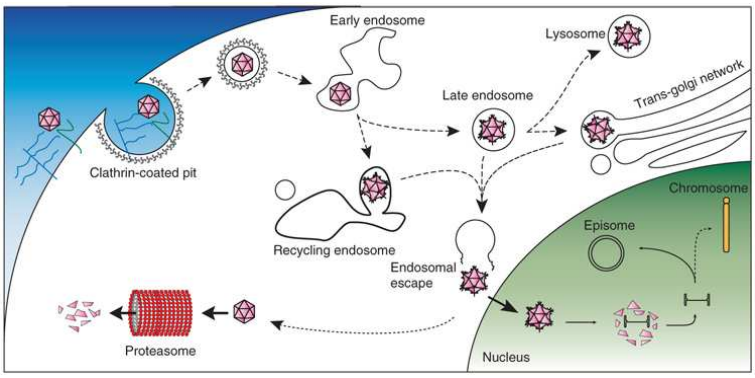

Figure 13. Intracellular trafficking of AAV. After extracellular docking to the plasma membrane, AAV is internalised by clathrin-dependent endocytosis. Nuclear translocation occurs on alternative routes, the most prominent involving endosomal escape following induction of capsid-associated phospholipase activity during endosomal processing. Uncoating of virions and concomitant viral genome release takes place in the nucleus. Viral genomes may remain as stable concatemeric episomes or integrate into the host genome (detailed in the main text). Proteasomal degradation counteracts successful AAV transduction. From (Schultz and Chamberlain, 2008)

1.3.2 Adeno-associated virus as a somatic gene transfer vector

The general interest to employ viruses as gene therapy vectors is based on the inherent possibility to provide therapeutic cargo in a temporally controlled and tissue-specific manner. Moreover, successful viral transgene delivery to a diseased organ would ideally lead to stable long-term expression of the therapeutic gene product, and hence cure the existing problem without a need for recurrent therapeutic intervention. Obviously, monogenetic diseases with hypomorphic or defective gene expression appear particularly interesting targets for such gene therapy approaches, and clinical examples include hemophilia, Canavan disease, cystic fibrosis, and muscular dystrophies.

Many aspects of basic AAV virology detailed in the previous section render this virus an especially promising candidate for gene therapy purposes, and consequently great interest to exploit AAV arose in the field (e.g. Carter, 2004; Daya and Berns, 2008). These promising aspects include AAV's excellent safety profile related to its inherent non-pathogenicity and replication deficiency, as well as its property to elicit only weak immune responses which sets it apart from other viral vector systems like adenoviruses. AAV's ability to transduce a wide variety of cell types moreover allows its application in a broad range of tissues including those harbouring post-mitotic cells which are notoriously difficult to transduce by other methods. At the same time, the option to choose between several serotypes with different transduction spectra allows for the specific tailoring of an AAV gene transfer vector with respect to the target tissue in question. This latter option has received even further refinement in recent years by the finding that AAV tropism and transduction efficiency can be manipulated by at least two different methods, i.e. transcapsidation and the generation of chimeric vectors. Transcapsidation designates the process of packaging rAAV genomes flanked by ITRs of a given serotype into virion shells built from capsid proteins from another serotype (Rabinowitz et al., 2002). This approach helps altering AAV transduction profiles as both the ITRs and the capsid composition contribute critically to overall transduction efficiency (Choi et al., 2005). Chimeric vectors, on the other hand, are virions with capsid protein compositions derived from different serotypes. This approach is likewise able to alter both tissue tropism and

transduction efficiency compared to parental serotypes (Hauck et al., 2003). However, limitations exist with regard to the compatibility of capsid proteins of different serotypes to form functional virions (Rabinowitz et al., 2004). Amongst this background of major advantages, the only downside of AAV as a gene therapy vector is its limited packaging capacity which is restricted to the size of the wildtype AAV genome, thus precluding efficient delivery of therapeutic DNA exceeding 4.7 kb in length (Dong et al., 1996).

In contrast to retroviral transduction systems which integrate somewhat randomly into the host genome, and thus exhibit significant mutagenic potential, the propensity of wildtype AAV to integrate at a specific location (AAVS1) into the host genome attracted further attention. As chromosomal integration at AAVS1 does not occur with absolute reliability, however, it is thus regarded as a double-edged sword in the clinical setting (Dutheil et al., 2004). Nevertheless, this problem is virtually abolished in recombinant AAV (rAAV) vectors which retain only some 300 bp of non-transcribed ITR sequences from the wildtype AAV genome that are the only *cis*-acting signals required for genome replication and packaging. In addition, replacement of wildtype genomic sequences further reduces the probability of an immune response as no viral genes are expressed by infected cells. In the absence of wildtype AAV gene products, particularly Rep proteins, integration can not occur, and the AAV genomes remain in an episomal form, more precisely as head-to-tail, and less frequently as head-to-head or tail-to-tail concatemers (Nakai et al., 2000; Schultz and Chamberlain, 2008). Importantly, these episomal vector genomes are stable and contribute to long-term transgene expression (Nakai et al., 2001).

In central nervous system (CNS) research, AAV has proven a particularly valuable tool due to its dual properties to exclusively infect post-mitotic neurons with little if any transduction of glial or other cell types, and to facilitate stable, long-term ($\geq$ 2 years) neuronal transgene expression in both rodents and monkey (Davidson et al., 2000; Gao et al., 2002). The first evidence for an AAV-mediated functional improvement of disease conditions came from a study in which the authors ectopically expressed tyrosine hydroxylase in striatal neurons in a rat model of Parkinson's disease (Kaplitt et al., 1994). Thereafter, successful improvement of disease symptoms was reported in a large number of studies

using AAV-mediated *in vivo* somatic gene transfer to CNS neurons in animal models of various diseases including but not restricted to Parkinson's, Canavan, Alzheimer's, and Huntington's disease, epilepsy, and amyotrophic lateral sclerosis (reviewed in McCown, 2011; Henriques et al., 2011).

1.4 Aim of this Work

Granulocyte/macrophage colony stimulating factor (GM-CSF) has been originally identified as a hematopoietic growth factor but has recently been assigned important neurotrophic functions in the central nervous system under various disease conditions. In addition, pro-neurogenic effects on adult neural stem cells were established *in vitro*. These findings place GM-CSF along with the other two major hematopoietic proteins granulocyte colony stimulating factor (G-CSF) and erythropoietin (EPO) in a novel group of neuronally active growth factors. Because of the abundant expression of the GM-CSF receptor on neurons in regions associated with learning and memory such as the cortex and hippocampus, we asked whether GM-CSF signalling might be involved in aspects of cognitive processing. To address this question, we systematically tested learning and memory formation in GM-CSF deficient (GMko) mice by employing a battery of behavioural paradigms that assessed both cognitive and sensomotoric aspects of rodent behaviour. In a complementary approach, we altered expression levels of the ligand-specific GM-CSFRα subunit exclusively in the hippocampus of adult wildtype mice using adeno-associated virus vectors for GM-CSFRα overexpression and knock-down, respectively, and examined spatial memory formation in these animals in the Morris water maze. The induction of long-term potentiation in the CA1 hippocampal subfield of GMko mice was examined by electrophysiological recordings. Moreover, morphological studies on dentate gyrus and CA1 neurons were performed to determine the impact of GM-CSF deficiency on neuronal complexity, dendritic spine number, and spine maturation. In an independent effort, the generation of a conditional knock-out mouse line for the GM-CSF receptor alpha subunit was pursued to obtain a novel and valuable tool for future projects.

2 RESULTS

This study was focused on the elucidation of a putative role for GM-CSF in learning and memory. For this purpose, among other things, an extensive behavioural test battery was applied to GM-CSF-deficient (GMko) mice which included a variety of specific learning and memory tasks. These tests were preceded by an assessment of more basal aspects of behaviour to complement data from subsequent cognitive tests and allow for their proper interpretation.

2.1 Effects of GM-CSF deficiency on basal behaviour

2.1.1 Locomotor behaviour in the open field

The open field test primarily assesses spontaneous locomotor activity in a novel, slightly aversive environment which consisted in our case of a white cubicle box without a lid. In this exposed arena, animal behaviour is influenced by both anxiety and exploratory drive, and these parameters contribute to the amount of time spent in the corner or center areas of the arena and to the overall distance travelled within the testing period. To facilitate quantification, the open field was subdivided into 26 subregions (Fig. 14a), and mice were video-tracked while freely exploring the arena individually for 30 min. GMko mice showed reduced levels of locomotor activity throughout the 30 min testing period (Fig. 14b,c). This effect was not caused by elevated levels of anxiety as animals from both

groups spent similar amounts of time in the corner and center regions of the arena (Fig. 14d).

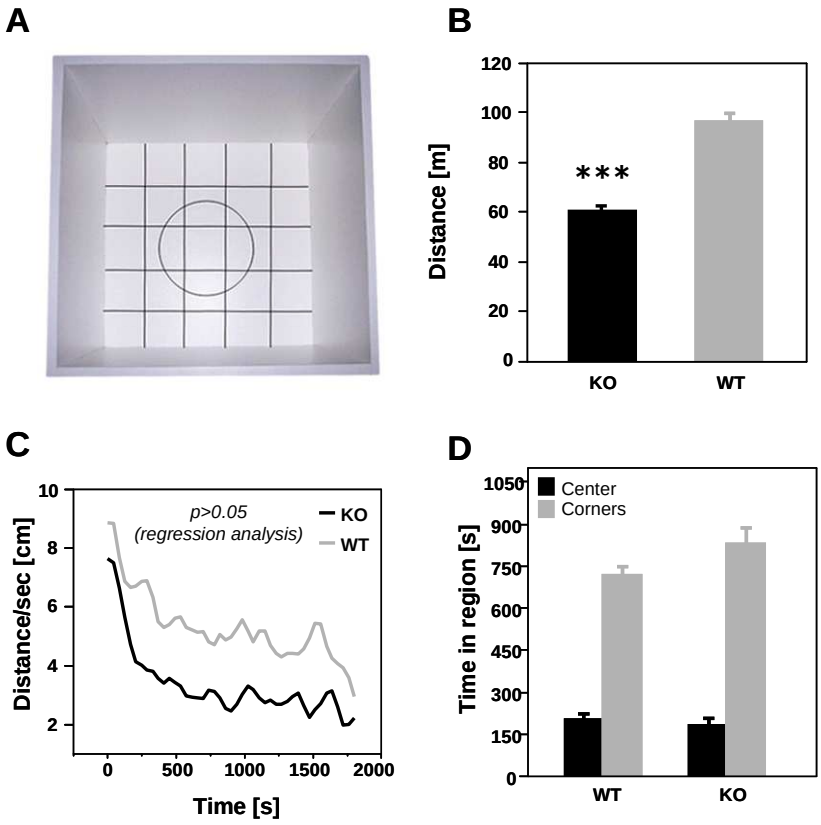

Figure 14. Open Field test. (***A***) The floor of the open field arena was subdivided *in silico* into 25 squares and a circular center region. (***B***) Spontaneous locomotor activity in the open field was reduced in GMko mice which travelled shorter overall distances over the course of a 30 min testing period ($p<0.001$). (***C***) Activity was consistently lower in GMko mice (genotype, $p<0.001$) and no initial anxiety-related immobility or altered habituation rate (genotype*time, $p>0.05$) was noted. (***D***) Times spent in the corner or center regions of the arena were similar between groups (both $p>0.05$). wt, n=18; ko, n=16 animals

2.1.2 Analysis of long-term activity

To confirm reduced spontaneous activity with a different assay, GMko and wildtype animals were next tested in a LABORAS cage, an automated device for the detection of rodent behaviour based on the analysis of force and vibration

patterns. Due to automated analysis, this paradigm facilitated long term observation of animals for 12 hours during their nocturnal activity phase, thus diminishing any potential experimenter related influences. Again, GMko mice travelled a shorter overall distance (Fig. 15a). They also spent less time with horizontal locomotion and cage climbing, but spent more time in an immobile state (Fig. 15 b-d), thus confirming the reduced spontaneous locomotor activity observed in the open field.

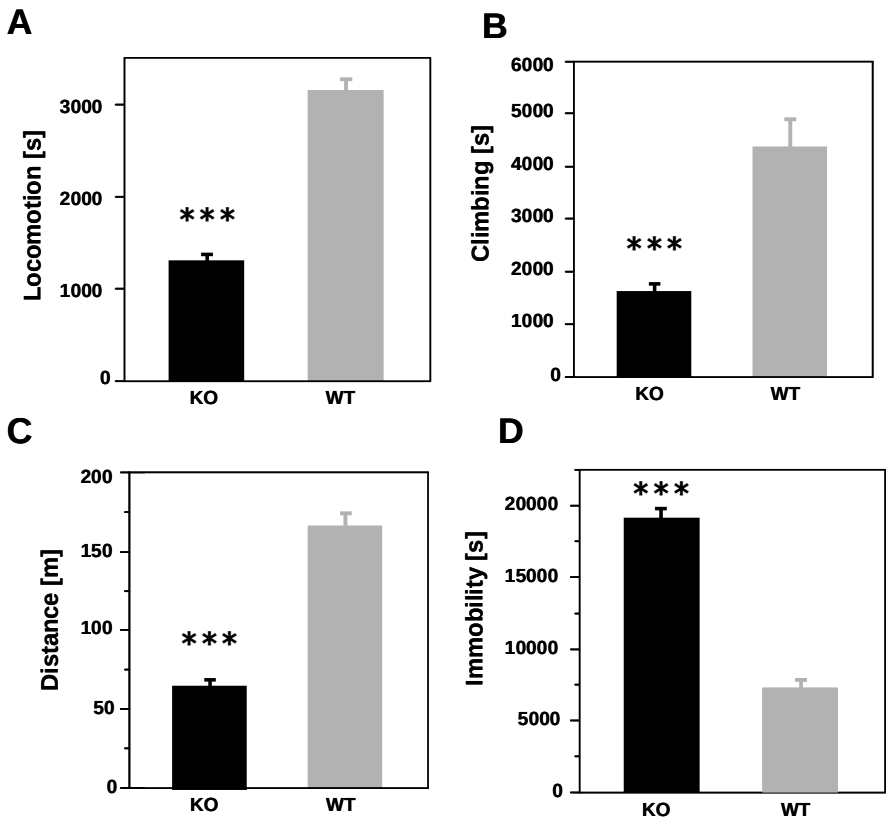

Figure 15. Spontaneous activity in a LABORAS cage. Spontaneous activity was reduced in GMko mice over a 12 hour nocturnal period in which GMko mice spent less time with locomotion (***A***) and cage climbing (***B***), covered a shorter overall distance (***C***), and spent more time in an immobile state (D). (***, $p<0.001$); wt, n=18; ko, n=16 animals

2.1.3 Assessment of motor function

To determine whether physical impairments of the motor system contributed to the reduced spontaneous locomotor activity of GMko mice, we next tested motor function under conditions of forced exercise on a rotating beam. To this end, mice were examined on a rotarod under a challenging acceleration protocol. Interestingly, this experiment indicated a positive rather than a negative influence of GM-CSF deficiency on both motor endurance and coordination as total fall-off latencies were increased in GMko mice, an effect that was due to superior performance during the first 5 days of testing (Fig. 16).

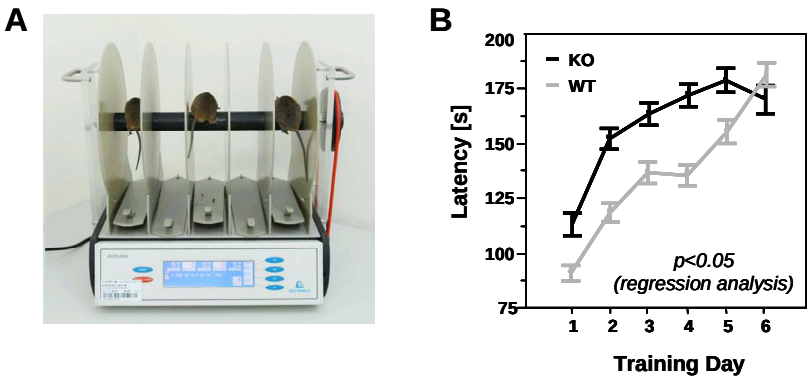

Figure 16. Motor performance on a Rotarod. (***A***) Animals were tested on a rotarod under a challenging acceleration protocol of 4-80 rpm over 300 seconds. (***B***) GMko mice did not show any impairments of the motor system. Instead, motor performance was superior in the early stages of training (genotype, $p<0.05$). wt, n=18; ko, n=16 animals

2.1.4 Analysis of anxiety-related behaviour and exploration

To fully exclude heightened anxiety levels as a reason for diminished locomotor activity, we employed the dark-light box paradigm, which offers a choice between occupation of a dark and protective environment on the one hand, and a brightly illuminated and exposed environment on the other (Fig. 17a). It thus utilizes the conflict situation arising from the tendency to explore novel environments and an

opposing innate avoidance of exposed areas, the latter increasing with elevated levels of inherent anxiety.

This analysis confirmed anxiety levels to be comparable between GMko and wildtype mice which spent similar times in the exposed lit compartment (Fig. 17b). Diminished rearing behaviour in the lit compartment of the dark-light box was noted as well, indicating reduced levels of exploratory activity (Fig. 17c).

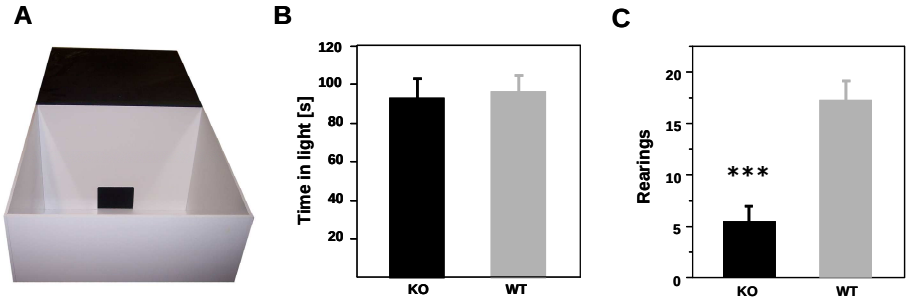

Figure 17. Dark-Light Box analysis. (***A***) The Dark-Light Box is split in two compartments, one protected from light, the other exposed and aversively brightly illuminated. (***B***) Both groups of animals spent similar amounts of time in the lit compartment ($p>0.05$). (***C***) Rearing behaviour, an index of exploratory activity, was greatly diminished in GMko animals ($p<0.001$). wt, n=18; ko, n=16 animals

2.1.5 Summary of basal aspects of behaviour

A strong reduction in spontaneous locomotor activity was noted in two different paradigms, i.e. the open field and an automated LABORAS detection system. This effect was neither paralleled by altered habituation characteristics nor by altered levels of inherent anxiety as judged by open field and dark-light box analysis. Physical motor deficits were also ruled out with a rotarod where knock-outs performed better rather than inferior compared to wildtype controls. This renders reduced exploratory drive as a likely explanation for the observed spontaneous hypoactivity, a notion confirmed by the reduced rearing activity of GMko mice in the lit compartment of a dark-light box.

2.2 Effects of GM-CSF Deficiency on Cognition

2.2.1 Active place avoidance and pain threshold levels

To examine hippocampus-dependent spatial learning and memory, we initially tested animals in an active place avoidance paradigm that has been described previously (Serrano et al., 2008). Briefly, animals were placed on a circular, rotating metal disk and learned to avoid one non-rotating 60° sector, entry to which was punished by mild foot shocks (Fig. 18a). Acquisition occurred rapidly within 8 training trials on a single day and both groups learned to avoid the shock sector as evidenced by increasing latencies to initial entry (Fig. 18b). However, task acquisition was inferior and reached an early plateau in GMko mice. Exemplary trajectories from the first and last training trials are shown for individual animals from both groups, illustrating inferior performance of knock-outs (Fig. 18c). When memory retention was assessed 24 hours after the last training trial, the inferior acquisition of GMko mice corresponded to a worse recall performance of these animals (Fig. 18d). Importantly, these observations were not due to altered plantar pain threshold levels as assessed by the paw withdrawal response following application of thermal stimulation (Fig. 18e,f)

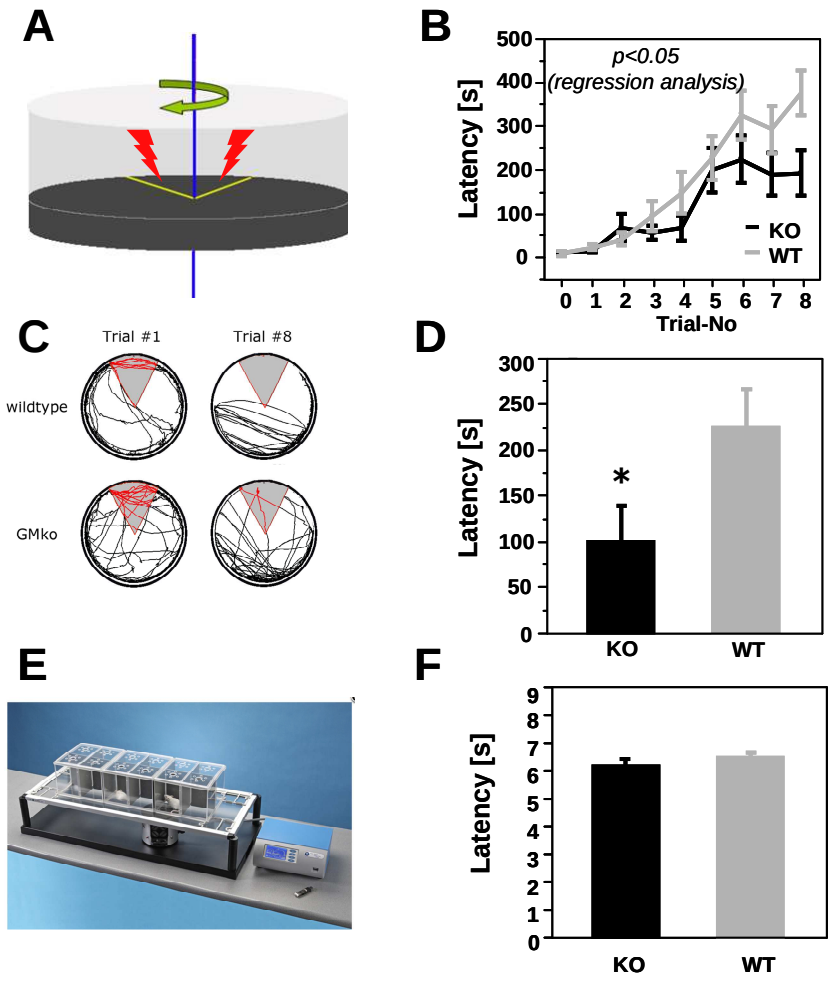

Figure 18. Spatial learning and memory by active place avoidance and plantar pain threshold levels. (***A***) Schematic illustration of rotating testing disk with pre-defined shock sector. (***B***) Spatial learning was impaired in GMko animals (genotype, $p<0.05$; genotype*trial, $p=0.010$). (***C***) Representative trajectories illustrating reduced spatial learning in knock-outs. (***D***) GM-CSF deficiency led to inferior performance levels when spatial memory was assessed 24 hours after training ($p<0.05$). (***E***) Picture of plantar test apparatus. Thermal stimulation to paws is administered with an infrared light emitter via the plastic floor. (Picture provided courtesy of Ugo Basile Srl) (***F***) Paw withdrawal latencies to thermal stimulation were identical between groups ($p>0.05$). wt, n=22; ko, n=21 animals

2.2.2 Morris water maze

In the Morris Water Maze (MWM) animals are required to learn the location of a hidden escape platform in a swimming pool by using extra-maze visual cues for

orientation. This task is widely considered the gold standard in rodent testing of hippocampus-dependent spatial learning and memory.

Gross visual and motivational deficits that might interfere with the animals' ability to mount the escape platform were ruled out in a visual platform version of the task. This analysis revealed no between-group differences of escape latency, path length, and velocity (Fig. 19).

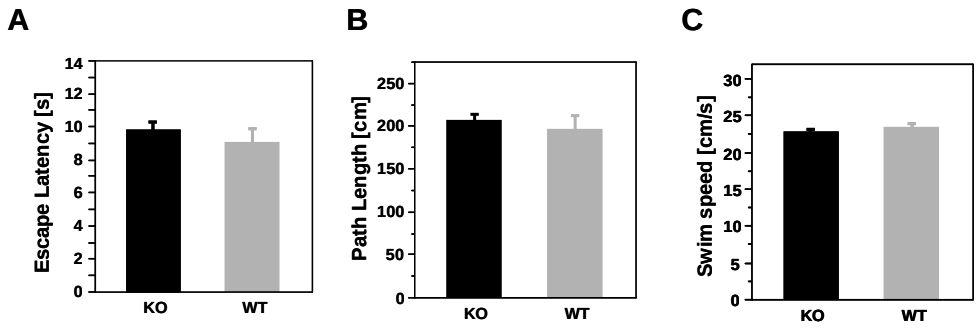

Figure 19. Visible platform version of the Morris water maze. Escape latency (***A***), total path length to platform (***B***), and average velocity (***C***) were all similar between groups (all p>0.05). wt, n=22; ko, n=21 animals

Over the course of 12 training days (D1-D12), both groups learned the location of the platform as monitored by decreasing escape latencies and path lengths (Fig. 20a,b). While a considerable offset difference was noted between groups in both acquisition curves, the slopes of these curves were similar, indicating some general performance deficit in GMko mice but no specific learning impairment. To better understand the underlying behavioural differences between groups, a frequency density map was generated by accumulative overlay of swim path trajectories. This analysis revealed that knock-outs were more likely to be found near pool entry sites during early training sessions and needed longer to develop a search pattern in closer vicinity to the platform (Fig. 20c). This suggested that increased stress susceptibility interfered with efficient development of goal-directed search strategies in knock-outs. In line with this, GMko mice displayed other erratic behaviours like high initial velocity (Fig. 20d) and frequent platform jump-offs (Fig. 20e) during early training. However, we did not observe

any floating behaviour. Due to the differential velocity profiles between groups, further analyses were based on escape path length as a swim speed-independent parameter.

The probe trial at D13 revealed a significant difference in the time spent in the target area defined as a circle (radius r = 20 cm) around the former platform center (Fig. 20f). Covariate analysis using genotype, path length at D12, and their interaction as factors revealed an influence of genotype on recall performance ($p<0.05$) that was independent of D12 path length. Therefore, GM-CSF deficiency resulted in impaired spatial memory recall 24 h after acquisition. Representative probe trial trajectories and cumulative density heat maps for both groups are shown as well (Fig. 20g,h).

To investigate potential differences in platform search strategies during the probe trial, we next analysed occupancy of the target area in bins of 10 seconds. Apart from an overall offset difference (genotype $p<0.01$), the slopes of the curves were significantly different ($p<0.05$), suggesting that strategies differed between groups. In contrast to controls, knock-outs failed to perform an initially focused search in the target area and did not reduce their visiting time markedly upon failure to find a platform (Fig. 20i). Importantly, however, the latter was not due to a ground effect as both groups occupied the target area well above chance levels throughout the 120 s probe trial.

As this indicated a diminished flexibility of GMko mice to adapting to task variations, we consequently explored reversal learning where pre-trained animals were subjected to a 5-day (RD1-RD5) protocol with the platform position changed from the NW to the SE quadrant. Indeed, reversal learning was clearly impaired in GMko mice ($p<0.05$) in this scenario (Fig. 20j). Collectively, these results show that GM-CSF deficiency causes profound spatial memory impairments and affects the animals' behavioural flexibility to respond to altered environmental conditions.

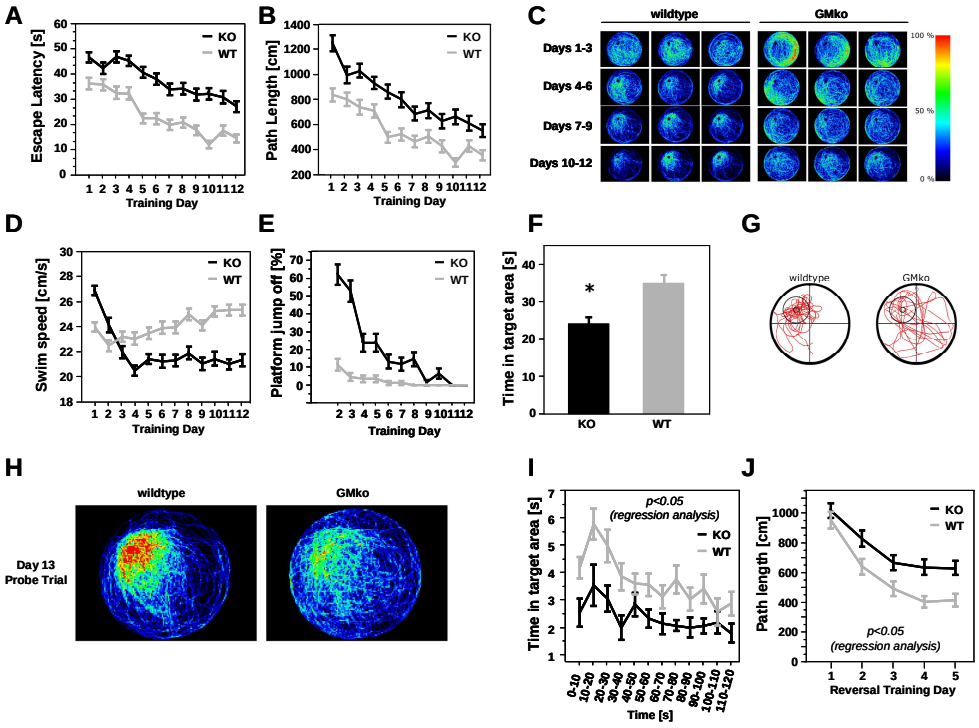

Figure 20. Effects of GM-CSF deficiency on spatial learning and memory in the Morris water maze. (***A***,***B***) Escape latencies and swim path lengths were increased in GMko mice at all times compared to controls with a main effect of genotype ($p<0.001$). However, learning progress was comparable between groups as reflected by similar relative decreases in escape latency and trajectory lengths, respectively (genotype*day, $p>0.05$). (***C***) Frequency density analysis of accumulated trajectories reveals thigmotactic behaviour of knock-outs during early training with an initial focus on pool entry sites. Platform-focused trajectories develop later and to a lesser extent compared to wildtypes. (***D***) Velocity profiles during training differed between groups (genotype, $p<0.01$, genotype*day, $p<0.001$). In contrast to controls, knock-outs displayed signs of an elevated stress response with initial hyper- and subsequent hypoactivity. (***E***) Knock-outs also displayed pronounced platform jump-off behaviour (genotype, $p<0.001$). This only subsided towards the end of the acquisition period. (***F***) Spatial memory was impaired in GMko mice which spent significantly less time in the target area during the probe trial ($p<0.05$). While performance at D12 clearly affected this parameter ($p<0.01$), genotype had an independent effect ($p<0.05$). (***G***) Representative probe trial trajectories illustrating reduced memory accuracy in GMko mice. (***H***) Frequency density maps illustrating inferior memory performance of GMko mice. (***I***) Occupancy of target area during the probe trial in bins of 10 seconds indicates differential platform search patterns between groups (genotype, $p=0.010$; genotype*time, $p<0.05$). Controls initially perform a focused search at the former platform location (FPL) before screening other regions, while, at an overall lower rate, knock-outs keep constantly visiting the FPL. (***J***) Reversal learning was impaired in GMko mice (both genotype and genotype*time, $p<0.05$). Note that path lengths were indistinguishable at RD1. wt, n=22; ko, n=21 animals

2.2.3 Fear conditioning

To determine whether other memory systems that are not involved in spatial navigation were also affected by GM-CSF deficiency, we tested GMko and wildtype mice in a fear conditioning experiment that assesses associative memory formation. Both groups showed substantial but indistinguishable freezing behaviour in response to repetitive cue-shock pairings during acquisition indicating similar associative learning abilities (Fig. 21a). Similarly, fear responses to context challenge 24 hours later were comparable between groups (Fig. 21a). However, when cue-related fear memory was assessed by challenge with the conditioning cue 48 hours after training, fear responses were strongly reduced in GMko mice (Fig. 21b). Temporal analysis of freezing behaviour at 1 s resolution confirmed that the overall difference was due to different levels of fear responses to cue presentations (Fig. 21c).

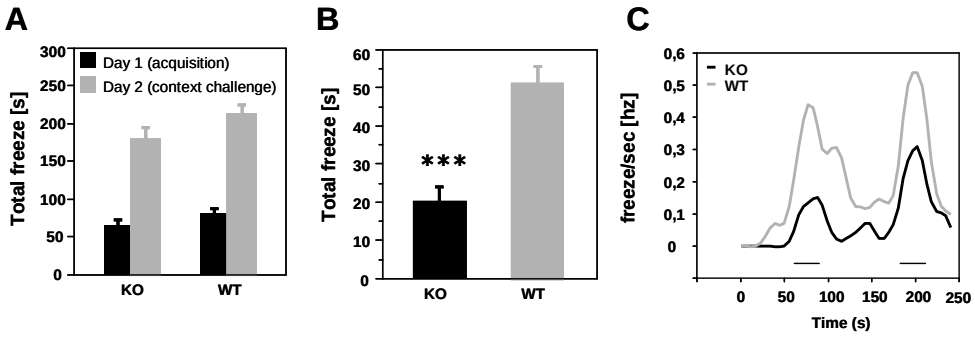

Figure 21. Effects of GM-CSF deficiency on fear memory formation. (***A***) Freezing responses were identical during both fear conditioning at day 1 and context challenge at day 2 (both $p>0.05$). (***B***) Freezing responses to conditioned stimulus 48 hours after training were reduced in GMko mice indicating fear memory impairments in these animals. (***C***) Temporal analysis of freezing behaviour at day 3 illustrates that differential fear responses between groups are due to different response levels to cue presentations. Bars indicate duration of cue presentation. (***, $p<0.001$); wt, n=22; ko, n=21 animals

2.2.4 Summary of cognitive aspects of behaviour

GM-CSF deficiency was clearly associated with performance deficits in all behavioural learning and memory paradigms conducted in this study. Specifically, GMko mice showed both spatial learning and spatial memory deficits in the active place avoidance (APA) and MWM paradigms, respectively, and reduced fear memory formation to cue-shock associations in a fear conditioning (FC) experiment. Importantly, altered pain threshold levels were ruled out as a cause for reduced performance levels in the APA and FC paradigms which relied on aversive foot shock stimulation via the animals' paws. Moreover, diminished behavioural flexibility to adapt to novel environmental configurations was noted in knock-outs in both the MWM memory recall trial and a subsequent re-learning protocol. Apart from that, these animals displayed a variety of erratic behaviours in the MWM, indicating GM-CSF deficiency to additionally cause enhanced stress susceptibility.

2.3 Effects of GM-CSF Deficiency on Hippocampal Morphology

Brains of GMko and wildtype mice were analyzed at both the structural, cellular and subcellular level to investigate whether the behavioural deficits associated with GM-CSF deficiency were paralleled by morphological defects in the hippocampus.

2.3.1 Neurite outgrowth

Primary hippocampal neurons from E18.5 rat embryos were grown in the absence or presence of 20 ng/ml GM-CSF to examine a potential any stimulatory effect of the neurotrophin on the neurite outgrowth of these cells. Indeed, after 48 hours in culture, total neurite length was significantly increased by approximately 13 % in the presence of GM-CSF (Fig. 22).

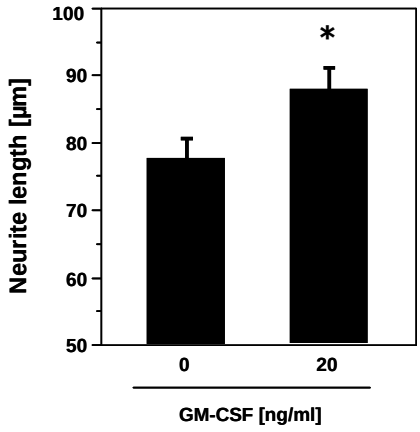

Figure 22. GM-CSF stimulated neurite outgrowth *in vitro*. Application of 20 ng/ml GM-CSF to cultures of primary rat hippocampal neurons increased total neurite length per cell by >13 % (*, $p<0.05$). n=100 cells per group

2.3.2 Gross hippocampal morphology

Based on this *in vitro* result, we next asked whether GM-CSF deficiency was associated with morphological deficits *in vivo*. Measures of hippocampal volume, maximal hippocampal width, and distance between dorsal tips of the CA1 and DG layers of nuclei revealed no between-group differences, thus ruling out gross structural deficits in hippocampal anatomy (Fig. 23a-c). Nevertheless, other measures of distances between characteristic points within various planes along the rostro-caudal axis indicated minor alterations of unclear relevance in GMko hippocampal anatomy including a slight compression of the DG with reduced gap width between upper and lower blades of the granule cell layers (Fig. 23d-f).

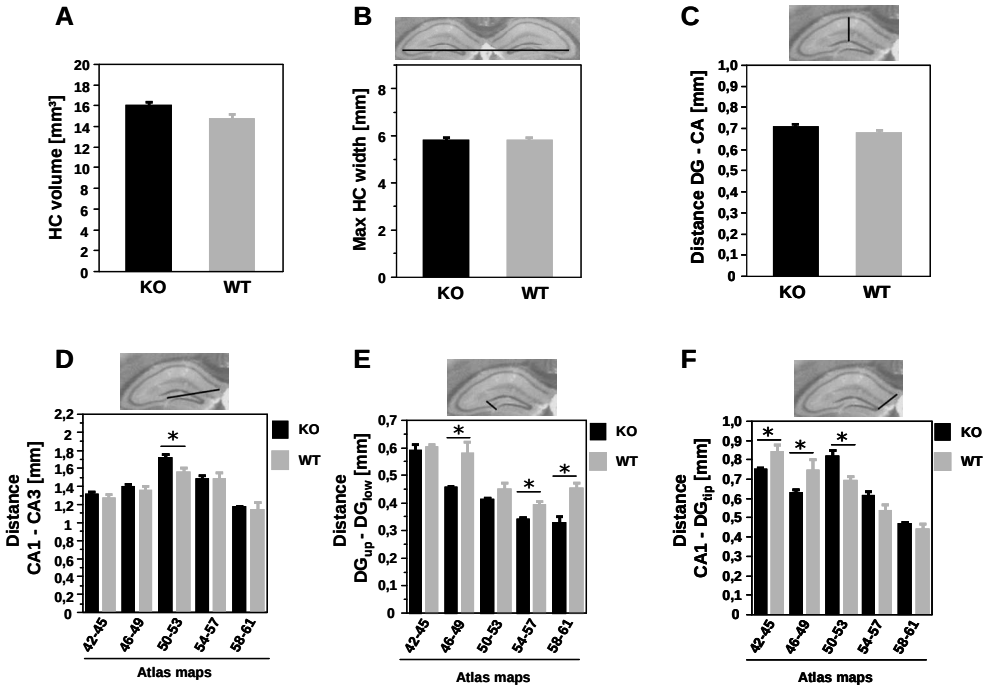

Figure 23. Effects of GMko on gross hippocampal morphology. (***A***) Hippocampal volume was similar between GMko and wildtype mice ($p>0.05$). (***B***) Maximal hippocampal width was similar between GMko groups ($p>0.05$). (***C***) Distance between dorsal tips of CA pyramidal cell and DG granule cell layers was similar ($p>0.05$). (***D***) Distance between CA1 and CA3 ends of CA pyramidal cell layer were increased in medial ($p<0.05$) but not in rostral, rostromedial, mediocaudal, and caudal sections of the hippocampus (all $p>0.05$). (***E***) Distance between open ends of upper and lower blade granule cell layers were decreased in rostromedial, mediocaudal, and caudal sections (all $p<0.05$). (***F***) Distance between junction of upper and lower blade granule cell layers and the CA1 end of CA pyramidal cell layer were reduced in rostral and rostromedial (both $p<0.05$) and increased in medial sections ($p<0.01$). Labelling of x-axis in (***D***)-(***F***) denotes map numbers in (Paxinos and Franklin, 2004). n=6 animals per group

2.3.3 Dendritic arborisation

To investigate the impact of GM-CSF deficiency on hippocampal morphology at the cellular level, we next performed full reconstruction of DG neurons from GMko and wildtype mice (n=17 and 19, respectively). To this end, hippocampal sections stained by the Golgi-Cox method were subjected to image acquisition by confocal microscopy, and individual neurons were subsequently reconstructed from image stacks using Neuromantic software (http://www.reading.ac.uk/neuromantic/). This analysis revealed a shortening by 33 % in total dendritic length and a decrease by 30% in the number of dendritic bifurcations in GMko brains (Fig. 24), thus indicating a reduction of dendritic complexity in DG granule cells by approximately one third.

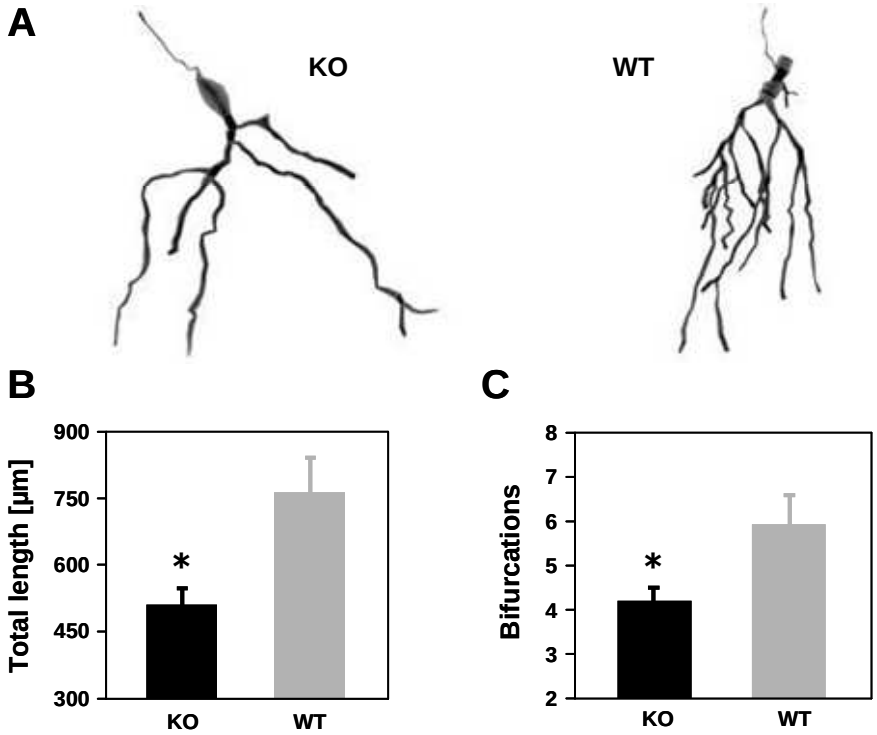

Figure 24. Effects of GM-CSF deficiency on dendritic morphology. (***A***) Representative reconstructions of GMko and wildtype DG granule cells showing reduced dendritic complexity of GMko neurons. (***B,C***) Quantification of total dendritic length and dendritic branch points of DG granule cells confirming rudimentary arborisation of GMko neurons. (*, $p<0.05$); wt, n=19; ko, n=17 cells

2.3.4 Dendritic spine density

We subsequently examined the density of dendritic spines in GMko and wildtype animals to address the question whether GM-CSF deficiency was also associated with morphological deficits at the subcellular level. This analysis was performed in two different hippocampal subregions, i.e. the DG and CA1 subfield. In GMko mice, we found dendritic spine density to be reduced in these areas by 15 % and 31 %, respectively (Fig. 25), thus demonstrating reduced dendritic complexity at the subcellular level.

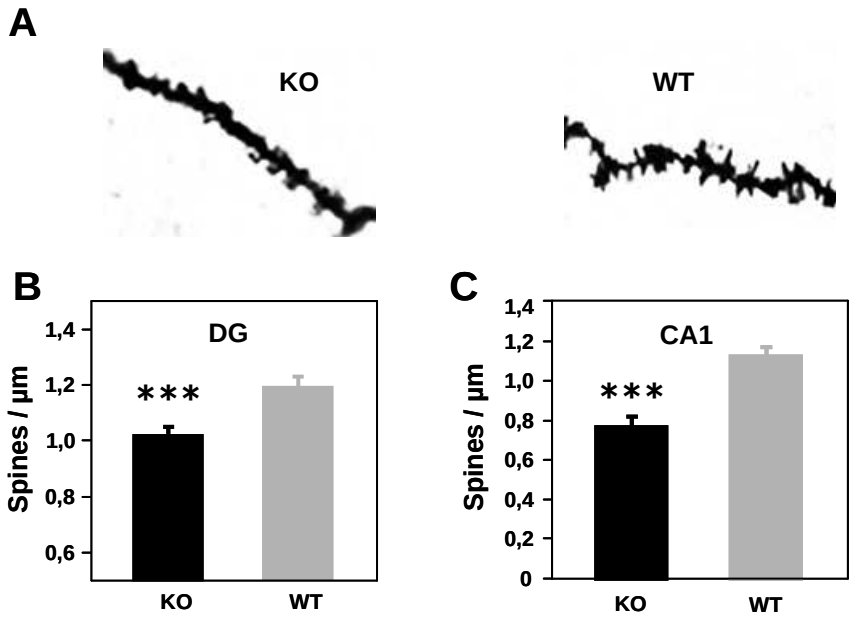

Figure 25. Effects of GM-CSF deficiency on dendritic spine numbers. (***A***) Representative examples of dendrites from GMko and wildtype DG granule cells illustrating reduced spine density in knock-outs. (***B,C***) Spine density quantification of DG granule cells (str. moleculare) and CA1 pyramidal neurons (str. radiatum) showing reduced dendritic spine densities in both regions of the GMko brain. (***, $p<0.001$); wt, n=49; ko, n=54 cells from 3 animals each.

2.3.5 Dendritic spine morphology

Dendritic spines are frequently classified into three morphological categories, i.e. thin filopodial, stubby, and mushroom-shaped spines. Although controversy exists about the functional characteristics of these different spine types, mushroom spines have been frequently associated with high synaptic strength and efficient synaptic transmission. We thus examined whether the relative abundance of this spine type in the DG and CA1 subfields would differ between genotypes. In fact, GMko mice displayed a smaller percentage of mushroom-like dendritic spines in both hippocampal subfields with a reduction of 32 % in the DG, and 37 % in the CA1 region (Fig. 26).

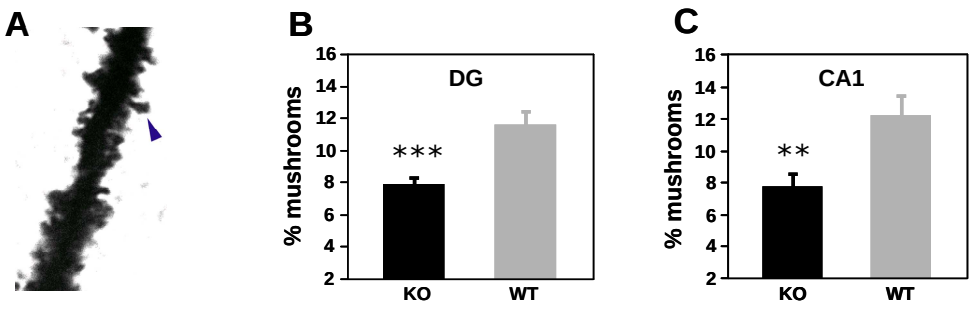

Figure 26. Effects of GM-CSF deficiency on the numbers of mushroom-shaped dendritic spines. (***A***) Representative example of a dendritic spine with mushroom-like morphology (arrowhead). (***B***,***C***) Percentage of mushroom-shaped dendritic spines was reduced in both dentate gyrus and CA1. (**, $p<0.01$; ***, $p<0.001$); wt, n=49; ko, n=54 cells from 3 animals each.

Collectively, these results consistently show a reduction in dendritic complexity at various cellular and subcellular levels and suggest that excitatory synaptic input is reduced by approximately one third in the GM-CSF deficient hippocampus.

2.4 Effects of GM-CSF Deficiency on Hippocampal Electrophysiology

In light of the behavioural deficits of GMko mice and their morphological aberrations in the hippocampus, we next asked whether GM-CSF deficiency might have an effect on hippocampal long-term potentiation (LTP). We thus investigated whether LTP between CA3 Schaffer collaterals and the CA1 dendritic region might be altered in the absence of GM-CSF (wt, n=21 slices; GMko, n=23 slices; n=8 mice each). These measurements were performed in collaboration with the group of Prof. Draguhn at the Institute of Physiology and Pathophysiology by Dr. Martin Both and Simon A. Kranig.

2.4.1 Induction and persistence of long-term potentiation

Prior to induction of LTP, maximal population spike amplitudes and spontaneous activity were monitored as described previously (Weiss et al., 2008) to rule out genotype-related differences in baseline properties of important electrophysiological parameters such as electrical excitability and endogenous firing rate. This analysis revealed no between-group differences (Fig. 27a-e).

Long-term potentiation at Schaffer collaterals was then successfully induced in both groups using a delta burst protocol adjusted to evoke population spikes with 50 % of the maximal amplitude, and was monitored for 60 min following induction. However, no impairment of LTP induction or maintenance was noted in GMko animals as judged by both slope and population spike analysis (Fig. 27f).

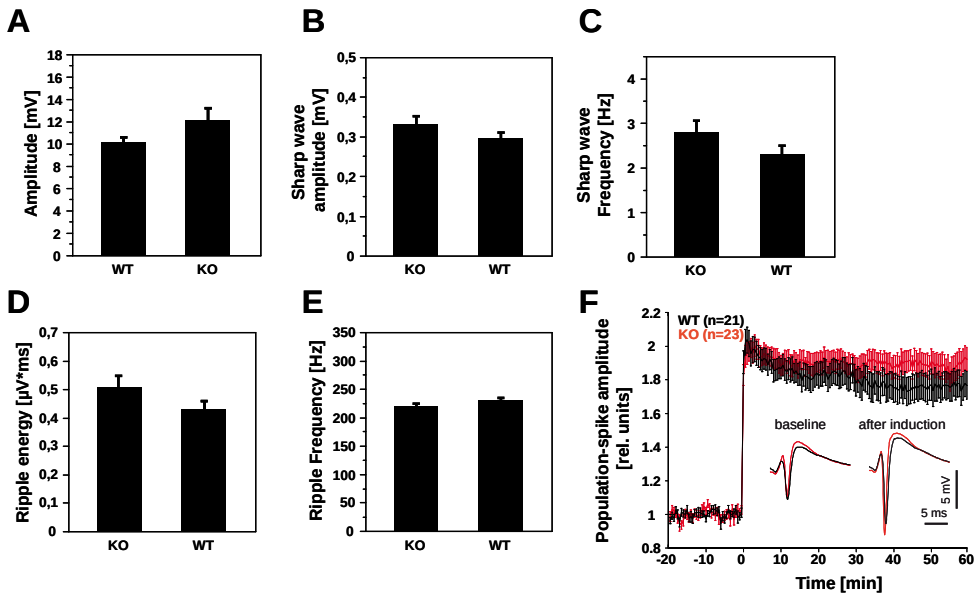

Figure 27. Effects of GM-CSF deficiency on baseline electrophysiological parameters and long-term potentiation. (***A***) Maximal population spike amplitudes were similar between groups (p>0.05). (***B***,***C***) Both sharp wave amplitudes and frequencies were identical between groups (both p>0.05). (***D***,***E***) Both ripple energy and ripple frequency were identical between genotypes (both p>0.05). (***F***) LTP between CA3 Schaffer collaterals and the CA1 dendritic region was induced using a delta burst protocol at timepoint 0 min, and monitored for 60 min after induction. Shown are population spike amplitudes as means ± s.e.m. GMko mice do not show impaired LTP induction when comparing the last 10 min of the protocol. Insets depict individual traces of wt and ko animals prior and after LTP induction. (wt, n=21 slices; GMko, n=23 slices; n=8 mice each)

2.4.2 Paired-pulse analysis

To test for potential genotype-related alterations in short-term plasticity and in the probability of presynaptic transmitter release, paired-pulse facilitation was assessed in GMko and wildtype mice. Again, no between-group differences were observed when responses to paired-pulse stimulation at 20 ms delay were examined both before and after induction of LTP (Fig. 28). As expected, paired-pulse stimulation did not lead to further enhancement of response intensities following LTP induction.

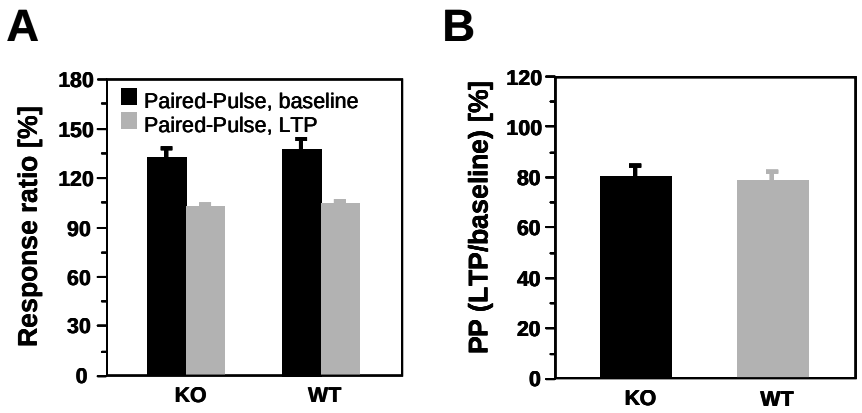

Figure 28. Effects of GM-CSF deficiency on paired-pulse facilitation. (***A***) Paired-pulse facilitation was similar between groups both prior to and following LTP induction (both $p>0.05$). As expected, no further response increase was obtained by paired-pulse stimulation after LTP induction. (***B***) Paired-pulse facilitation decreased by approximately 20 % after LTP induction. This effect was similar in both groups ($p>0.05$). (wt, n=21 slices; GMko, n=23 slices; n=8 mice each)

From these data we conclude that no major electrophysiological distortions are obvious in GM-CSF deficient animals, despite the morphological deficits observed in GMko mice.

2.5 Acute Manipulation of Adult Hippocampal GM-CSF Signalling

Constitutive deficiency for GM-CSF in the GMko mouse line may impact on neuronal development, and thus cause secondary effects on behaviour and cognition. To confirm our hypothesis that the observed cognitive deficits in GM-CSF knock-out mice were, at least partially, due to an acute lack of GM-CSF signalling in the adult brain, we chose a second, independent approach of AAV-mediated somatic gene transfer to complement the knock-out study in several ways by 1) use of wildtype animals that developed normally until adulthood; 2) strictly hippocampus-specific targeting by stereotaxic viral vector delivery; 3) exclusively neuron-specific modulation of GM-CSF signalling due to strict neurotropism of AAV in the CNS; 4) modulation of ligand-specific GM-CSF receptor alpha levels instead of GM-CSF ligand.

2.5.1 Adeno-associated virus vector constructs and functional characterisation

Vectors were designed to overexpress (AAV-GMCSFRα) or knock-down (AAV-shRNA) hippocampal GM-CSFRα levels in adult mice, while a third group of animals received vector AAV-UNC carrying a universal negative control construct (Fig. 29).

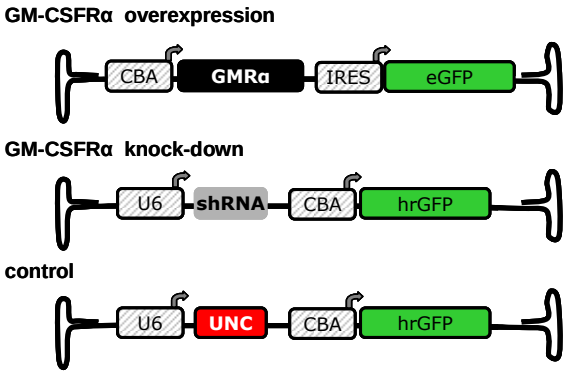

Figure 29. AAV constructs employed in this study. Vectors were designed to modulate GM-CSFRα levels in a bidirectional manner. CBA, chicken beta actin promoter; GMRα, GM-CSF receptor alpha subunit; IRES, internal ribosome entry site; eGFP, enhanced green fluorescent protein; U6, human U6 promoter; shRNA, small hairpin RNA; hrGFP, humanized renilla green fluorescen protein; UNC, universal negative control

Initially, a screen was conducted with four candidate AAV-shRNA constructs (sh427, sh845, sh1274, sh1542) to identify one that robustly knocked-down GM-CSFRα levels. We first tried to estimate knock-down efficiency at the mRNA level in the murine neural cell line NSC34 (Cashman et al., 1992). Attempts to quantify knock-down of endogenous transcript levels failed repetitively due to the low abundance of GM-CSFRα mRNA. We thus measured knock-down efficiency of our candidates on a background of artificially enhanced GM-CSFRα transcript levels by co-transfecting the shRNA constructs with plasmid AAV-GMCSFRα into NSC34 cells. Quantitative real-time PCR on cDNA from these cells indicated a 40 % - 50 % knock-down by constructs sh427, sh845, and sh1542, while sh1274 showed an unusually high variance in replicate experiments and was therefore no longer considered. Importantly, co-transfection of the negative control construct AAV-UNC with pAAV-GMCSFRα did not reduce GM-CSFRα transcript levels (Fig. 30).

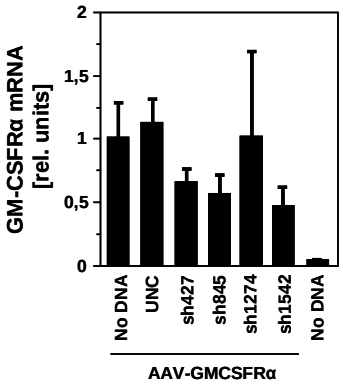

Figure 30. ***In vitro*** **GM-CSFRα knock-down screening at mRNA level.** Three of four shRNA candidates knocked-down artificially enhanced GM-CSFRα levels in NSC34 cells following co-transfection with plasmid AAV-GMCSFRα. (n=2)

Subsequently, candidate shRNA function was assessed on the protein level by immunocytochemical analysis of HEK293 cells co-transfected with plasmids pAAV-GMCSFRα-3xFlag and the individual candidate shRNA constructs. Transfected HEK293 cells were stained for the Flag tag to indirectly detect murine GM-CSFRα using Cy3-labelled secondary antibodies. Cy3 fluorescence signal intensity was then correlated at the single cell level to shRNA construct-derived GFP intensity. This analysis confirmed reliable shRNA-mediated reduction of Flag-tagged GM-CSFRα protein levels by 40 % - 80 % for all four candidates (Fig. 31).

Based on these results we focused on sh427 and sh1542 for assessment of knock-down function on endogenous hippocampal GM-CSFRα protein levels *in vivo*. Western blot analysis on hippocampal protein samples prepared from adult wildtype mice three weeks following unilateral hippocampal injection of AAV constructs expressing the respective candidate shRNAs revealed slightly better knock-down effects for sh427 (Fig. 32). We thus employed construct AAV-sh427 in this study.

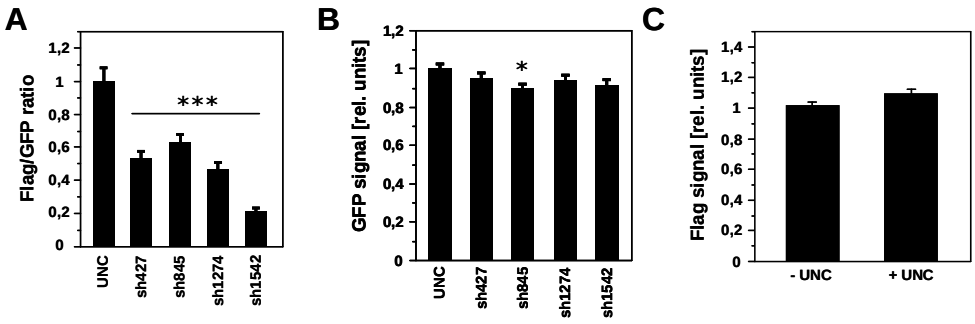

Figure 31. ***In vitro*** **GM-CSFRα knock-down screening at protein level.** HEK293 cells were co-transfected with plasmids AAV-GMCSFRα-3xFlag and individual shRNA candidate constructs. (***A***) All shRNA constructs reduced the Flag/GFP ratio in co-transfected HEK293 cells indicating knock-down of 3xFlag-tagged GM-CSFRα protein levels (ANOVA, $p<0.001$; Tukey-Kramer HSD, $p<0.001$ for UNC versus any other group). (***B***) Reductions in Flag/GFP ratios in (*A*) were not due to higher levels of GFP expression in UNC. In fact, GFP levels were similar in all groups except for sh845 which led to slightly lower GFP expression levels (ANOVA, $p<0.05$; Tukey-Kramer HSD, $p<0.05$ for UNC versus sh845). (***C***) Likewise, reductions of Flag/GFP ratios in (*A*) were not due to increased expression of Flag-tagged GM-CSFRα in response to co-transfection with UNC plasmid ($p>0.05$). n>100 cells per group

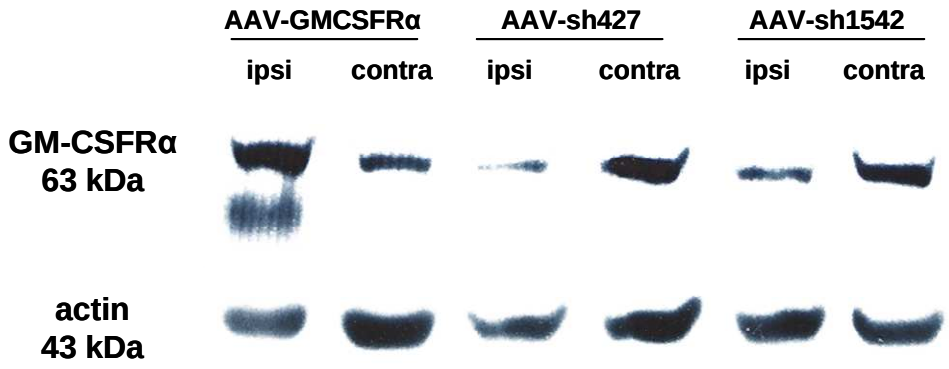

Figure 32. ***In vivo*** **GM-CSFRα knock-down screening at endogenous protein level.** Western blots on hippocampal protein samples of unilaterally injected mice 3 weeks after surgery revealed successful up- and down-regulation of endogenous GM-CSFRα protein levels by AAV-GMCSFRα and both AAV-shRNA constructs, respectively. Knock-down was more efficient with AAV-sh427 compared to AAV-sh1542. (ipsi, ipsilateral side; contra, contralateral side)

All viral constructs, AAV-GMCSFRα, AAV-sh427, and AAV-UNC, led to robust hippocampal transduction based on reporter gene expression as exemplified for AAV-UNC in (Fig 32a), and hippocampal GM-CSFRα protein levels differed in

the expected construct-dependent manner after bilateral stereotaxic injection (Fig 32b). Quantification of Western blots revealed GM-CSFRα levels to be knocked-down by approximately 42 % and increased by approximately 1000 % following injection of AAV-sh427 and AAV-GMCSFRα, respectively, as compared to AAV-UNC.

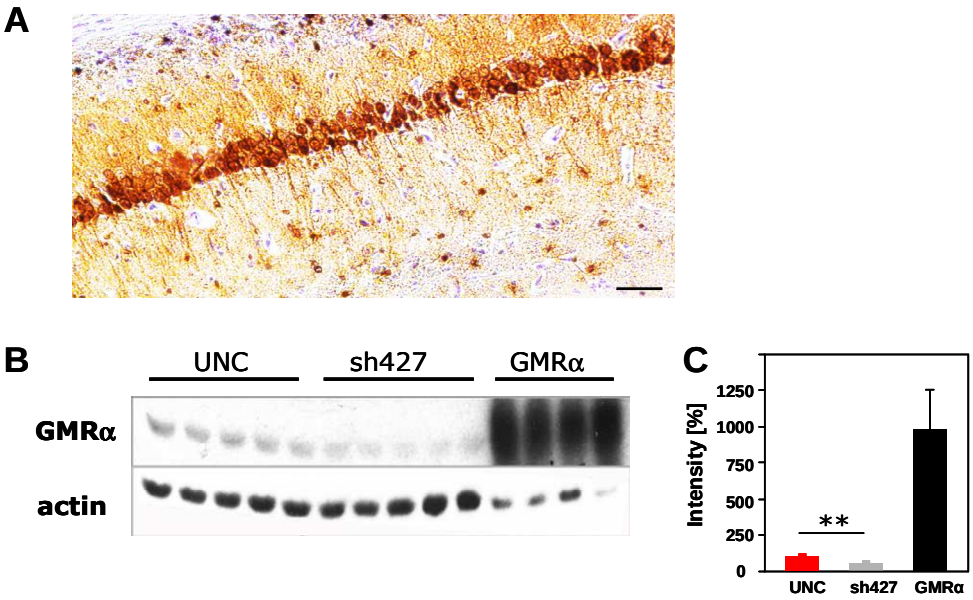

Figure 33. AAV-mediated transgene delivery to the adult murine hippocampus for bidirectional manipulation of GM-CSFRα levels in wildtypes. (***A***) Representative example of robust hippocampal reporter gene expression (AAV-UNC; CA1 region). Reference bar, 50 µm (***B***) GM-CSFRα levels in western blots of AAV-treated hippocampal samples differ in the expected construct-dependent manner. (***C***) Quantification of blot in (B). (**, $p<0.01$)

2.5.2 Effects of viral constructs on baseline activity

Animals were bilaterally infused intrahippocampally with viral vector solutions by a stereotaxic approach. Three weeks following surgery, when AAV-mediated transgene expression reached stable peak levels, all animals were examined in an open field experiment to assess aspects of baseline behaviour. No between-group differences were found in total distance travelled, and time spent in the corner or center regions of the arena (Fig 33). Thus, baseline activity and anxiety-related behaviour was similar irrespective of AAV treatment.

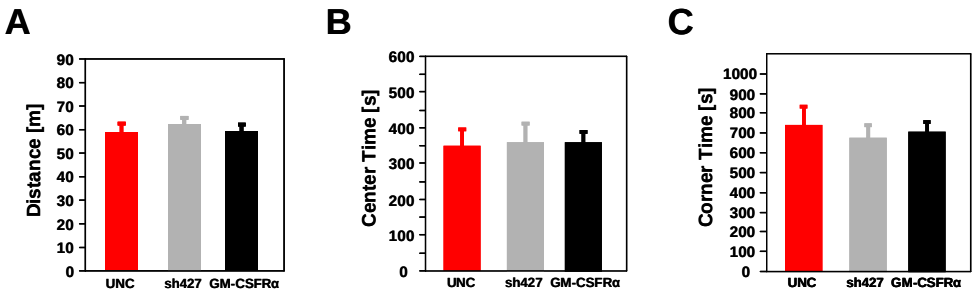

Figure 34. Effects of hippocampus-specific AAV treatment on basal behaviour in an open field. (***A***) Locomotor activity was not different between groups which travelled similar distances over the course of a 30 min examination ($p>0.05$). (***B,C***) Anxiety-related behaviour was not different between groups as judged by similar amounts of time spent in the center (*B*) and corner (*C*) regions of the arena (both $p>0.05$). n=19 animals per group

2.5.3 Effects of viral constructs on spatial learning and memory

When tested in the MWM, all three groups performed similarly during task acquisition over 11 training days indicating comparable spatial learning abilities (Fig 34a,b). However, memory recall in the probe trial was dependent on viral constructs as time spent in the target area was increased or reduced in AAV-GMCSFRα and AAV-sh427, respectively (Fig 34c, ANOVA, $p=0.05$; Tukey-Kramer HSD, $p<0.05$ for AAV-GMCSFRα vs. AAV-sh427).

These findings corroborate the results obtained with the GMko animals and demonstrate that adult hippocampal GM-CSF signalling affects learning and memory independent of potential developmental effects of GM-CSF deficiency.

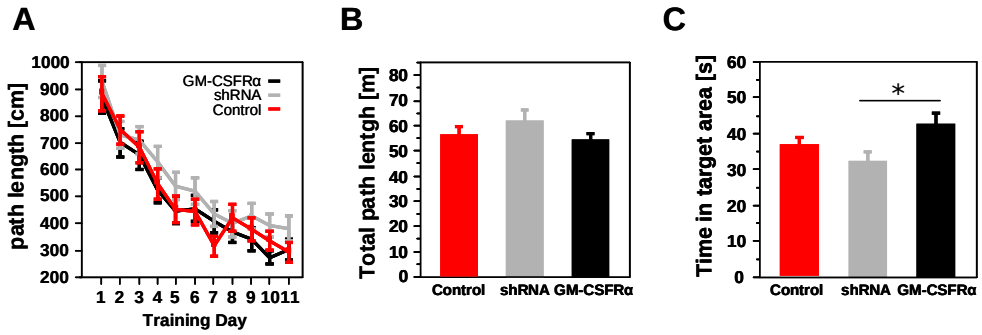

Figure 35. Impact of AAV-mediated manipulation of hippocampal GM-CSFRα levels on spatial learning and memory in the MWM. (***A***) Learning curves were indistinguishable between groups (genotype*day $p>0.05$). (***B***) Area under the curve plot of spatial learning in the MWM (genotype $p>0.05$). (***C***) Memory accuracy of the former platform location during the probe trial was dependent on hippocampal GM-CSFRα levels with an impairment and improvement caused by treatment with AAV-sh427 and AAV-GMCSFRα, respectively, as judged by the time spent in the target area. (*, $p<0.05$); n=19 animals per group

2.6 Generation of GM-CSF Receptor alpha Conditional Knock-Out Mice

The conditional ablation of genes in a tissue-specific manner has become a powerful tool in neuroscience research as it provides an option to study targeted genetic loss-of-function in adult animals without effects on prior developmental stages. The generation of a GM-CSFRα conditional knock-out (GM-CSFRα-cko) mouse line was intended to facilitate future studies on GM-CSF function that are not feasible with currently available tools, such as investigating the effects of GM-CSF signalling in particular hippocampal subregions. Notably, however, other fields of biological research might benefit from GM-CSFRα-cko mice as well given the pleiotropic peripheral functions of this cytokine. The engineering of this mouse line was expected to be potentially challenging as, to date, the European Conditional Mouse Mutagenesis Program (EUCOMM) run by an international consortium struggling to generate conditional knock-out mouse lines for every protein-coding gene, failed to obtain a gene targeting vector for the GM-CSFRα gene (http://www.knockoutmouse.org/).

2.6.1 Gene targeting vector design

Physically located on chromosome 19 of the murine genome, the GM-CSFRα gene *Csf2ra* spans 4 kb of sequence, consists of 12 exons, and generates a spliced transcript of approximately 1850 nucleotides. The introns are very small with only 87-159 nucleotides in length, except for intron #1 which comprises almost 1 kb of sequence. Its adjacent exons #1 and #2 are remarkable as the former is entirely composed of 5’ untranslated region (5’-UTR), while the latter immediately begins with the start codon ATG where translation of the receptor chain is initiated (Fig. 36a). Given these structural features, options for placing loxP sites were very limited as modifications of small introns pose the risk of interfering with the

splicing machinery in the conditional allele. Hence, loxP sites were placed in direct orientation in the last third of intron #1 and downstream of the last exon, respectively, such that Cre-mediated recombination would excise the full-length *Csf2ra* coding sequence except for the non-coding exon #1 (Fig. 36b). To facilitate screening of homologously recombined embryonic stem cells by both positive and negative selection, an FRT-flanked neomycin resistance cassette (neo^R) was included upstream to the second loxP site, and a herpes simplex virus thymidine kinase expression cassette downstream to the 3' homology arm, respectively (Fig. 36b). Flanking neo^R with FRT sites allows for Flp recombinase-mediated cassette removal from targeted ES cells prior to blastocyst injection.

To allow for convenient monitoring of the Cre-mediated conversion to a *Csf2ra* knock-out allele, the vector was further equipped downstream of the second loxP site with a promoterless eYFP-coding ORF carrying (i) upstream stop codons in all frames to prevent leaky reporter gene expression from cryptic promoters in the conditional allele, and (ii) splice acceptor sequences derived from *Csf2ra* intron #1 at its 5' end (Fig. 36b). In this way, excision of the *Csf2ra* coding sequence would concomitantly bring the previously silent reporter cassette under transcriptional control of the endogenous *Csf2ra* promoter and facilitate splicing of *Csf2ra* exon#1 to eYFP using endogenous *Csf2ra* exon #2 splice acceptor sequences (Fig. 36c).

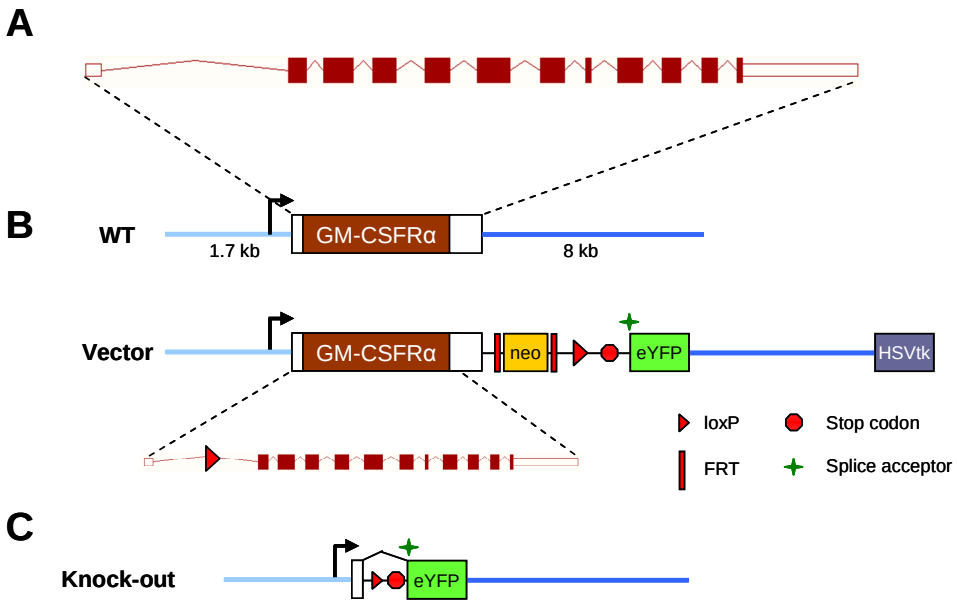

Figure 36. Design of the Csf2ra gene targeting vector and strategy. (***A***) The full-length *Csf2ra* transcript consists of 12 small exons. (***B***) The wildtype *Csf2ra* gene is converted to a targeting vector with a short 5' and a longer 3' homology arm. The rationale behind the overall design is detailed in the main text. Note the location of loxP sites (red triangles) in *Csf2ra* intron #1 and downstream of the *Csf2ra* coding sequence, respectively. (***C***) Cre-mediated excision of *Csf2ra* coding sequences causes splicing of the untranslated *Csf2ra* exon #1 to the eYFP reporter, thus skipping the artificial stop codons upstream of the eYFP translation initiation site. *Csf2ra* sequences: open boxes, untranslated regions; filled boxes, translated regions

2.6.2 Gene targeting vector characterisation

The expected vector size of 21.3 kb was confirmed by restriction enzyme digest (Fig. 37a). Additionally, all junctions between functional elements of the targeting vector were sequence-verified on both strands. Subsequently, feasibility of Flp recombinase-mediated excision of the neomycin resistance cassette was confirmed by PCR on plasmid DNA preparations from circular targeting vector / Flp recombinase co-transfections of the neural cell line NSC34 (Fig. 37b). Finally, generation of a Csf2ra exon #1-eYFP fusion transcript was confirmed by PCR on cDNA from ES cells co-electroporated with targeting vector / Cre recombinase. Importantly, formation of fusion transcripts occurred in a strictly Cre-dependent manner, as evidenced by PCR specific for the

fusion transcript followed by subsequent fragment sequencing, thus ruling out spontaneous formation of fusion transcripts by illegitimate splicing (Fig. 37c).

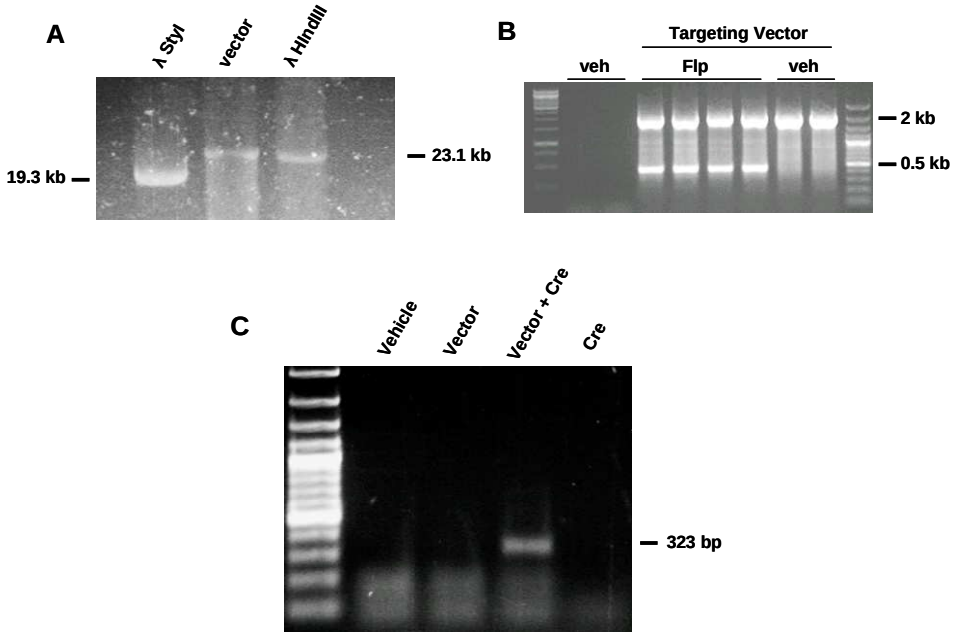

Figure 37. Characterisation of *Csf2ra* targeting vector. (***A***) Linearization by SbfI digest reveals expected vector size of approximately 23.1 kb. (***B***) PCR with primers flanking the neo cassette on plasmid DNA preparations from NSC34 cells obtained 48 hours after transfection. Band sizes: neo cassette, 2033 bp; Flp-recombined neo cassette, 449 bp. Note that removal of neo cassette occurs only in the presence of Flp recombinase. (***C***) PCR with primers located within *Csf2ra* exon #1 and eYFP ORF, respectively, on cDNA preparations from murine ES cells obtained 24 hours after (co-)transfection. Note that a exon #1-eYFP fusion transcript is only found after co-transfection of the targeting vector with Cre recombinase.

2.6.3 Targeting and screening in embryonic stem cells

Following electroporation of the linear targeting vector into ES cells, candidate ES cell clones growing under neomycin selection were isolated and analyzed by PCR for homologous recombination. Screening involved verification of site-specific recombination at both ends of the vector and verification of heterozygosity for neo^R (Fig. 38). A total of 4 clones positive for all parameters were identified. These are ready for future clonal expansion and subsequent blastocyst injection.

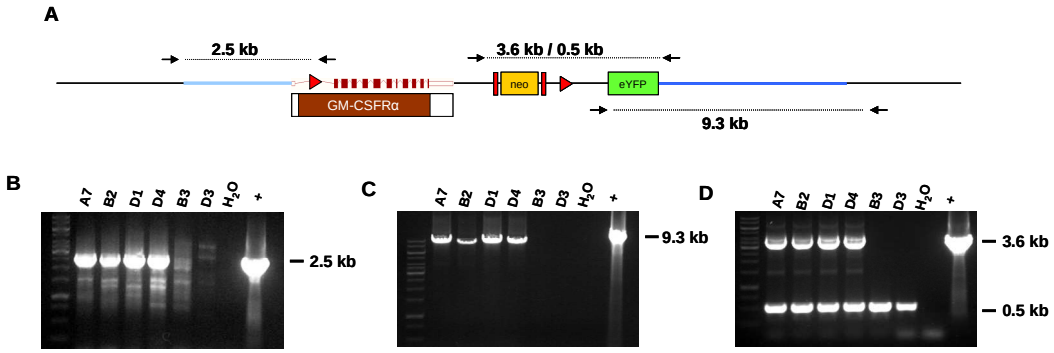

Figure 38. Screening of *Csf2ra* conditional knock-out ES cells. (***A***) Illustration of PCR screening strategy. Note that wildtype alleles will not generate any bands in both the 5' and 3' homology arm PCRs as the 3' end of one primer of each pair lies in vector-specific sequences. Note also that, conversely, the PCR involving neo^R sequences yields bands of different size for wildtype *Csf2ra* and vector templates. (***B***) Four clones positive (A7, B2, D1, D4), and two clones negative (B3, D3) for 5' homologous recombination are shown. (***C***) The same banding pattern observed in (*B*) is found for all six clones when homologous recombination is assessed at the longer 3' homology arm. (***D***) Clones A7, B2, D1, and D4 show both wildtype (0.5 kb) and vector-derived (3.6 kb) bands when neo^R / eYFP sequences were analyzed, thus confirming heterozygosity for the targeting vector. Instead, clones B3 and D3 only carry wildtype *Csf2ra* alleles. All symbols in (*A*) as in Fig. 36.

3 DISCUSSION

The data presented here demonstrates that GM-CSF signalling in the murine brain plays a hitherto unrecognized important role in processes underlying learning and memory. This conclusion is reached by assessing a broad array of cognitive functions in GM-CSF knock-out mice, and in mice with targeted manipulations of GM-CSF receptor α levels specifically in the adult hippocampus.

3.1 GM-CSF deficiency causes specific memory deficits

The GM-CSF-deficient mouse line displayed broadly impaired learning and memory performances in all cognitive paradigms investigated including an active place avoidance task, the Morris water maze, and a fear conditioning experiment. These deficits were detected amongst a background of other behavioural alterations including reduced spontaneous locomotor activity which appeared to be caused by a diminished central drive for exploration in the absence of motor unit defects. While this activity reduction might potentially perturb the interpretation of the learning tasks, close behavioural analysis negates the existence of such conflict.

For example, in the fear conditioning paradigm, low levels of activity could lead to an overestimation of freezing behaviour and fear memory retention as the absence of motor activity during challenge with a previously shock-associated stimulus serves as the behavioural read-out of successful fear memory formation. Since we observed reduced rather than enhanced freezing responses in

knock-outs, detection of locomotion-related false positive effects appears unlikely. Instead, diminished levels of activity might, if any, have rather caused an underestimation of the fear memory deficit observed in knock-out mice.

In the MWM, on the contrary, decreased activity could prolong escape latencies, and hence overshadow learning progress which might lead to false positive acquisition deficits. If very pronounced, reduced motor activity might even prevent goal-directed behaviour in the MWM altogether. While the latter was clearly ruled out by the continuous decrease in escape latencies over time in both groups, we circumvented the latency problem by using escape path length as a swim speed-independent parameter that is gradually reduced during acquisition through increasingly direct trajectories. Moreover, absence of both visual and motivational deficits to mount the platform during visually cued trials further indicates that deficits of GMko mice were correctly ascribed to spatial memory impairments.

In summary, inferior performance of GMko mice in our cognitive behavioural test battery appears due to genuine learning and memory deficits. In line with this, the presence of aversive stimuli during cognitive testing apparently led to disinhibition of voluntary activity in knock-outs as exemplified by the comparable activity levels between groups in the active place avoidance paradigm.

3.2 Mechanisms for reduced memory performance

The cognitive deficit of GMko mice was paralleled by marked reductions of hippocampal dendritic complexity. We observed decreased hippocampal dendritic spine densities and a relative loss of the likely more mature mushroom-shaped spines (Matsuzaki et al., 2001) in the CA1 and DG subfields. These alterations present a convincing morphological correlate of cognitive impairment given the paramount role the hippocampus plays in learning and memory, and the fact that neuronal circuit formation is known to critically depend on dendritogenesis since the dendritic compartment serves as the primary input site for neuronal information processing. As the elaboration of the dendritic tree determines both

the amount and distribution of synaptic input sites, it may thus limit the available cellular substrate for plasticity events required in learning and memory, and hence limit the capacity of pyramidal neurons to partake in complex neuronal networks.

Moreover, on the background of GMko-associated reductions in dendritic complexity, we observed concomitant morphological changes in the population of dendritic spines in the DG and the CA1 subfield including both a decrease in dendritic spine density and a relative loss of mushroom-shaped spines. Although conclusive evidence is still missing, this type of spine has been correlated with high synaptic strength by numerous studies (Chakravarthy et al., 2006; Geinisman et al., 1991; Matsuzaki et al., 2001). These alterations in the spinogenesis of the GMko brain could thus have aggravated the impact of reduced dendritic arborisation on hippocampal malfunction both individually or synergistically, as they represent a further reduction in the quantity of excitatory synaptic input sites, as well as a presumably disadvantageous qualitative change in the composition of the dendritic spine population.

It was shown previously that Akt, Stat3 and Erk pathways are major pathways activated by GM-CSF in neurons (Schabitz et al., 2008). Both PI3K/Akt and Ras/MAPK pathways have been implicated in dendritic size and complexity regulation (Kumar et al., 2005; Jan and Jan, 2010; Jaworski et al., 2005), and therefore present likely candidates to mediate the observed effects of GM-CSF in dendritic morphology.

Despite these morphological limitations we did not observe a reduction in long-term potentiation (LTP). Obviously, the excitatory postsynaptic potential (EPSP) generated by fewer synaptic inputs in the markedly pruned dendritic tree of CA1 pyramidal neurons is relatively larger than the one elicited in wildtype neurons, possibly because of the smaller surface area and volume of the dendrites. Although overall strength of post-tetanic EPSP is not impaired, it is straightforward to assume that the ability to form complex neuronal networks for memory retention is strongly affected by the decreased number of possible excitatory synaptic input sites. The GMko animals are therefore an interesting counterexample for the often claimed straight correlation of LTP and learning and

memory performance, and rather underline that the relationship between the two phenomena is more complicated (Neves et al., 2008).

3.3 Spatio-temporally regulated alterations of GM-CSF signalling affect spatial memory

The relevance of neuronal GM-CSF signalling for cognitive processes was further confirmed by a fully independent and complementary *in vivo* approach in which AAV-mediated somatic gene transfer was employed to specifically transduce hippocampal neurons of genotypic wildtype mice. Here, in contrast to the knock-out mice, we targeted a different component of the GM-CSF signalling pathway by modulating expression levels of the ligand-specific GM-CSF receptor α subunit in a bidirectional manner. This alteration was confined to the hippocampus, and occurred only after animals had reached adulthood. The higher developmental and spatial confinement of changes in GM-CSF signalling likely explains the very specific effects on spatial memory recall. We believe that GM-CSF likely acts on both a developmental or chronic and on a more acute level, and while all of these components are compromised in the knock-out animals, only the more acute effects are perturbed in the AAV-treated mice. While the strong morphological alterations in the dendritic structure are likely one component of the long-term alteration of the GM-CSF system, it remains to be defined what physiological and ultrastructural changes occur in the more acute adult manipulation of this system.

3.4 Other hematopoietic cytokines in the brain

GM-CSF is closely related at the functional level to other hematopoietic growth factors like erythropoietin (EPO) and granulocyte-colony stimulating factor (G-CSF). Recently, neuronal receptor expression for all of these growth factors has been demonstrated with particularly high expression levels in cortical and

hippocampal neurons (Digicaylioglu et al., 1995; Schneider et al., 2005; Schabitz et al., 2008). Subcutaneous injections of G-CSF improved spatial learning in wildtype rats (Diederich et al., 2009a) while, conversely, a phenotypic analysis of G-CSF knock-out mice revealed disruptions of memory formation along with decreased neuronal complexity in the hippocampus (Diederich et al., 2009b). Intraperitoneal EPO injections enhanced hippocampus-dependent memory in wildtype mice (Adamcio et al., 2008; El-Kordi et al., 2009). This was also observed in transgenic mice expressing constitutively active EPO receptors in cortical and hippocampal pyramidal neurons (Sargin et al., 2011). Enhanced levels of adult hippocampal neurogenesis after peripheral EPO injections have been reported as well (Leconte et al., 2011). Clinical studies with EPO suggest that these findings may be translatable to patients with cognitive problems (Ehrenreich et al., 2007a; Ehrenreich et al., 2007b; Marsh et al., 1991). Our data establish that the group of these hematopoietic factors as a whole shares highly analogous functions in the CNS, extending from basic anti-apoptotic to high level neuronal network functions. In line with this, all three factors have been established as neuroprotective agents with beneficial effects in a variety of neurodegenerative diseases and cerebrovascular events including stroke (Schabitz et al., 2003; Schneider et al., 2005; Wang et al., 2004; Schabitz et al., 2008), amyotrophic lateral sclerosis (Henriques et al., 2011; Pitzer et al., 2008; Grunfeld et al., 2007; Tanaka et al., 2006) and Parkinson’s disease (Ganser et al., 2010; Meuer et al., 2006; Kim et al., 2009). These properties are shared with other neurotrophic factors such as BDNF (brain-derived neurotrophic factor) which is known as a key determinant for memory formation and synaptic strength in the hippocampus (Korte et al., 1996; Korte et al., 1998).

3.5 Therapeutic potential

Collectively, our results suggest that GM-CSF signalling plays a novel role in learning and memory. Unlike most other neurotrophic proteins, GM-CSF is able to pass the intact blood-brain barrier, and is well-tolerated in humans. Importantly, we have shown in the AAV experiment that while a decrease in signalling

worsens memory performance, an increase improves it. Although it remains to be determined if and at what doses peripherally applied GM-CSF is able to improve cognitive deficits, it certainly is a bona fide candidate for cognitive enhancement. It is interesting in this regard that peripheral application of GM-CSF counteracted scopolamine-induced acute cognitive deficits (Bianchi et al., 1996), and that a recent report by Boyd and co-workers indicated that GM-CSF treatment was able to reverse cognitive deficits in a mouse model of Alzheimer's disease (Boyd et al., 2010). Although the authors ascribed the beneficial effect of GM-CSF treatment to the reduction of amyloidosis, it is tempting to assume in the light of our findings that direct effects on cognitive processing were involved.

4 MATERIALS AND METHODS

4.1 Animals

Animals were housed in groups of 3-5 under standard conditions on a 12-h light/dark cycle with lights on at 7:00 AM and water and food available *ad libitum*. The GM-CSF-deficient mouse line was a gift from Jeffrey A. Whitsett and has previously been described in many studies (Berclaz et al., 2007; LeVine et al., 1999; Yoshida et al., 2001). Wildtype C57Bl/6 mice were obtained from Charles River (CRL, Sulzfeld, Germany). All experiments were performed in accordance with the European Communities Council Directive 86/609/EEC for the care and use of laboratory animals for experiments and were approved by the responsible local authorities (Regierungspräsidium Karlsruhe, Germany).

4.2 Design of AAV expression constructs

The vector for overexpression of GM-CSFRα was based on AAV expression cassette pAAV-CBA-pl-IRES-EGFP-WPRE-bGHpA (provided by Dr. Matthias Klugmann, University of New South Wales, Sydney, Australia) containing a CMV immediate early enhancer / chicken β-actin hybrid promoter (CBA), a polylinker (pl), an IRES element, the EGFP cDNA, the woodchuck hepatitis virus post-transcriptional regulatory element (WPRE), and the bovine growth hormone polyadenylation sequence (bGHpA). This cassette was flanked

by AAV2 inverted terminal repeats (ITRs). Vector AAV-GMCSFRα was constructed by PCR amplification of the murine GM-CSFRα ORF from a murine cDNA library using primers GMCSFRα_s (GGG GAC AAG TTT GTA CAA AAA AGC AGG CTC TAC CAT GGC AGG AAG CCC CCT GTC TC) and GMCSFRα_as (GGG GAC CAC TTT GTA CAA GAA AGC TGG GTC CTA GGG CTG CAG GAG GTC CTT C) and subsequent subcloning into the pl site. The final construct was sequence verified on both strands.

Vectors for small hairpin RNA (shRNA) expression were based on the AAV2 ITR-flanked shRNA expression cassette pAM/U6-pl-CBA-hrGFP-WPRE-bGHpA described earlier (Franich et al., 2008). This vector harbours a humanized renilla GFP (hrGFP) reporter gene expression cassette under control of a CBA hybrid promoter along with a shRNA expression cassette with a RNA polymerase III compatible human U6 promoter. For knock-down of GM-CSFRα transcript levels, target sequence GGA GGC TGA GCT TCG TCA ACG was identified with Invitrogen's BLOCK-iT™ RNAi Designer web tool, and complementary DNA oligonucleotides encoding shRNAs directed against this target sequence were generated using Ambion's pSilencer™ Expression Vectors Insert Design Tool. For the loop structure, sequence GTG AAG CCA CAG ATG was used as described previously (Zeng and Cullen, 2004). Annealed oligonucleotides were BamHI x HIndIII-subcloned into the pl site downstream of the U6 promoter. Based on the location of the target sequence in the GM-CSFRα ORF, the resulting vector was termed AAV-sh427. The same expression cassette and cloning strategy was used for generation of a control vector which drove expression of the universal negative control shRNA "UNC" with the validated non-targeting sequence ACT ACC GTT GTT ATA GGT G (Yang et al., 2005).

4.3 Production of AAV

Chimeric AAV vectors containing AAV serotype 1 and 2 capsid proteins in a 1:1 ratio were generated as described earlier (Klugmann et al., 2006). Briefly, HEK293 cells were $CaPO_4$-transfected with the respective AAV expression

plasmid, the adenoviral helper plasmid (pFΔ6) and equal amounts of both AAV1 (pH21) and AAV2 (pRV1) helper plasmids. Cells were harvested sixty hours following transfection and vectors were purified using heparin affinity columns (HiTrap Heparin HP; Amersham Pharmacia Biotech, Uppsala, Sweden). Quantitative PCR (SYBR-Green; Lightcycler™, Roche Diagnostics) using primers derived from the WPRE sequence were used for genomic titration of viral vector preparations. For *in vivo* application, vectors were diluted in sterile PBS to a concentration of 2.5×10^8 vector genomes/µl.

4.4 Stereotaxic surgery

For AAV-treatment, 57 adult male C57Bl/6 mice (25–30 g, Charles River Laboratories, Sulzfeld, Germany) were randomly allocated to three groups of 19 animals. Mice were anesthetized by i.p. injection of a mixture of ketamine (120 mg/kg body weight; Pharmanovo, Hannover, Germany) and xylazine (Rompun, 16 mg/kg body weight; Bayer, Leverkusen, Germany), and placed in a stereotaxic frame (David Kopf Instruments, Tujunga, CA) before receiving bilateral infusions of 1.5 µl vector solution at a flow rate of 150 nl/min through a 35G stainless steel beveled NanoFil needle (WPI, Berlin, Germany). Coordinates for hippocampal injection were (relative to bregma): RC -2.0 mm, ML ±2.0 mm, DV -2.0 mm. Following infusion, needles were left in place for 2 min to allow fluid distribution away from the injection site depot. After surgery, mice were left in their home cages for 3 weeks to allow AAV-mediated transgene expression to reach stable peak levels.

4.5 Behavioural testing

4.5.1 Open field

Locomotor activity was measured in an open field arena (40x40x40 cm) made of white melamine resin-coated wooden board. The arena was located in a dedicated testing cubicle and was homogeneously illuminated at lux intensities well below aversive levels. Animals were entered into the center of the arena and allowed to freely explore for 30 min. Movement was recorded with a top-mounted video camera, and analyzed using proprietary high-resolution tracking software (SYGNIS tracker v4.1.4). Analysis was based on both a virtual grid subdividing the arena into 25 squares of 64 cm^2 each and a circle with radius r = 12 cm around the center of the arena. Total distance travelled and time spent in the circular center and the four corner squares of the open field were recorded.

4.5.2 Active place avoidance

The active place avoidance apparatus (Serrano et al., 2008) was located in a testing cubicle with visual cues on the inside walls. It consisted of a slowly rotating (1 rpm), circular platform (radius r = 40 cm) surrounded by a transparent wall. One randomly chosen 60° sector of the arena was designated as the non-rotating shock zone where animals received a mild 0.4 mA electric shock upon entry, and further identical shocks every 1.5 s if they failed to leave the sector. The shock zone was identical for all animals and its location only identifiable relative to the extra-maze visual cues. Due to platform rotation, any passive strategy was inevitably associated with foot-shocks, and animals quickly learned to actively avoid the shock zone. After a 10 min pre-training trial without shocks, 8 training trials of 10 min each were conducted at inter-trial intervals of 12 min which animals spent in their home cages. After 24 hours, one retention trial was run without triggering foot shocks. Latency to shock zone entry was recorded during all trials.

4.5.3 Fear conditioning

Mice were placed in a conditioning chamber with transparent walls and a stainless steel grid rod floor which was set up inside a sound attenuating cubicle containing an exhaust fan as a source of white noise and a video camera connected to video tracking software (Med Associates Inc, St. Albans, Vermont) recording animals' locomotive behaviour. The chamber was thoroughly cleaned after every animal. For conditioning, mice spent 6 min inside the chamber under dim illumination with visible light, and were exposed to an acoustic signal (5 kHz, 85 dB, 30 s) at 90-120 s, 150-180 s, 210-240 s, and 270-300 s (conditioned stimulus, CS). At the last second of each tone segment, one foot shock (0.6 mA, 1 s) was applied via the floor grid (unconditioned stimulus, US). Freezing was defined as a change in less than 11 out of 76800 pixels between two adjacent frames (33 ms apart) over a time period of at least 1 s. After 24 hours, animals were re-introduced to the chamber for 6 min in the absence of CS or US to evaluate contextual fear memory. 48 hours after training, cue-related fear memory was assessed. To hinder recognition of the chamber from haptic, olfactory, or visual cues the chamber was remodelled with a flat plastic floor panel covering the steel grid and a black roof-shaped insert, by replacement of visible light with near infrared illumination, and by use of a different disinfectant for cleaning. Mice were exposed to this altered context for 4 min during which the 30 s CS was presented twice, terminating at 60 and 180 s. Locomotive behaviour was analyzed as before.

4.5.4 Morris water maze

A circular pool (170 cm in diameter) was filled with opaque water (24 ± 1 °C) to a height of 35 cm with a circular escape platform (10 cm in diameter) submerged 1 cm below the water surface at a constant position in the center of the North-West (NW) quadrant during training. The pool openly faced the testing room which provided ample distal cues for visual spatial navigation. Mice were habituated to the maze 24 hours prior to training by a session of 4 trials in which the platform was located once in every quadrant. Here, the platform was visible by both elevation above water level and marking by a coloured mesh cage

structure. Training consisted of 4 daily trials on 11 (AAV animals) or 12 (GMko animals) consecutive days with inter-trial intervals (ITI) of 90 min. Cages were placed under infra-red lamps during the first 45 min of the ITI to prevent hypothermia. Animals were introduced into the pool from start positions East (E), South-East (SE), South (S), and South-West (SW) to avoid close initial proximity to the platform. Starting positions were block-randomized with 4 different starting positions in random order on every day. After successfully mounting the platform, animals were left there for 15 s. Cut-off time for trials was set to 60 s, after which animals failing to locate the platform were guided with a wooden rod and also left there for 15 s. Abandoning the platform during these 15 s was considered a platform jump-off. One probe trial of 120 s with the platform removed from the pool was conducted 24 hours after the last training day. Here, animals entered the pool from position S. On the following day, a cued platform test was conducted to rule out gross visual deficits. This test was similar to the pre-training session except that the pool was shielded from all extra-maze cues by black curtains to prevent animals from adopting previously learned search strategies. For GMko analysis, an additional 5-day reversal learning protocol started 48 hours later. Here, all positions were inverted compared to the former setup, i.e. platform now at SE and starting points pseudorandomized between W, NW, N, and NE. Frequency density maps were generated by accumulative addition of tracked trajectories (1 pixel wide) such that pixel density was analyzed in blocks of 5x5 pixels and normalized to performance of wildtypes at the last training day.

4.5.5 Rotarod

Animals were tested for motor function on a rotarod (Ugo Basile, Comerio, Italy) on 6 consecutive days with 5 daily trials at ITIs of 8 min using a challenging protocol with constant acceleration (4-80 rpm in 300 s). Latencies to falling off the rod were recorded. In the rare event of an animal clinging to the rod and passively rotating with it for at least 10 s, time of onset of this behaviour was recorded as latency.

4.5.6 Dark-light box

The dark-light test was conducted in a white 42x42x33 cm open field, of which the center of one side was linked at floor level by a door (8.5 x 10 cm) to a black 21x42x33 cm compartment that was covered with a lid to keep it dark. The open field was brightly illuminated from above to provide 120 lx in the center and 95 lx at the junction door. The whole apparatus was located in a dedicated testing cubicle and was monitored by an overhead-mounted video camera. Mice were placed into the dark compartment for a 60 s habituation period with the exit closed. After that, the door was opened and animals were left to freely explore for 330 s. For every animal, the following parameters were recorded: Time spent and number of rearings in the lit compartment. Presence in lit compartment required all four paws to be placed in the lit compartment.

4.5.7 Plantar pain test

Plantar pain threshold of rear paws was assessed by the Hargreaves method using an apparatus (Cat. Nr 7371, Ugo Basile, Comerio, Italy) to measure the response to infrared (IR) heat stimuli applied with an IR emitter over 5 trials with ITIs of 10 min through the plastic floor of the test box. Mice were tested between 2 and 6:30 h PM at an IR intensity of approximately 220 mW/cm². Because this test required animals to keep their hind paws motionless on the ground, habituation to the test chamber was allowed for at least 15 min. Care was taken to only test animals in alert, yet immobile states with dry paws. If an initiated trial was interrupted by grooming or locomotion-related paw movement, the trial was re-started no earlier than 10 min later to allow for the reversal of any pain sensitization triggered during the failed attempt.

4.5.8 Spontaneous behaviour assessment by LABORAS

The Laboratory Animal Behaviour Observation, Registration and Analysis System (LABORAS, Metris, Hoofddorp, Netherlands) is a fully automated system

for the vibration and force pattern-based detection and discrimination of a variety of rodent behaviours including locomotion, immobility, and cage climbing. Mice were individually placed in LABORAS cages at 6:00 h PM and spontaneous behaviour was monitored for 12 hours starting at 7:00 h PM.

4.6 Hippocampal anatomy

After deep anaesthesia, GMko and wildtype mice (n=6 per group) were transcardially perfused with phosphate buffered saline followed by 4 % paraformaldehyde. Brains were removed, embedded in paraffin and cut on a microtom to 10 µm coronal sections of which three consecutive slices were mounted to the same microscope slide. Starting with the slide carrying the rostralmost hippocampal section, every 10^{th} slide was subjected to Masson's Trichrom staining (Sigma Aldrich, Steinheim, Germany) such that always 9 slides (27 sections) were skipped. Stained sections were compared to a mouse brain atlas (Paxinos and Franklin, 2004) to exclude those from further analysis that were not covered by maps #42-#61 (i.e. bregma -1.34 mm to -3.64 mm). Sections were scanned and hippocampal areas were determined using ImageJ software (Rasband, 1997-2011). From these values hippocampal volumes were calculated by the Cavalieri method using equation $V = \sum(A_1, A_2, \ldots, A_n) * d$, where V = hippocampal volume, A_x = mean hippocampal area of three sections on slide x, and d = distance between sections on consecutive slides (270 µm).

Next, sections were subdivided into five groups (G1-G5) of rostral (G1), rostromedial (G2), medial (G3), mediocaudal (G4), and caudal (G5) location covering four atlas maps each with a rostrocaudal extent of 0.36 to 0.4 mm per group. Within these groups, lengths of distances D1-D5 between characteristic hippocampal structures were determined. These were defined as follows: D1 = maximal interhemispheric distance between CA3 pyramidal cell nuclei; D2 = distance between dorsal tips of DG granule cell and CA1 pyramidal cell layers; D3 = distance between ends of CA cell layer (CA1-CA3); D4 = distance between open ends of DG upper and lower blades; D5 = distance between CA1 end of CA cell layer and junction of DG upper and lower blades. However, D1

and D2 were only determined on the one section per animal in which hippocampal width was maximal and no CA3 pyramidal cell nuclei lay ventral relative to DG granule cell nuclei.

4.7 Neuronal morphology and dendritic spine analysis

Brains were removed from deeply anesthetized animals and subjected to Golgi-Cox staining using the FD Rapid GolgiStain kit (FD NeuroTechnologies, Ellicott City, USA) according to manufacturer's instructions. Tissue was cut on a cryostat into 100 µm sections and confocal microscopic image acquisition was perfomed with a Leica TCS SP5 laser scanning microscope (Leica Microsystems, Wetzlar, Germany). For whole neuron reconstruction, stacks of images (step size 0.5 µm) were taken from individual DG granule cells and used for manual reconstruction with the Neuromantic software v1.6.3. Spine analysis was conducted on both CA1 pyramidal and DG granule cells. Here, stacks of images (step size 0.2 µm) were taken of the first dendritic bifurcation in either stratum radiatum (CA1) or stratum moleculare (DG), and analysis was done from this bifurcation onwards to the distal end of the neurite, either until the neurite ended or disappeared from the display window, or the next bifurcation appeared.

4.8 Electrophysiology

All electrophysiological recordings were performed at the Interdisciplinary Center for Neurosciences in the group of Prof. Dr. Draguhn by Dr. Martin Both and Simon A. Kranig. Experiments were performed on 24 mice aged 6-10 weeks by experimenters blinded to genotype. Animals were anesthetized with CO_2, decapitated and brains removed. Brains were kept in cooled (1-4°C) artificial cerebrospinal fluid (ACSF), containing (mM): NaCl 124, KCl 3, $MgSO_4$ 1.8, $CaCl_2$ 1.6, glucose 10, NaH_2PO_4 1.25, $NaHCO_3$ 26, saturated with

95% O_2 / 5% CO_2 with a pH of 7.4 at 35°C. After removal of the cerebellum and frontal brain structures, horizontal hippocampal slices (450 µm) were cut on a vibratome (Leica, VT 1000S, Germany). Slices were maintained at 35 ± 0.5°C in a Haas-type interface chamber and rested for ≥ 2.5 hours prior to experiments. Extracellular glass microelectrodes (tip diameter ~5 µm) filled with ACSF were placed in CA1 str. pyramidale and str. radiatum. Electrical stimulation to Schaffer collaterals was achieved by a bipolar platinum / iridium electrode (Science Products, 100 kΩ at 1 kHz, 75 µm tip distance). Stimulation strength was adjusted to evoke population spikes with 50 % of the maximal amplitude. Test pulses were applied every 30 s. LTP was induced by a delta burst protocol (consisting of 10 bursts within 8 s, each at 100 Hz with 40 ms duration). If baseline recording was stable over ≥ 20 min, potentials were amplified 100-fold, low pass-filtered at 10 kHz, high pass-filtered at 0.3 Hz (EXT10-2FX amplifiers, npi electronics, Tamm, Germany), digitized at 20 kHz for offline analysis (1401 interface and Spike-2 data acquisition program, CED, Cambridge, UK), and analyzed offline using custom routines written in Matlab (The MathWorks, Natick, MA).

4.9 Neurite outgrowth analysis

Primary hippocampal neurons were prepared from E18.5 rat embryos and seeded on coverslips in 24-well plates at a density of 10000 cells per well. Six hours after seeding, GM-CSF or vehicle was added and neurons were fixed with 4 % paraformaldehyde 48 hours after stimulation. Cells were stained for neurofilament-L (AB9568, 1:200, Millipore, Schwalbach, Germany) in 1 % BSA / TBS o/n at 4°C. FITC-labelled secondary antibody was applied for 1 h at room temperature in 0.1 % BSA / TBS (1:200, Dianova, Hamburg, Germany). Image acquisition at 40x magnification was done in a grid of 7x7 pictures to yield composits of 49 individual images covering a total area of 1.8 mm². Each composit was screened in a predefined pattern by a blinded observer for fully traceable neurons, and total neurite length per cell was determined using the NeuronJ plug-in for ImageJ. A maximum of 15 neurons was traced per coverslip to ultimately yield 100 neurons per group.

4.10 *Csf2ra* targeting vector construction

The targeting vector was based on BAC clone 367J9 from the bMQ library generated from murine AB2.2 ES cell DNA. This library covers > 99 % of all Ensembl genes at 3.6-fold autosome coverage and an average insert size of 110.7 kb (Adams et al., 2005). The vector was constructed using both conventional cloning and Red/ET recombineering (Zhang et al., 1998; Zhang et al., 2000). Both loxP sites were introduced by Red/ET recombineering using commercially available kits (Cat. No. K005, Gene Bridges GmbH, Heidelberg, Germany). The 373 bp intronic splice acceptor sequence was PCR-amplified from bMQ367J9 (nucleotides 35296-35668) using the following primers: intron_s, 5'-CTGTCAGTCAGATGAGTGGGCAGAG-3' and intron_as, 5'-CCACTTAGCTGGtgaatgaatgaaGCTGAGCTTGGAGCACGGCGGGGTT-3'. The eYFP-ORF was amplified from pDEST-N-eYFP using primers eYFP_s 5'-cccactcatctgactgacagATGGTGAGCAAGGGCGAGGAGCTGT-3' and eYFP_as 5'-ccagctaagtggACAAACCACAACTAGAATGCAGTGA-3'. Both amplicons were used as templates in a 2-fragment PCR approach using primers sa-eYFP_s: 5'-ccagctaagtggACAAACCACAACTAGAATG-3' and sa-eYFP_as: 5'-ccacttagctggTGAATGAATGAAGCTGAGC-3', thus generating a BstXI-flanked splice acceptor-eYFP fusion fragment with upstream stop codons in all frames. This cassette was subsequently subcloned to the BAC using a BstXI-compatible artificial I-CeuI recognition sequence. The herpes simplex virus thymidine kinase (HSVtk) ORF was BamHI x ClaI-isolated from plasmid pIC19R_MC1-tk and subcloned into the targeting vector which was transferred prior to that to a plasmid backbone by Red/ET recombineering (Cat. No. K003, Gene Bridges GmbH, Heidelberg, Germany). Subsequently, FRT sites were introduced flanking the downstream neo cassette by PCR in a stretch of sequences located between unique PmeI / NheI restriction sites. These sites were used to exchange the non-FRT by the FRT-flanked cassette. The targeting vector was linearized by an artificial SbfI site introduced adjacent to the HSVtk gene prior to ES cell transfection.

4.11 Embryonic stem cells

PluriStem 129/SvEv (S6) murine ES cells (Millipore GmbH, Schwalbach, Germany) were used for generation of the *Csf2ra* conditional knock-out mouse line. ES cells were grown on mitomycin C-treated primary mouse embryonic feeder cells (Millipore GmbH, Schwalbach, Germany) in serum-containing EmbryoMax medium from the same manufacturer.

4.12 Statistics

Comparisons between two conditions were made with the two-sided t-test. More conditions were analyzed using ANOVA with a post-hoc Tukey-Kramer test. Serial tests were analyzed using regression analysis. In addition, AUC analyses were performed. A p-value of < 0.05 was considered significant for all tests. All analyses were performed using JMP v8.02 (SAS Institute).

5 ACKNOWLEDGMENTS

Many people have contributed to this thesis. To them I am indebted and wish to express my gratitude.

I am grateful to Prof. Dr. Armin Schneider for providing me with the opportunity to conduct this work at Sygnis Bioscience GmbH & Co. KG, for initiation and supervision of the project, for general support, and numerous scientific discussions.

I would like to thank Prof. Dr. Stephan Frings for project supervision and general support.

I also would like to thank Prof. Dr. Peter H. Seeburg and PD Dr. Anne Régnier-Vigouroux for agreeing to join the board of examiners for this thesis.

Everyday's lab work would have been much harder without the help, advice, and the good spirits of Ulrike Bolz, Gisela Eisenhardt, Simone Hoppe, Verena Kamuf-Schenk, Friederike Kirsch, Carola Krüger, Melanie Motsch, Claudia Pitzer, Joanna Schwammel, Vera Sonntag-Buck, Angela Vogt-Eisele, Daniela Weber, Frank Herzog, and Christian Plaas, all of whom helped me out many times in their respective fields of expertise. Thanks a million.

Another big thank you is due to Paul Ruf and Gerhard Rimner who saved me lots of time and effort by taking perfectly good care of my animals.

I also wish to thank Gerhard Vogt who developed and contributed wonderful software tools.

Quality time on and off the bench was frequently provided by Alexandre Henriques, Armin Keller, Rico Laage, and Renzo Wolbold. That helped, thank you.

Matthias Klugmann and Miriam Schneider were always approachable and a reliable source of valuable advice on AAV and rodent behaviour. Matthias also commented on the manuscript. Thanks for all of that.

I am much obliged to Prof. Dr. Andreas Draguhn and his group members Dr. Martin Both and Simon A. Kranig who shared with us their expertise on electrophysiology, conducted the respective experiments, and helped writing the sections related to this.

I also wish to thank Dr. Jeffrey A. Whitsett of the Cincinnati Children's Hospital Medical Center who kindly provided the GM-CSF knock-out mouse line.

Of course I wish to thank my family for their constant support.

And most of all, for your patience, for your endurance, and your lenience when the thesis was, again, strangely more important than anything else: Danke Kathrin.

6 LIST OF ABBREVIATIONS

Å	Angström
AAV	adeno-associated virus
AAVS1	AAV integration site 1
ACSF	artificial cerebrospinal fluid
AD	Alzheimer's disease
ANOVA	analysis of variance
APA	active place avoidance
Aβ	amyloid beta
BAC	bacterial artificial chromosome
BAD	Bcl-2 associated death promoter
Bcl-2	B-cell lymphoma 2
BDNF	brain derived neurotrophic factor
bGHpA	bovine growth hormone polyadenylation signal
bp	base pair
BSA	bovine serum albumin
CA	cornu ammonis
cAMP	cyclic adenosine monophosphate
CBA	chicken beta actin
cDNA	complementary DNA
CNS	central nervous system
CRE	cAMP response element
Cre	Causes recombination
CREB	cAMP response element binding protein
CRM	cytokine receptor module
CS	conditioned stimulus
Csf2ra	alpha subunit of the GM-CSFR
Cy3	cyanine-3
DG	dentate gyrus
DNA	deoxyribonucleic acid
dsDNA	double stranded DNA
DV	dorso-ventral axis
E18.5	embryonic day 18.5
EC	entorhinal cortex
eGFP	enhanced green fluorescent protein
EPO	erythropoietin
EPOR	erythropoietin receptor

EPSP	excitatory postsynaptic potential
ERK	extracellular signal-regulated kinase
ES cell	embryonic stem cell
eYFP	enhanced yellow fluorescent protein
FC	fear conditioning
FITC	fluorescein isothiocyanate
FNIII	fibronectin III
GABA	γ-aminobutyric acid
G-CSF	granulocyte colony stimulating factor
G-CSFR	G-CSF receptor
GFP	green fluorescent protein
GM-CSF	granulocyte/macrophage colony stimulating factor
GM-CSFR	GM-CSF receptor
GM-CSFRα	alpha subunit of the GM-CSFR
GMko	GM-CSF knock-out
Grb2	growth factor receptor-bound protein 2
GTP	gunaosine-5'-triphosphate
HEK	human embryonic kidney
hrGFP	humanized renilla GFP
HSD	honestly significant difference
HSVtk	herpes simplex virus thymidin kinase
IκB	inhibitor of kappa B
IKK	IκB kinase
IL	interleukin
IRES	internal ribosome entry site
ITI	inter-trial interval
ITR	inverted terminal repeat
JAK	Janus kinase
JMML	juvenile myelomonocytic leukemia
JNK	c-Jun N-terminal kinase
Kb	kilobases
K_D	dissociation constant
loxP	locus of crossover in phage P1
LPP	lateral perforant path
LTP	long-term potentiation
Lx	lux
MAPK	mitogen-activated protein kinase
ML	medio-lateral axis
mM	millimolar
MPP	medial perforant path
MPTP	1-methyl-4-phenyl-1,2,3,6-tetrahydropyridine
mRNA	messenger ribonucleic acid
MTL	medial temporal lobe
MWM	Morris water maze
neo^R	neomycin resistance
NFkB	nuclear factor kappa-light-chain enhancer of activated B cells
NMDA	*N*-Methyl-*D*-aspartate

NR1	NMDA receptor subunit 1
NR2	NMDA receptor subunit 2
NSC34	neuroblastoma × spinal cord hybrid cell line
ORF	open reading frame
PAP	pulmonary alveolar proteinosis
PBS	phosphate-buffered saline
PCR	polymerase chain reaction
PDK1	3-phosphoinositide dependent protein kinase-1
PH	pleckstrin homology
PI3K	phosphoinositide3-kinase
PIP2	Phosphatidylinositol 4,5-bisphosphate
PIP3	Phosphatidylinositol (3,4,5)-triphosphate
PKC	protein kinase C
pM	picomolar
PP	perforant path
RA	rheumatoid arthritis
rAAV	recombinant AAV
RC	rostro-caudal axis
REM	rapid eye movement
rGM-CSF	recombinant GM-CSF
RNA	ribonucleic acid
RNAi	RNA interference
rpm	revolutions per minute
RSK	p90 ribosomal S6 kinase
s.e.m.	standard error of the mean
S6K	p70 ribosomal S6 kinase
SAPK	stress-activated protein kinase
SCI	spinal cord injury
SGK	glucocorticoid-induced protein kinase
Shc	Src homology 2 domain containing protein
shRNA	small hairpin RNA
ssDNA	single-stranded DNA
STAT	signal transducer and activator of transcription
str.	stratum
TBS	TRIS-buffered saline
TRIS	Tris(hydroxymethyl)-aminomethan
UNC	universal negative control
US	unconditioned stimulus
UTR	untranslated region
WPRE	woodchuck hepatitis virus post-transcriptional regulatory element
wt	wildtype
β_c	common beta subunit

7 REFERENCES

Adamcio, B., Sargin, D., Stradomska, A., Medrihan, L., Gertler, C., Theis, F., Zhang, M., *et al.* (2008). Erythropoietin Enhances Hippocampal Long-Term Potentiation and Memory. *BMC Biol* 6, 37.

Adams, D.J., Quail, M.A., Cox, T., van der Weyden, L., Gorick, B.D., Su, Q., Chan, W.I., *et al.* (2005). A Genome-Wide, End-Sequenced 129sv Bac Library Resource for Targeting Vector Construction. *Genomics* 86, 753-758.

al-Shami, A., Bourgoin, S.G., and Naccache, P.H. (1997). Granulocyte-Macrophage Colony-Stimulating Factor-Activated Signaling Pathways in Human Neutrophils. I. Tyrosine Phosphorylation-Dependent Stimulation of Phosphatidylinositol 3-Kinase and Inhibition by Phorbol Esters. *Blood* 89, 1035-1044.

Arnaout, M.A., Wang, E.A., Clark, S.C., and Sieff, C.A. (1986). Human Recombinant Granulocyte-Macrophage Colony-Stimulating Factor Increases Cell-to-Cell Adhesion and Surface Expression of Adhesion-Promoting Surface Glycoproteins on Mature Granulocytes. *J Clin Invest* 78, 597-601.

Atchison, R.W., Casto, B.C., and Hammon, W.M. (1965). Adenovirus-Associated Defective Virus Particles. *Science* 149, 754-756.

Baldwin, G.C., Benveniste, E.N., Chung, G.Y., Gasson, J.C., and Golde, D.W. (1993). Identification and Characterization of a High-Affinity Granulocyte-Macrophage Colony-Stimulating Factor Receptor on Primary Rat Oligodendrocytes. *Blood* 82, 3279-3282.

Bannerman, D.M., Good, M.A., Butcher, S.P., Ramsay, M., and Morris, R.G. (1995). Distinct Components of Spatial Learning Revealed by Prior Training and Nmda Receptor Blockade. *Nature* 378, 182-186.

Barco, A., Alarcon, J.M., and Kandel, E.R. (2002). Expression of Constitutively Active Creb Protein Facilitates the Late Phase of Long-Term Potentiation by Enhancing Synaptic Capture. *Cell* 108, 689-703.

Bayascas, J.R. (2008). Dissecting the Role of the 3-Phosphoinositide-Dependent Protein Kinase-1 (Pdk1) Signalling Pathways. *Cell Cycle* 7, 2978-2982.

Bayer, K.U., De Koninck, P., Leonard, A.S., Hell, J.W., and Schulman, H. (2001). Interaction with the Nmda Receptor Locks Camkii in an Active Conformation. *Nature* 411, 801-805.

Bayer, K.U., LeBel, E., McDonald, G.L., O'Leary, H., Schulman, H., and De Koninck, P. (2006). Transition from Reversible to Persistent Binding of Camkii to Postsynaptic Sites and Nr2b. *J Neurosci* 26, 1164-1174.

Bazan, J.F. (1990). Structural Design and Molecular Evolution of a Cytokine Receptor Superfamily. *Proc Natl Acad Sci U S A* 87, 6934-6938.

Bekinschtein, P., Cammarota, M., Igaz, L.M., Bevilaqua, L.R., Izquierdo, I., and Medina, J.H. (2007). Persistence of Long-Term Memory Storage Requires a Late Protein Synthesis- and Bdnf- Dependent Phase in the Hippocampus. *Neuron* 53, 261-277.

Berclaz, P.Y., Carey, B., Fillipi, M.D., Wernke-Dollries, K., Geraci, N., Cush, S., Richardson, T., *et al.* (2007). Gm-Csf Regulates a Pu.1-Dependent Transcriptional Program Determining the Pulmonary Response to Lps. *Am J Respir Cell Mol Biol* 36, 114-121.

Bianchi, M., Clavenna, A., Bondiolotti, G.P., Ferrario, P., and Panerai, A.E. (1997). Gm-Csf Affects Hypothalamic Neurotransmitter Levels in Mice: Involvement of Interleukin-1. *Neuroreport* 8, 3587-3590.

Bianchi, M., Sacerdote, P., and Panerai, A.E. (1996). Peripherally Administered Gm-Csf Interferes with Scopolamine-Induced Amnesia in Mice: Involvement of Interleukin-1. *Brain Res* 729, 285-288.

Blacklow, N.R., Hoggan, M.D., and Rowe, W.P. (1967). Isolation of Adenovirus-Associated Viruses from Man. *Proc Natl Acad Sci U S A* 58, 1410-1415.

Bourtchuladze, R., Frenguelli, B., Blendy, J., Cioffi, D., Schutz, G., and Silva, A.J. (1994). Deficient Long-Term Memory in Mice with a Targeted Mutation of the Camp-Responsive Element-Binding Protein. *Cell* 79, 59-68.

Boyd, T.D., Bennett, S.P., Mori, T., Governatori, N., Runfeldt, M., Norden, M., Padmanabhan, J., *et al.* (2010). Gm-Csf Upregulated in Rheumatoid Arthritis Reverses Cognitive Impairment and Amyloidosis in Alzheimer Mice. *J Alzheimers Dis* 21, 507-518.

Bradley, T.R., and Metcalf, D. (1966). The Growth of Mouse Bone Marrow Cells in Vitro. *Aust J Exp Biol Med Sci* 44, 287-299.

Brines, M.L., Ghezzi, P., Keenan, S., Agnello, D., de Lanerolle, N.C., Cerami, C., Itri, L.M., and Cerami, A. (2000). Erythropoietin Crosses the Blood-Brain

Barrier to Protect against Experimental Brain Injury. *Proc Natl Acad Sci U S A* 97, 10526-10531.

Brown, C.B., Beaudry, P., Laing, T.D., Shoemaker, S., and Kaushansky, K. (1995). In Vitro Characterization of the Human Recombinant Soluble Granulocyte-Macrophage Colony-Stimulating Factor Receptor. *Blood* 85, 1488-1495.

Burgess, A.W., Camakaris, J., and Metcalf, D. (1977). Purification and Properties of Colony-Stimulating Factor from Mouse Lung-Conditioned Medium. *J Biol Chem* 252, 1998-2003.

Carr, P.D., Conlan, F., Ford, S., Ollis, D.L., and Young, I.G. (2006). An Improved Resolution Structure of the Human Beta Common Receptor Involved in Il-3, Il-5 and Gm-Csf Signalling Which Gives Better Definition of the High-Affinity Binding Epitope. *Acta Crystallogr Sect F Struct Biol Cryst Commun* 62, 509-513.

Carr, P.D., Gustin, S.E., Church, A.P., Murphy, J.M., Ford, S.C., Mann, D.A., Woltring, D.M., Walker, I., Ollis, D.L., and Young, I.G. (2001). Structure of the Complete Extracellular Domain of the Common Beta Subunit of the Human Gm-Csf, Il-3, and Il-5 Receptors Reveals a Novel Dimer Configuration. *Cell* 104, 291-300.

Carter, B.J. (2004). Adeno-Associated Virus and the Development of Adeno-Associated Virus Vectors: A Historical Perspective. *Mol Ther* 10, 981-989.

Casadio, A., Martin, K.C., Giustetto, M., Zhu, H., Chen, M., Bartsch, D., Bailey, C.H., and Kandel, E.R. (1999). A Transient, Neuron-Wide Form of Creb-Mediated Long-Term Facilitation Can Be Stabilized at Specific Synapses by Local Protein Synthesis. *Cell* 99, 221-237.

Cashman, N.R., Durham, H.D., Blusztajn, J.K., Oda, K., Tabira, T., Shaw, I.T., Dahrouge, S., and Antel, J.P. (1992). Neuroblastoma X Spinal Cord (Nsc) Hybrid Cell Lines Resemble Developing Motor Neurons. *Dev Dyn* 194, 209-221.

Chakravarthy, S., Saiepour, M.H., Bence, M., Perry, S., Hartman, R., Couey, J.J., Mansvelder, H.D., and Levelt, C.N. (2006). Postsynaptic Trkb Signaling Has Distinct Roles in Spine Maintenance in Adult Visual Cortex and Hippocampus. *Proc Natl Acad Sci U S A* 103, 1071-1076.

Choi, V.W., McCarty, D.M., and Samulski, R.J. (2005). Aav Hybrid Serotypes: Improved Vectors for Gene Delivery. *Curr Gene Ther* 5, 299-310.

Ciabarra, A.M., Sullivan, J.M., Gahn, L.G., Pecht, G., Heinemann, S., and Sevarino, K.A. (1995). Cloning and Characterization of Chi-1: A Developmentally Regulated Member of a Novel Class of the Ionotropic Glutamate Receptor Family. *J Neurosci* 15, 6498-6508.

Clark-Lewis, I., Lopez, A.F., To, L.B., Vadas, M.A., Schrader, J.W., Hood, L.E., and Kent, S.B. (1988). Structure-Function Studies of Human Granulocyte-Macrophage Colony-Stimulating Factor. Identification of Residues Required for Activity. *J Immunol* 141, 881-889.

Conway, J.E., Zolotukhin, S., Muzyczka, N., Hayward, G.S., and Byrne, B.J. (1997). Recombinant Adeno-Associated Virus Type 2 Replication and Packaging Is Entirely Supported by a Herpes Simplex Virus Type 1 Amplicon Expressing Rep and Cap. *J Virol* 71, 8780-8789.

Corkin, S. (1984). Lasting Consequences of Bilateral Medial Temporal Lobectomy: Clinical Course and Experimental Findings in H.M. *Semin. Neurol.* 4, 249-259.

Corkin, S. (2002). What's New with the Amnesic Patient H.M.? *Nat Rev Neurosci* 3, 153-160.

Crawford, L.V., Follett, E.A., Burdon, M.G., and McGeoch, D.J. (1969). The DNA of a Minute Virus of Mice. *J Gen Virol* 4, 37-46.

Croning, M.D., Marshall, M.C., McLaren, P., Armstrong, J.D., and Grant, S.G. (2009). G2cdb: The Genes to Cognition Database. *Nucleic Acids Res* 37, D846-851.

Dame, J.B., Christensen, R.D., and Juul, S.E. (1999). The Distribution of Granulocyte-Macrophage Colony-Stimulating Factor and Its Receptor in the Developing Human Fetus. *Pediatr Res* 46, 358-366.

Dash, P.K., Hochner, B., and Kandel, E.R. (1990). Injection of the Camp-Responsive Element into the Nucleus of Aplysia Sensory Neurons Blocks Long-Term Facilitation. *Nature* 345, 718-721.

Davidson, B.L., Stein, C.S., Heth, J.A., Martins, I., Kotin, R.M., Derksen, T.A., Zabner, J., Ghodsi, A., and Chiorini, J.A. (2000). Recombinant Adeno-Associated Virus Type 2, 4, and 5 Vectors: Transduction of Variant Cell Types and Regions in the Mammalian Central Nervous System. *Proc Natl Acad Sci U S A* 97, 3428-3432.

Daya, S., and Berns, K.I. (2008). Gene Therapy Using Adeno-Associated Virus Vectors. *Clin Microbiol Rev* 21, 583-593.

de Groot, R.P., Coffer, P.J., and Koenderman, L. (1998). Regulation of Proliferation, Differentiation and Survival by the Il-3/Il-5/Gm-Csf Receptor Family. *Cell Signal* 10, 619-628.

Deng, W., Aimone, J.B., and Gage, F.H. (2010). New Neurons and New Memories: How Does Adult Hippocampal Neurogenesis Affect Learning and Memory? *Nat Rev Neurosci* 11, 339-350.

Diederich, K., Schabitz, W.R., Kuhnert, K., Hellstrom, N., Sachser, N., Schneider, A., Kuhn, H.G., and Knecht, S. (2009a). Synergetic Effects of Granulocyte-Colony Stimulating Factor and Cognitive Training on Spatial Learning and Survival of Newborn Hippocampal Neurons. *PLoS One* 4, e5303.

Diederich, K., Sevimli, S., Dorr, H., Kosters, E., Hoppen, M., Lewejohann, L., Klocke, R., *et al.* (2009b). The Role of Granulocyte-Colony Stimulating Factor (G-Csf) in the Healthy Brain: A Characterization of G-Csf-Deficient Mice. *J Neurosci* 29, 11572-11581.

Diederichs, K., Boone, T., and Karplus, P.A. (1991). Novel Fold and Putative Receptor Binding Site of Granulocyte-Macrophage Colony-Stimulating Factor. *Science* 254, 1779-1782.

Digicaylioglu, M., Bichet, S., Marti, H.H., Wenger, R.H., Rivas, L.A., Bauer, C., and Gassmann, M. (1995). Localization of Specific Erythropoietin Binding Sites in Defined Areas of the Mouse Brain. *Proc Natl Acad Sci U S A* 92, 3717-3720.

Dijkers, P.F., van Dijk, T.B., de Groot, R.P., Raaijmakers, J.A., Lammers, J.W., Koenderman, L., and Coffer, P.J. (1999). Regulation and Function of Protein Kinase B and Map Kinase Activation by the Il-5/Gm-Csf/Il-3 Receptor. *Oncogene* 18, 3334-3342.

Dong, J.Y., Fan, P.D., and Frizzell, R.A. (1996). Quantitative Analysis of the Packaging Capacity of Recombinant Adeno-Associated Virus. *Hum Gene Ther* 7, 2101-2112.

Doyle, S.E., and Gasson, J.C. (1998). Characterization of the Role of the Human Granulocyte-Macrophage Colony-Stimulating Factor Receptor Alpha Subunit in the Activation of Jak2 and Stat5. *Blood* 92, 867-876.

Duan, D., Li, Q., Kao, A.W., Yue, Y., Pessin, J.E., and Engelhardt, J.F. (1999). Dynamin Is Required for Recombinant Adeno-Associated Virus Type 2 Infection. *J Virol* 73, 10371-10376.

Dutheil, N., Yoon-Robarts, M., Ward, P., Henckaerts, E., Skrabanek, L., Berns, K.I., Campagne, F., and Linden, R.M. (2004). Characterization of the Mouse Adeno-Associated Virus Aavs1 Ortholog. *J Virol* 78, 8917-8921.

Ebner, K., Bandion, A., Binder, B.R., de Martin, R., and Schmid, J.A. (2003). Gmcsf Activates Nf-Kappab Via Direct Interaction of the Gmcsf Receptor with Ikappab Kinase Beta. *Blood* 102, 192-199.

Ehrenreich, H., Fischer, B., Norra, C., Schellenberger, F., Stender, N., Stiefel, M., Siren, A.L., Paulus, W., Nave, K.A., Gold, R., and Bartels, C. (2007a). Exploring Recombinant Human Erythropoietin in Chronic Progressive Multiple Sclerosis. *Brain* 130, 2577-2588.

Ehrenreich, H., Hinze-Selch, D., Stawicki, S., Aust, C., Knolle-Veentjer, S., Wilms, S., Heinz, G., *et al.* (2007b). Improvement of Cognitive Functions in Chronic Schizophrenic Patients by Recombinant Human Erythropoietin. *Mol Psychiatry* 12, 206-220.

Eichenbaum, H. (1997). How Does the Brain Organize Memories? *Science* 277, 330-332.

Eichenbaum, H. (2000). Hippocampus: Mapping or Memory? *Curr Biol* 10, R785-787.

Eichenbaum, H., Dudchenko, P., Wood, E., Shapiro, M., and Tanila, H. (1999). The Hippocampus, Memory, and Place Cells: Is It Spatial Memory or a Memory Space? *Neuron* 23, 209-226.

Ekstrom, A.D., Kahana, M.J., Caplan, J.B., Fields, T.A., Isham, E.A., Newman, E.L., and Fried, I. (2003). Cellular Networks Underlying Human Spatial Navigation. *Nature* 425, 184-188.

El-Kordi, A., Radyushkin, K., and Ehrenreich, H. (2009). Erythropoietin Improves Operant Conditioning and Stability of Cognitive Performance in Mice. *BMC Biol* 7, 37.

Erles, K., Sebokova, P., and Schlehofer, J.R. (1999). Update on the Prevalence of Serum Antibodies (Igg and Igm) to Adeno-Associated Virus (Aav). *J Med Virol* 59, 406-411.

Figurov, A., Pozzo-Miller, L.D., Olafsson, P., Wang, T., and Lu, B. (1996). Regulation of Synaptic Responses to High-Frequency Stimulation and Ltp by Neurotrophins in the Hippocampus. *Nature* 381, 706-709.

Fleischmann, J., Golde, D.W., Weisbart, R.H., and Gasson, J.C. (1986). Granulocyte-Macrophage Colony-Stimulating Factor Enhances Phagocytosis of Bacteria by Human Neutrophils. *Blood* 68, 708-711.

Franich, N.R., Fitzsimons, H.L., Fong, D.M., Klugmann, M., During, M.J., and Young, D. (2008). Aav Vector-Mediated Rnai of Mutant Huntingtin Expression Is Neuroprotective in a Novel Genetic Rat Model of Huntington's Disease. *Mol Ther* 16, 947-956.

Gambrill, A.C., and Barria, A. (2011). Nmda Receptor Subunit Composition Controls Synaptogenesis and Synapse Stabilization. *Proc Natl Acad Sci U S A* 108, 5855-5860.

Ganser, C., Papazoglou, A., Just, L., and Nikkhah, G. (2010). Neuroprotective Effects of Erythropoietin on 6-Hydroxydopamine-Treated Ventral Mesencephalic Dopamine-Rich Cultures. *Exp Cell Res* 316, 737-746.

Gao, G.P., Alvira, M.R., Wang, L., Calcedo, R., Johnston, J., and Wilson, J.M. (2002). Novel Adeno-Associated Viruses from Rhesus Monkeys as

Vectors for Human Gene Therapy. *Proc Natl Acad Sci U S A* 99, 11854-11859.

Gasson, J.C., Weisbart, R.H., Kaufman, S.E., Clark, S.C., Hewick, R.M., Wong, G.G., and Golde, D.W. (1984). Purified Human Granulocyte-Macrophage Colony-Stimulating Factor: Direct Action on Neutrophils. *Science* 226, 1339-1342.

Geinisman, Y., deToledo-Morrell, L., and Morrell, F. (1991). Induction of Long-Term Potentiation Is Associated with an Increase in the Number of Axospinous Synapses with Segmented Postsynaptic Densities. *Brain Res* 566, 77-88.

Griffiths, D., Dickinson, A., and Clayton, N. (1999). Episodic Memory: What Can Animals Remember About Their Past? *Trends Cogn Sci* 3, 74-80.

Groopman, J.E., Mitsuyasu, R.T., DeLeo, M.J., Oette, D.H., and Golde, D.W. (1987). Effect of Recombinant Human Granulocyte-Macrophage Colony-Stimulating Factor on Myelopoiesis in the Acquired Immunodeficiency Syndrome. *N Engl J Med* 317, 593-598.

Grunfeld, J.F., Barhum, Y., Blondheim, N., Rabey, J.M., Melamed, E., and Offen, D. (2007). Erythropoietin Delays Disease Onset in an Amyotrophic Lateral Sclerosis Model. *Exp Neurol* 204, 260-263.

Guthridge, M.A., Stomski, F.C., Thomas, D., Woodcock, J.M., Bagley, C.J., Berndt, M.C., and Lopez, A.F. (1998). Mechanism of Activation of the Gm-Csf, Il-3, and Il-5 Family of Receptors. *Stem Cells* 16, 301-313.

Ha, Y., Kim, Y.S., Cho, J.M., Yoon, S.H., Park, S.R., Yoon, D.H., Kim, E.Y., and Park, H.C. (2005). Role of Granulocyte-Macrophage Colony-Stimulating Factor in Preventing Apoptosis and Improving Functional Outcome in Experimental Spinal Cord Contusion Injury. *J Neurosurg Spine* 2, 55-61.

Hall, J., Thomas, K.L., and Everitt, B.J. (2000). Rapid and Selective Induction of Bdnf Expression in the Hippocampus During Contextual Learning. *Nat Neurosci* 3, 533-535.

Han, J.H., Kushner, S.A., Yiu, A.P., Cole, C.J., Matynia, A., Brown, R.A., Neve, R.L., Guzowski, J.F., Silva, A.J., and Josselyn, S.A. (2007). Neuronal Competition and Selection During Memory Formation. *Science* 316, 457-460.

Hansen, G., Hercus, T.R., McClure, B.J., Stomski, F.C., Dottore, M., Powell, J., Ramshaw, H., *et al.* (2008). The Structure of the Gm-Csf Receptor Complex Reveals a Distinct Mode of Cytokine Receptor Activation. *Cell* 134, 496-507.

Hauck, B., Chen, L., and Xiao, W. (2003). Generation and Characterization of Chimeric Recombinant Aav Vectors. *Mol Ther* 7, 419-425.

Hauswirth, W.W., and Berns, K.I. (1977). Origin and Termination of Adeno-Associated Virus DNA Replication. *Virology* 78, 488-499.

Hayashi, K., Ohta, S., Kawakami, Y., and Toda, M. (2009). Activation of Dendritic-Like Cells and Neural Stem/Progenitor Cells in Injured Spinal Cord by Gm-Csf. *Neurosci Res* 64, 96-103.

Heldt, S.A., Stanek, L., Chhatwal, J.P., and Ressler, K.J. (2007). Hippocampus-Specific Deletion of Bdnf in Adult Mice Impairs Spatial Memory and Extinction of Aversive Memories. *Mol Psychiatry* 12, 656-670.

Henke, K. (2010). A Model for Memory Systems Based on Processing Modes Rather Than Consciousness. *Nat Rev Neurosci* 11, 523-532.

Henriques, A., Pitzer, C., Dittgen, T., Klugmann, M., Dupuis, L., and Schneider, A. (2011). Cns-Targeted Viral Delivery of G-Csf in an Animal Model for Als: Improved Efficacy and Preservation of the Neuromuscular Unit. *Mol Ther* 19, 284-292.

Hercus, T.R., Cambareri, B., Dottore, M., Woodcock, J., Bagley, C.J., Vadas, M.A., Shannon, M.F., and Lopez, A.F. (1994). Identification of Residues in the First and Fourth Helices of Human Granulocyte-Macrophage Colony-Stimulating Factor Involved in Biologic Activity and in Binding to the Alpha- and Beta-Chains of Its Receptor. *Blood* 83, 3500-3508.

Hercus, T.R., Thomas, D., Guthridge, M.A., Ekert, P.G., King-Scott, J., Parker, M.W., and Lopez, A.F. (2009). The Granulocyte-Macrophage Colony-Stimulating Factor Receptor: Linking Its Structure to Cell Signaling and Its Role in Disease. *Blood* 114, 1289-1298.

Hernandez, Y.J., Wang, J., Kearns, W.G., Loiler, S., Poirier, A., and Flotte, T.R. (1999). Latent Adeno-Associated Virus Infection Elicits Humoral but Not Cell-Mediated Immune Responses in a Nonhuman Primate Model. *J Virol* 73, 8549-8558.

Hetherington, P.A., and Shapiro, M.L. (1997). Hippocampal Place Fields Are Altered by the Removal of Single Visual Cues in a Distance-Dependent Manner. *Behav Neurosci* 111, 20-34.

Hill, A.D., Naama, H.A., Calvano, S.E., and Daly, J.M. (1995). The Effect of Granulocyte-Macrophage Colony-Stimulating Factor on Myeloid Cells and Its Clinical Applications. *J Leukoc Biol* 58, 634-642.

Hoang, T., De Lean, A., Haman, A., Beauchemin, V., Kitamura, T., and Clark, S.C. (1993). The Structure and Dynamics of the Granulocyte Macrophage Colony-Stimulating Factor Receptor Defined by the Ternary Complex Model. *J Biol Chem* 268, 11881-11887.

Hoggan, M.D., Blacklow, N.R., and Rowe, W.P. (1966). Studies of Small DNA Viruses Found in Various Adenovirus Preparations: Physical, Biological,

and Immunological Characteristics. *Proc Natl Acad Sci U S A* 55, 1467-1474.

Huang, X., Kim, J.M., Kong, T.H., Park, S.R., Ha, Y., Kim, M.H., Park, H., *et al.* (2009). Gm-Csf Inhibits Glial Scar Formation and Shows Long-Term Protective Effect after Spinal Cord Injury. *J Neurol Sci* 277, 87-97.

Ichikawa, Y., Pluznik, D.H., and Sachs, L. (1966). In Vitro Control of the Development of Macrophage and Granulocyte Colonies. *Proc Natl Acad Sci U S A* 56, 488-495.

Iversen, P.O., To, L.B., and Lopez, A.F. (1996). Apoptosis of Hemopoietic Cells by the Human Granulocyte-Macrophage Colony-Stimulating Factor Mutant E21r. *Proc Natl Acad Sci U S A* 93, 2785-2789.

Jan, Y.N., and Jan, L.Y. (2010). Branching Out: Mechanisms of Dendritic Arborization. *Nat Rev Neurosci* 11, 316-328.

Jaworski, J., Spangler, S., Seeburg, D.P., Hoogenraad, C.C., and Sheng, M. (2005). Control of Dendritic Arborization by the Phosphoinositide-3'-Kinase-Akt-Mammalian Target of Rapamycin Pathway. *J Neurosci* 25, 11300-11312.

Kafitz, K.W., Rose, C.R., Thoenen, H., and Konnerth, A. (1999). Neurotrophin-Evoked Rapid Excitation through Trkb Receptors. *Nature* 401, 918-921.

Kanakura, Y., Druker, B., Wood, K.W., Mamon, H.J., Okuda, K., Roberts, T.M., and Griffin, J.D. (1991). Granulocyte-Macrophage Colony-Stimulating Factor and Interleukin-3 Induce Rapid Phosphorylation and Activation of the Proto-Oncogene Raf-1 in a Human Factor-Dependent Myeloid Cell Line. *Blood* 77, 243-248.

Kandel, E.R. (2001). The Molecular Biology of Memory Storage: A Dialogue between Genes and Synapses. *Science* 294, 1030-1038.

Kaplitt, M.G., Leone, P., Samulski, R.J., Xiao, X., Pfaff, D.W., O'Malley, K.L., and During, M.J. (1994). Long-Term Gene Expression and Phenotypic Correction Using Adeno-Associated Virus Vectors in the Mammalian Brain. *Nat Genet* 8, 148-154.

Kaushansky, K., Shoemaker, S.G., Alfaro, S., and Brown, C. (1989). Hematopoietic Activity of Granulocyte/Macrophage Colony-Stimulating Factor Is Dependent Upon Two Distinct Regions of the Molecule: Functional Analysis Based Upon the Activities of Interspecies Hybrid Growth Factors. *Proc Natl Acad Sci U S A* 86, 1213-1217.

Kelley, A.E., Andrzejewski, M.E., Baldwin, A.E., Hernandez, P.J., and Pratt, W.E. (2003). Glutamate-Mediated Plasticity in Corticostriatal Networks: Role in Adaptive Motor Learning. *Ann N Y Acad Sci* 1003, 159-168.

Kida, S., Josselyn, S.A., Pena de Ortiz, S., Kogan, J.H., Chevere, I., Masushige, S., and Silva, A.J. (2002). Creb Required for the Stability of New and Reactivated Fear Memories. *Nat Neurosci* 5, 348-355.

Kim, J.K., Choi, B.H., Park, H.C., Park, S.R., Kim, Y.S., Yoon, S.H., Park, H.S., Kim, E.Y., and Ha, Y. (2004). Effects of Gm-Csf on the Neural Progenitor Cells. *Neuroreport* 15, 2161-2165.

Kim, N.K., Choi, B.H., Huang, X., Snyder, B.J., Bukhari, S., Kong, T.H., Park, H., Park, H.C., Park, S.R., and Ha, Y. (2009). Granulocyte-Macrophage Colony-Stimulating Factor Promotes Survival of Dopaminergic Neurons in the 1-Methyl-4-Phenyl-1,2,3,6-Tetrahydropyridine-Induced Murine Parkinson's Disease Model. *Eur J Neurosci* 29, 891-900.

Kimura, M., Kodama, T., Aguila, M.C., Zhang, S.Q., and Inoue, S. (2000). Granulocyte-Macrophage Colony-Stimulating Factor Modulates Rapid Eye Movement (Rem) Sleep and Non-Rem Sleep in Rats. *J Neurosci* 20, 5544-5551.

Klugmann, M., Leichtlein, C.B., Symes, C.W., Klaussner, B.C., Brooks, A.I., Young, D., and During, M.J. (2006). A Novel Role of Circadian Transcription Factor Dbp in Hippocampal Plasticity. *Mol Cell Neurosci* 31, 303-314.

Koczot, F.J., Carter, B.J., Garon, C.F., and Rose, J.A. (1973). Self-Complementarity of Terminal Sequences within Plus or Minus Strands of Adenovirus-Associated Virus DNA. *Proc Natl Acad Sci U S A* 70, 215-219.

Kong, T., Choi, J.K., Park, H., Choi, B.H., Snyder, B.J., Bukhari, S., Kim, N.K., Huang, X., Park, S.R., Park, H.C., and Ha, Y. (2009). Reduction in Programmed Cell Death and Improvement in Functional Outcome of Transient Focal Cerebral Ischemia after Administration of Granulocyte-Macrophage Colony-Stimulating Factor in Rats. Laboratory Investigation. *J Neurosurg* 111, 155-163.

Korte, M., Carroll, P., Wolf, E., Brem, G., Thoenen, H., and Bonhoeffer, T. (1995). Hippocampal Long-Term Potentiation Is Impaired in Mice Lacking Brain-Derived Neurotrophic Factor. *Proc Natl Acad Sci U S A* 92, 8856-8860.

Korte, M., Griesbeck, O., Gravel, C., Carroll, P., Staiger, V., Thoenen, H., and Bonhoeffer, T. (1996). Virus-Mediated Gene Transfer into Hippocampal Ca1 Region Restores Long-Term Potentiation in Brain-Derived Neurotrophic Factor Mutant Mice. *Proc Natl Acad Sci U S A* 93, 12547-12552.

Korte, M., Kang, H., Bonhoeffer, T., and Schuman, E. (1998). A Role for Bdnf in the Late-Phase of Hippocampal Long-Term Potentiation. *Neuropharmacology* 37, 553-559.

Kotin, R.M., Siniscalco, M., Samulski, R.J., Zhu, X.D., Hunter, L., Laughlin, C.A., McLaughlin, S., Muzyczka, N., Rocchi, M., and Berns, K.I. (1990). Site-Specific Integration by Adeno-Associated Virus. *Proc Natl Acad Sci U S A* 87, 2211-2215.

Kruger, C., Laage, R., Pitzer, C., Schabitz, W.R., and Schneider, A. (2007). The Hematopoietic Factor Gm-Csf (Granulocyte-Macrophage Colony-Stimulating Factor) Promotes Neuronal Differentiation of Adult Neural Stem Cells in Vitro. *BMC Neurosci* 8, 88.

Kumar, V., Zhang, M.X., Swank, M.W., Kunz, J., and Wu, G.Y. (2005). Regulation of Dendritic Morphogenesis by Ras-Pi3k-Akt-Mtor and Ras-Mapk Signaling Pathways. *J Neurosci* 25, 11288-11299.

Kumaran, D., and Maguire, E.A. (2005). The Human Hippocampus: Cognitive Maps or Relational Memory? *J Neurosci* 25, 7254-7259.

Leconte, C., Bihel, E., Lepelletier, F.X., Bouet, V., Saulnier, R., Petit, E., Boulouard, M., Bernaudin, M., and Schumann-Bard, P. (2011). Comparison of the Effects of Erythropoietin and Its Carbamylated Derivative on Behaviour and Hippocampal Neurogenesis in Mice. *Neuropharmacology* 60, 354-364.

Lee, Y.S., and Silva, A.J. (2009). The Molecular and Cellular Biology of Enhanced Cognition. *Nat Rev Neurosci* 10, 126-140.

LeVine, A.M., Reed, J.A., Kurak, K.E., Cianciolo, E., and Whitsett, J.A. (1999). Gm-Csf-Deficient Mice Are Susceptible to Pulmonary Group B Streptococcal Infection. *J Clin Invest* 103, 563-569.

Lock, P., Metcalf, D., and Nicola, N.A. (1994). Histidine-367 of the Human Common Beta Chain of the Receptor Is Critical for High-Affinity Binding of Human Granulocyte-Macrophage Colony-Stimulating Factor. *Proc Natl Acad Sci U S A* 91, 252-256.

Lopez, A.F., Shannon, M.F., Hercus, T., Nicola, N.A., Cambareri, B., Dottore, M., Layton, M.J., Eglinton, L., and Vadas, M.A. (1992). Residue 21 of Human Granulocyte-Macrophage Colony-Stimulating Factor Is Critical for Biological Activity and for High but Not Low Affinity Binding. *EMBO J* 11, 909-916.

Lopez de Armentia, M., Jancic, D., Olivares, R., Alarcon, J.M., Kandel, E.R., and Barco, A. (2007). Camp Response Element-Binding Protein-Mediated Gene Expression Increases the Intrinsic Excitability of Ca1 Pyramidal Neurons. *J Neurosci* 27, 13909-13918.

Lukashenko, P.V., Lukashenko, T.M., Savanovich, II, Sandakov, D.B., and Gerein, V. (2004). Granulocyte Macrophage Colony-Stimulating Factor Regulates Activity of the Nervous System. *Neuroimmunomodulation* 11, 36-40.

Manczak, M., Mao, P., Nakamura, K., Bebbington, C., Park, B., and Reddy, P.H. (2009). Neutralization of Granulocyte Macrophage Colony-Stimulating Factor Decreases Amyloid Beta 1-42 and Suppresses Microglial Activity in a Transgenic Mouse Model of Alzheimer's Disease. *Hum Mol Genet* 18, 3876-3893.

Marsh, J.T., Brown, W.S., Wolcott, D., Carr, C.R., Harper, R., Schweitzer, S.V., and Nissenson, A.R. (1991). Rhuepo Treatment Improves Brain and Cognitive Function of Anemic Dialysis Patients. *Kidney Int* 39, 155-163.

Matsuzaki, M., Ellis-Davies, G.C., Nemoto, T., Miyashita, Y., Iino, M., and Kasai, H. (2001). Dendritic Spine Geometry Is Critical for Ampa Receptor Expression in Hippocampal Ca1 Pyramidal Neurons. *Nat Neurosci* 4, 1086-1092.

Maurer, M.H., Schabitz, W.R., and Schneider, A. (2008). Old Friends in New Constellations--the Hematopoetic Growth Factors G-Csf, Gm-Csf, and Epo for the Treatment of Neurological Diseases. *Curr Med Chem* 15, 1407-1411.

McCown, T.J. (2011). Adeno-Associated Virus (Aav) Vectors in the Cns. *Curr Gene Ther* 11, 181-188.

McLay, R.N., Kimura, M., Banks, W.A., and Kastin, A.J. (1997). Granulocyte-Macrophage Colony-Stimulating Factor Crosses the Blood--Brain and Blood--Spinal Cord Barriers. *Brain* 120 (Pt 11), 2083-2091.

Meropol, N.J., Altmann, S.W., Shanafelt, A.B., Kastelein, R.A., Johnson, G.D., and Prystowsky, M.B. (1992). Requirement of Hydrophilic Amino-Terminal Residues for Granulocyte-Macrophage Colony-Stimulating Factor Bioactivity and Receptor Binding. *J Biol Chem* 267, 14266-14269.

Metcalf, D. (1989). The Molecular Control of Cell Division, Differentiation Commitment and Maturation in Haemopoietic Cells. *Nature* 339, 27-30.

Metcalf, D. (2008). Hematopoietic Cytokines. *Blood* 111, 485-491.

Metcalf, D., Begley, C.G., Williamson, D.J., Nice, E.C., De Lamarter, J., Mermod, J.J., Thatcher, D., and Schmidt, A. (1987). Hemopoietic Responses in Mice Injected with Purified Recombinant Murine Gm-Csf. *Exp Hematol* 15, 1-9.

Metcalf, D., Johnson, G.R., and Burgess, A.W. (1980). Direct Stimulation by Purified Gm-Csf of the Proliferation of Multipotential and Erythroid Precursor Cells. *Blood* 55, 138-147.

Meuer, K., Pitzer, C., Teismann, P., Kruger, C., Goricke, B., Laage, R., Lingor, P., *et al.* (2006). Granulocyte-Colony Stimulating Factor Is

Neuroprotective in a Model of Parkinson's Disease. *J Neurochem* 97, 675-686.

Milner, B., Corkin, S., and Teuber, H.L. (1968). Further Analysis of the Hippocampal Amnesic Syndrome: 14-Year Follow-up Study of H.M. *Neuropsychologia* 6, 215-234.

Minichiello, L. (2009). Trkb Signalling Pathways in Ltp and Learning. *Nat Rev Neurosci* 10, 850-860.

Monyer, H., Burnashev, N., Laurie, D.J., Sakmann, B., and Seeburg, P.H. (1994). Developmental and Regional Expression in the Rat Brain and Functional Properties of Four Nmda Receptors. *Neuron* 12, 529-540.

Moser, E., Moser, M.B., and Andersen, P. (1993). Spatial Learning Impairment Parallels the Magnitude of Dorsal Hippocampal Lesions, but Is Hardly Present Following Ventral Lesions. *J Neurosci* 13, 3916-3925.

Moser, M.B., Moser, E.I., Forrest, E., Andersen, P., and Morris, R.G. (1995). Spatial Learning with a Minislab in the Dorsal Hippocampus. *Proc Natl Acad Sci U S A* 92, 9697-9701.

Mu, J.S., Li, W.P., Yao, Z.B., and Zhou, X.F. (1999). Deprivation of Endogenous Brain-Derived Neurotrophic Factor Results in Impairment of Spatial Learning and Memory in Adult Rats. *Brain Res* 835, 259-265.

Muto, A., Watanabe, S., Itoh, T., Miyajima, A., Yokota, T., and Arai, K. (1995). Roles of the Cytoplasmic Domains of the Alpha and Beta Subunits of Human Granulocyte-Macrophage Colony-Stimulating Factor Receptor. *J Allergy Clin Immunol* 96, 1100-1114.

Nakai, H., Storm, T.A., and Kay, M.A. (2000). Recruitment of Single-Stranded Recombinant Adeno-Associated Virus Vector Genomes and Intermolecular Recombination Are Responsible for Stable Transduction of Liver in Vivo. *J Virol* 74, 9451-9463.

Nakai, H., Yant, S.R., Storm, T.A., Fuess, S., Meuse, L., and Kay, M.A. (2001). Extrachromosomal Recombinant Adeno-Associated Virus Vector Genomes Are Primarily Responsible for Stable Liver Transduction in Vivo. *J Virol* 75, 6969-6976.

Neves, G., Cooke, S.F., and Bliss, T.V. (2008). Synaptic Plasticity, Memory and the Hippocampus: A Neural Network Approach to Causality. *Nat Rev Neurosci* 9, 65-75.

O'Keefe, J., and Dostrovsky, J. (1971). The Hippocampus as a Spatial Map. Preliminary Evidence from Unit Activity in the Freely-Moving Rat. *Brain Res* 34, 171-175.

O'Keefe, J., and Nadel, L. (1978). The Hippocampus as a Cognitive Map (Oxford University Press).

O'Keefe, J., and Speakman, A. (1987). Single Unit Activity in the Rat Hippocampus During a Spatial Memory Task. *Exp Brain Res* 68, 1-27.

Olson, N.J., Masse, T., Suzuki, T., Chen, J., Alam, D., and Kelly, P.T. (1995). Functional Identification of the Promoter for the Gene Encoding the Alpha Subunit of Calcium/Calmodulin-Dependent Protein Kinase Ii. *Proc Natl Acad Sci U S A* 92, 1659-1663.

Pavlov, I.P. (1927). Conditioned Reflexes: An Investigation of the Physiological Activity of the Cerebral Cortex (London: Oxford University Press).

Paxinos, G., and Franklin, K.B.J. (2004). The Mouse Brain in Stereotaxic Coordinates, 2nd edn (Elsevier Academic Press).

Perazzona, B., Isabel, G., Preat, T., and Davis, R.L. (2004). The Role of Camp Response Element-Binding Protein in Drosophila Long-Term Memory. *J Neurosci* 24, 8823-8828.

Perugini, M., Brown, A.L., Salerno, D.G., Booker, G.W., Stojkoski, C., Hercus, T.R., Lopez, A.F., Hibbs, M.L., Gonda, T.J., and D'Andrea, R.J. (2010). Alternative Modes of Gm-Csf Receptor Activation Revealed Using Activated Mutants of the Common Beta-Subunit. *Blood* 115, 3346-3353.

Pitzer, C., Kruger, C., Plaas, C., Kirsch, F., Dittgen, T., Muller, R., Laage, R., *et al.* (2008). Granulocyte-Colony Stimulating Factor Improves Outcome in a Mouse Model of Amyotrophic Lateral Sclerosis. *Brain* 131, 3335-3347.

Polotskaya, A., Zhao, Y., Lilly, M.L., and Kraft, A.S. (1993). A Critical Role for the Cytoplasmic Domain of the Granulocyte-Macrophage Colony-Stimulating Factor Alpha Receptor in Mediating Cell Growth. *Cell Growth Differ* 4, 523-531.

Qing, K., Mah, C., Hansen, J., Zhou, S., Dwarki, V., and Srivastava, A. (1999). Human Fibroblast Growth Factor Receptor 1 Is a Co-Receptor for Infection by Adeno-Associated Virus 2. *Nat Med* 5, 71-77.

Quelle, F.W., Sato, N., Witthuhn, B.A., Inhorn, R.C., Eder, M., Miyajima, A., Griffin, J.D., and Ihle, J.N. (1994). Jak2 Associates with the Beta C Chain of the Receptor for Granulocyte-Macrophage Colony-Stimulating Factor, and Its Activation Requires the Membrane-Proximal Region. *Mol Cell Biol* 14, 4335-4341.

Quirk, G.J., Muller, R.U., and Kubie, J.L. (1990). The Firing of Hippocampal Place Cells in the Dark Depends on the Rat's Recent Experience. *J Neurosci* 10, 2008-2017.

Rabinowitz, J.E., Bowles, D.E., Faust, S.M., Ledford, J.G., Cunningham, S.E., and Samulski, R.J. (2004). Cross-Dressing the Virion: The

Transcapsidation of Adeno-Associated Virus Serotypes Functionally Defines Subgroups. *J Virol* 78, 4421-4432.

Rabinowitz, J.E., Rolling, F., Li, C., Conrath, H., Xiao, W., Xiao, X., and Samulski, R.J. (2002). Cross-Packaging of a Single Adeno-Associated Virus (Aav) Type 2 Vector Genome into Multiple Aav Serotypes Enables Transduction with Broad Specificity. *J Virol* 76, 791-801.

Rajotte, D., Cadieux, C., Haman, A., Wilkes, B.C., Clark, S.C., Hercus, T., Woodcock, J.A., Lopez, A., and Hoang, T. (1997). Crucial Role of the Residue R280 at the F'-G' Loop of the Human Granulocyte/Macrophage Colony-Stimulating Factor Receptor Alpha Chain for Ligand Recognition. *J Exp Med* 185, 1939-1950.

Rasband, W.S. (1997-2011). Imagej. (Bethesda, Maryland, U. S. National Institutes of Health).

Rauner, C., and Kohr, G. (2011). Triheteromeric Nr1/Nr2a/Nr2b Receptors Constitute the Major N-Methyl-D-Aspartate Receptor Population in Adult Hippocampal Synapses. *J Biol Chem* 286, 7558-7566.

Redish, A.D. (2001). The Hippocampal Debate: Are We Asking the Right Questions? *Behav Brain Res* 127, 81-98.

Reed, J.A., Clegg, D.J., Smith, K.B., Tolod-Richer, E.G., Matter, E.K., Picard, L.S., and Seeley, R.J. (2005). Gm-Csf Action in the Cns Decreases Food Intake and Body Weight. *J Clin Invest* 115, 3035-3044.

Riedel, G., Platt, B., and Micheau, J. (2003). Glutamate Receptor Function in Learning and Memory. *Behav Brain Res* 140, 1-47.

Robertson, S.A., and Seamark, R.F. (1992). Granulocyte-Macrophage Colony Stimulating Factor (Gm-Csf): One of a Family of Epithelial Cell-Derived Cytokines in the Preimplantation Uterus. *Reprod Fertil Dev* 4, 435-448.

Rosas, M., Gordon, S., and Taylor, P.R. (2007). Characterisation of the Expression and Function of the Gm-Csf Receptor Alpha-Chain in Mice. *Eur J Immunol* 37, 2518-2528.

Rose, J.A., Berns, K.I., Hoggan, M.D., and Koczot, F.J. (1969). Evidence for a Single-Stranded Adenovirus-Associated Virus Genome: Formation of a DNA Density Hybrid on Release of Viral DNA. *Proc Natl Acad Sci U S A* 64, 863-869.

Sakamoto, K.M., Bardeleben, C., Yates, K.E., Raines, M.A., Golde, D.W., and Gasson, J.C. (1991). 5' Upstream Sequence and Genomic Structure of the Human Primary Response Gene, Egr-1/Tis8. *Oncogene* 6, 867-871.

Sakimura, K., Kutsuwada, T., Ito, I., Manabe, T., Takayama, C., Kushiya, E., Yagi, T., Aizawa, S., Inoue, Y., Sugiyama, H., and et al. (1995). Reduced

Hippocampal Ltp and Spatial Learning in Mice Lacking Nmda Receptor Epsilon 1 Subunit. *Nature* 373, 151-155.

Sallusto, F., and Lanzavecchia, A. (1994). Efficient Presentation of Soluble Antigen by Cultured Human Dendritic Cells Is Maintained by Granulocyte/Macrophage Colony-Stimulating Factor Plus Interleukin 4 and Downregulated by Tumor Necrosis Factor Alpha. *J Exp Med* 179, 1109-1118.

Sargin, D., El-Kordi, A., Agarwal, A., Muller, M., Wojcik, S.M., Hassouna, I., Sperling, S., Nave, K.A., and Ehrenreich, H. (2011). Expression of Constitutively Active Erythropoietin Receptor in Pyramidal Neurons of Cortex and Hippocampus Boosts Higher Cognitive Functions in Mice. *BMC Biol* 9, 27.

Satoh, T., Nakafuku, M., Miyajima, A., and Kaziro, Y. (1991). Involvement of Ras P21 Protein in Signal-Transduction Pathways from Interleukin 2, Interleukin 3, and Granulocyte/Macrophage Colony-Stimulating Factor, but Not from Interleukin 4. *Proc Natl Acad Sci U S A* 88, 3314-3318.

Sayani, F., Montero-Julian, F.A., Ranchin, V., Prevost, J.M., Flavetta, S., Zhu, W., Woodman, R.C., Brailly, H., and Brown, C.B. (2000). Identification of the Soluble Granulocyte-Macrophage Colony Stimulating Factor Receptor Protein in Vivo. *Blood* 95, 461-469.

Schabitz, W.R., Kollmar, R., Schwaninger, M., Juettler, E., Bardutzky, J., Scholzke, M.N., Sommer, C., and Schwab, S. (2003). Neuroprotective Effect of Granulocyte Colony-Stimulating Factor after Focal Cerebral Ischemia. *Stroke* 34, 745-751.

Schabitz, W.R., Kruger, C., Pitzer, C., Weber, D., Laage, R., Gassler, N., Aronowski, J., *et al.* (2008). A Neuroprotective Function for the Hematopoietic Protein Granulocyte-Macrophage Colony Stimulating Factor (Gm-Csf). *J Cereb Blood Flow Metab* 28, 29-43.

Schacter, D.L., Dobbins, I.G., and Schnyer, D.M. (2004). Specificity of Priming: A Cognitive Neuroscience Perspective. *Nat Rev Neurosci* 5, 853-862.

Schallenberg, M., Charalambous, P., and Thanos, S. (2009). Gm-Csf Regulates the Erk1/2 Pathways and Protects Injured Retinal Ganglion Cells from Induced Death. *Exp Eye Res* 89, 665-677.

Schneider, A., Kruger, C., Steigleder, T., Weber, D., Pitzer, C., Laage, R., Aronowski, J., *et al.* (2005). The Hematopoietic Factor G-Csf Is a Neuronal Ligand That Counteracts Programmed Cell Death and Drives Neurogenesis. *J Clin Invest* 115, 2083-2098.

Schultz, B.R., and Chamberlain, J.S. (2008). Recombinant Adeno-Associated Virus Transduction and Integration. *Mol Ther* 16, 1189-1199.

Scoville, W.B., and Milner, B. (1957). Loss of Recent Memory after Bilateral Hippocampal Lesions. *J Neurol Neurosurg Psychiatry* 20, 11-21.

Seeburg, P.H. (1993). The Tins/Tips Lecture. The Molecular Biology of Mammalian Glutamate Receptor Channels. *Trends Neurosci* 16, 359-365.

Seeburg, P.H., Burnashev, N., Kohr, G., Kuner, T., Sprengel, R., and Monyer, H. (1995). The Nmda Receptor Channel: Molecular Design of a Coincidence Detector. *Recent Prog Horm Res* 50, 19-34.

Serrano, P., Friedman, E.L., Kenney, J., Taubenfeld, S.M., Zimmerman, J.M., Hanna, J., Alberini, C., *et al.* (2008). Pkmzeta Maintains Spatial, Instrumental, and Classically Conditioned Long-Term Memories. *PLoS Biol* 6, 2698-2706.

Seymour, J.F., and Presneill, J.J. (2002). Pulmonary Alveolar Proteinosis: Progress in the First 44 Years. *Am J Respir Crit Care Med* 166, 215-235.

Shanafelt, A.B., Johnson, K.E., and Kastelein, R.A. (1991). Identification of Critical Amino Acid Residues in Human and Mouse Granulocyte-Macrophage Colony-Stimulating Factor and Their Involvement in Species Specificity. *J Biol Chem* 266, 13804-13810.

Sheng, M., McFadden, G., and Greenberg, M.E. (1990). Membrane Depolarization and Calcium Induce C-Fos Transcription Via Phosphorylation of Transcription Factor Creb. *Neuron* 4, 571-582.

Sheng, M., Thompson, M.A., and Greenberg, M.E. (1991). Creb: A Ca(2+)-Regulated Transcription Factor Phosphorylated by Calmodulin-Dependent Kinases. *Science* 252, 1427-1430.

Shi, Y., Liu, C.H., Roberts, A.I., Das, J., Xu, G., Ren, G., Zhang, Y., *et al.* (2006). Granulocyte-Macrophage Colony-Stimulating Factor (Gm-Csf) and T-Cell Responses: What We Do and Don't Know. *Cell Res* 16, 126-133.

Shimizu, E., Tang, Y.P., Rampon, C., and Tsien, J.Z. (2000). Nmda Receptor-Dependent Synaptic Reinforcement as a Crucial Process for Memory Consolidation. *Science* 290, 1170-1174.

Shingo, T., Sorokan, S.T., Shimazaki, T., and Weiss, S. (2001). Erythropoietin Regulates the in Vitro and in Vivo Production of Neuronal Progenitors by Mammalian Forebrain Neural Stem Cells. *J Neurosci* 21, 9733-9743.

Socinski, M.A., Cannistra, S.A., Elias, A., Antman, K.H., Schnipper, L., and Griffin, J.D. (1988). Granulocyte-Macrophage Colony Stimulating Factor Expands the Circulating Haemopoietic Progenitor Cell Compartment in Man. *Lancet* 1, 1194-1198.

Sprengel, R., Suchanek, B., Amico, C., Brusa, R., Burnashev, N., Rozov, A., Hvalby, O., *et al.* (1998). Importance of the Intracellular Domain of Nr2 Subunits for Nmda Receptor Function in Vivo. *Cell* 92, 279-289.

Stanley, E., Lieschke, G.J., Grail, D., Metcalf, D., Hodgson, G., Gall, J.A., Maher, D.W., Cebon, J., Sinickas, V., and Dunn, A.R. (1994). Granulocyte/Macrophage Colony-Stimulating Factor-Deficient Mice Show No Major Perturbation of Hematopoiesis but Develop a Characteristic Pulmonary Pathology. *Proc Natl Acad Sci U S A* 91, 5592-5596.

Sullivan, E.V., and Sagar, H.J. (1991). Double Dissociation of Short-Term and Long-Term Memory for Nonverbal Material in Parkinson's Disease and Global Amnesia. A Further Analysis. *Brain* 114 (Pt 2), 893-906.

Summerford, C., Bartlett, J.S., and Samulski, R.J. (1999). Alphavbeta5 Integrin: A Co-Receptor for Adeno-Associated Virus Type 2 Infection. *Nat Med* 5, 78-82.

Summerford, C., and Samulski, R.J. (1998). Membrane-Associated Heparan Sulfate Proteoglycan Is a Receptor for Adeno-Associated Virus Type 2 Virions. *J Virol* 72, 1438-1445.

Sweatt, J.D. (2004). Hippocampal Function in Cognition. *Psychopharmacology (Berl)* 174, 99-110.

Tanaka, M., Kikuchi, H., Ishizu, T., Minohara, M., Osoegawa, M., Motomura, K., Tateishi, T., Ohyagi, Y., and Kira, J. (2006). Intrathecal Upregulation of Granulocyte Colony Stimulating Factor and Its Neuroprotective Actions on Motor Neurons in Amyotrophic Lateral Sclerosis. *J Neuropathol Exp Neurol* 65, 816-825.

Tang, Y.P., Shimizu, E., Dube, G.R., Rampon, C., Kerchner, G.A., Zhuo, M., Liu, G., and Tsien, J.Z. (1999). Genetic Enhancement of Learning and Memory in Mice. *Nature* 401, 63-69.

Tao, X., Finkbeiner, S., Arnold, D.B., Shaywitz, A.J., and Greenberg, M.E. (1998). Ca2+ Influx Regulates Bdnf Transcription by a Creb Family Transcription Factor-Dependent Mechanism. *Neuron* 20, 709-726.

Terskikh, A.V., Easterday, M.C., Li, L., Hood, L., Kornblum, H.I., Geschwind, D.H., and Weissman, I.L. (2001). From Hematopoiesis to Neuropoiesis: Evidence of Overlapping Genetic Programs. *Proc Natl Acad Sci U S A* 98, 7934-7939.

Tolman, E.C. (1948). Cognitive Maps in Rats and Men. *Psychol Rev* 55, 189-208.

Tonges, L., Schlachetzki, J.C., Weishaupt, J.H., and Bahr, M. (2007). Hematopoietic Cytokines--on the Verge of Conquering Neurology. *Curr Mol Med* 7, 157-170.

Trapnell, B.C., Whitsett, J.A., and Nakata, K. (2003). Pulmonary Alveolar Proteinosis. *N Engl J Med* 349, 2527-2539.

Tulving, E., and Markowitsch, H.J. (1998). Episodic and Declarative Memory: Role of the Hippocampus. *Hippocampus* 8, 198-204.

Tulving, E., and Schacter, D.L. (1990). Priming and Human Memory Systems. *Science* 247, 301-306.

Ujike, H., and Sato, M. (2004). Clinical Features of Sensitization to Methamphetamine Observed in Patients with Methamphetamine Dependence and Psychosis. *Ann N Y Acad Sci* 1025, 279-287.

van Zundert, B., Yoshii, A., and Constantine-Paton, M. (2004). Receptor Compartmentalization and Trafficking at Glutamate Synapses: A Developmental Proposal. *Trends Neurosci* 27, 428-437.

Volmar, C.H., Ait-Ghezala, G., Frieling, J., Paris, D., and Mullan, M.J. (2008). The Granulocyte Macrophage Colony Stimulating Factor (Gm-Csf) Regulates Amyloid Beta (Abeta) Production. *Cytokine* 42, 336-344.

von Engelhardt, J., Doganci, B., Jensen, V., Hvalby, O., Gongrich, C., Taylor, A., Barkus, C., *et al.* (2008). Contribution of Hippocampal and Extra-Hippocampal Nr2b-Containing Nmda Receptors to Performance on Spatial Learning Tasks. *Neuron* 60, 846-860.

Wang, L., Zhang, Z., Wang, Y., Zhang, R., and Chopp, M. (2004). Treatment of Stroke with Erythropoietin Enhances Neurogenesis and Angiogenesis and Improves Neurological Function in Rats. *Stroke* 35, 1732-1737.

Weisbart, R.H., Kwan, L., Golde, D.W., and Gasson, J.C. (1987). Human Gm-Csf Primes Neutrophils for Enhanced Oxidative Metabolism in Response to the Major Physiological Chemoattractants. *Blood* 69, 18-21.

Weiss, E.K., Krupka, N., Bahner, F., Both, M., and Draguhn, A. (2008). Fast Effects of Glucocorticoids on Memory-Related Network Oscillations in the Mouse Hippocampus. *J Neuroendocrinol* 20, 549-557.

Woodcock, J.M., McClure, B.J., Stomski, F.C., Elliott, M.J., Bagley, C.J., and Lopez, A.F. (1997). The Human Granulocyte-Macrophage Colony-Stimulating Factor (Gm-Csf) Receptor Exists as a Preformed Receptor Complex That Can Be Activated by Gm-Csf, Interleukin-3, or Interleukin-5. *Blood* 90, 3005-3017.

Woodcock, J.M., Zacharakis, B., Plaetinck, G., Bagley, C.J., Qiyu, S., Hercus, T.R., Tavernier, J., and Lopez, A.F. (1994). Three Residues in the Common Beta Chain of the Human Gm-Csf, Il-3 and Il-5 Receptors Are Essential for Gm-Csf and Il-5 but Not Il-3 High Affinity Binding and Interact with Glu21 of Gm-Csf. *EMBO J* 13, 5176-5185.

Yang, N., Zhang, L., and Kazazian, H.H., Jr. (2005). L1 Retrotransposon-Mediated Stable Gene Silencing. *Nucleic Acids Res* 33, e57.

Yashiro, K., and Philpot, B.D. (2008). Regulation of Nmda Receptor Subunit Expression and Its Implications for Ltd, Ltp, and Metaplasticity. *Neuropharmacology* 55, 1081-1094.

Yin, J.C., Wallach, J.S., Del Vecchio, M., Wilder, E.L., Zhou, H., Quinn, W.G., and Tully, T. (1994). Induction of a Dominant Negative Creb Transgene Specifically Blocks Long-Term Memory in Drosophila. *Cell* 79, 49-58.

Yoshida, M., Ikegami, M., Reed, J.A., Chroneos, Z.C., and Whitsett, J.A. (2001). Gm-Csf Regulates Protein and Lipid Catabolism by Alveolar Macrophages. *Am J Physiol Lung Cell Mol Physiol* 280, L379-386.

Yoshida, N., Yagasaki, H., Xu, Y., Matsuda, K., Yoshimi, A., Takahashi, Y., Hama, A., *et al.* (2009). Correlation of Clinical Features with the Mutational Status of Gm-Csf Signaling Pathway-Related Genes in Juvenile Myelomonocytic Leukemia. *Pediatr Res* 65, 334-340.

Yoshimura, A., Ichihara, M., Kinjyo, I., Moriyama, M., Copeland, N.G., Gilbert, D.J., Jenkins, N.A., Hara, T., and Miyajima, A. (1996). Mouse Oncostatin M: An Immediate Early Gene Induced by Multiple Cytokines through the Jak-Stat5 Pathway. *EMBO J* 15, 1055-1063.

Zeng, Y., and Cullen, B.R. (2004). Structural Requirements for Pre-Microrna Binding and Nuclear Export by Exportin 5. *Nucleic Acids Res* 32, 4776-4785.

Zhang, Y., Buchholz, F., Muyrers, J.P., and Stewart, A.F. (1998). A New Logic for DNA Engineering Using Recombination in Escherichia Coli. *Nat Genet* 20, 123-128.

Zhang, Y., Muyrers, J.P., Testa, G., and Stewart, A.F. (2000). DNA Cloning by Homologous Recombination in Escherichia Coli. *Nat Biotechnol* 18, 1314-1317.

Zola-Morgan, S.M., and Squire, L.R. (1990). The Primate Hippocampal Formation: Evidence for a Time-Limited Role in Memory Storage. *Science* 250, 288-290.